ucc
Coláiste na hOllscoile Corcaigh, Éire
University College Cork, Ireland

THESIS:

DESIGN AND OPTIMISATION OF A SMALL, ROBUST OUTDOOR DUCKWEED BIOREACTOR FOR OPERATION UNDER 'ON-SITE' FARMYARD CONDITIONS

FOR THE DEGREE OF MENGSC BY RESEARCH

GRACE O' SULLIVAN, 118319761

DEPARTMENT OF PROCESS & CHEMICAL ENGINEERING.

SCHOOL OF ENGINEERING AND ARCHITECTURE.

SUPERVISORS: PROF EDMOND BYRNE AND DR FATEMEH KAVOUSI

JANUARY 2024

Abstract

Duckweed (*Lemnaceae*) is a small, aquatic plant that is ubiquitous across Ireland. It grows remarkably fast, with a doubling time of one to two days. Duckweed is typically found on slow moving water bodies, but it can grow on agricultural waste streams such as yard washings. Usefully, the plant removes excess nutrients (nitrogen and phosphorus) from wastewater to produce a high protein crop. Duckweed dry weight can contain up to 40% protein. Duckweed is currently being investigated for use in human nutrition, biofuel production, and the remediation of waste streams (Appenroth et al., 2017, Xu et al., 2012, Zhou et al., 2023).

The rising need for sustainable agriculture systems magnifies the importance of a circular economy approach to farming. This project involves the design and optimisation of an outdoor duckweed growth system suitable for use on farms. It offers farmers a plausible solution to managing the large volumes of nutrient-rich wastewater produced on farms daily, whilst also generating high-value biomass. Hence, it can help provide a circular economy approach to sustainable agriculture. Currently, two main styles of growth systems are used in the production of duckweed: ponds and raceway systems. A literature survey (undertaken as part of this research) reveals that limited studies have been completed on the effect of system design on duckweed cultivation.

The approach undertaken in this project involves a systematic analysis of fluid flow using Computational Fluid Dynamics (CFD) and tracer response experiments to inform the design of a system optimal for duckweed production. ANSYS Fluent is used to optimise the system geometry and interpret the effects of the geometry on nutrient distribution. Relative growth rate and nutrient uptake experiments were also employed to gain experiential knowledge and thus a holistic understanding of the impact of design on duckweed growth. From this study, it can be concluded that low levels of mixing within a cultivation system have a positive effect on both the relative growth rate of duckweed and its remediation ability. However, at higher flow rates the growth of duckweed is negatively impacted. The results also feature the design of a medium-scale outdoor duckweed cultivation system, informed by the literature review and experimental work.

This work will inform stakeholders on the most suitable system for duckweed production in a farm setting. In addition to this, it will provide guidance on the style of system that is most suitable for large scale duckweed production sites worldwide.

Acknowledgments

This Master's thesis marks the culmination of an exciting and rewarding years' work. The research was carried out between University College Cork's (UCC) Department of Process and Chemical Engineering (PCE), and the School of Biological, Earth, and Environmental Sciences (BEES). My undergraduate degree in biotechnology provided a unique bridge between both disciplines.

There are several people I am profoundly indebted to that I would like to thank. Firstly, I would like to express my deepest gratitude to my two supervisors Prof. Ed Byrne and Dr. Fatemeh Kavousi, whose unwavering guidance, encouragement, and support have been invaluable throughout this project. Their involvement, and enthusiasm to help at every stage was pivotal to the success of this Master's thesis. Moreover, the advice and expertise that you both afforded me over the last year has made the transition to engineering far less daunting.

In addition, I would like to extend special thanks to Prof. Marcel Jansen, Dr. Neil Coughlan, and Mr. Cian Redmond of the School of BEES for their contributions to this work. Their willingness to share their expertise of plant biology and work with duckweed, greatly enriched the quality and depth of this research. This interdisciplinary collaboration between the UCC's PCE and BEES departments was critical to the success of the project. Many thanks also to the wider DuckFeed team for their feedback and input throughout this past year.

I would also like to acknowledge Mr. Paul Conway (PCE) for his technical assistance during the project, particularly for his help in the construction of the growth systems. I really appreciated his astute perspective on both experimental setups, but also the next stages of the project. Furthermore, I want to extend my appreciation to my colleagues in the Postgraduate Office in PCE, particularly Mr. Vishal Kumar Singh for introducing me to Computational Fluid Dynamics (CFD) and offering invaluable advice on the software ANSYS.

Lastly, thank you to my family, and friends for the support I have received over the past year. I am incredibly grateful to you all. Again, thank you for being an integral part of this chapter in my academic journey.

Declaration

This is to certify that the work I am submitting is my own and has not been submitted for another degree, either at University College Cork or elsewhere. All external references and sources are clearly acknowledged and identified within the contents. I have read and understood the regulations of University College Cork concerning plagiarism and intellectual property.

Signature of the candidate: Grace O' Sullivan

Date: 05 January 2024

Table of Contents

List of Figures

List of Tables

Nomenclature

All abbreviations, scientific notation, and symbols from this Master's thesis can be found with their associated terminology in the tables below (units included where applicable).

Abbreviation	Terminology
BEES	Biological, Earth, and Environmental Sciences
CAP23	2023 Climate Action Plan
CFD	Computational Fluid Dynamics
COP28	28th Conference of the Parties
CORINE	Co-ORdinated INformation on the Environment
DAFM	Department of Agriculture, Food, and the Marine
EPA	Environmental Protection Agency
GHG	Greenhouse Gas Emissions
HRT	Hydraulic Retention Time (d)
IBC	Intermediate Bulk Container
IMTA	Integrated Multitrophic Aquaculture
IVF	Indoor Vertical Farm
PCE	Process and Chemical Engineering
P.I.	Principal Investigator
RGR	Relative Growth Rate (d^{-1})
TUD	Technical University Dublin
UCC	University College Cork

Symbol	Terminology
%	Percent
∇	Vector differential operator
ΔT	Number of days
°C	Degree Celsius
C(t)	Concentration curve
C_f	Final concentration (mol L^{-1})
C_i	Stock concentration (mol L^{-1})
d	Day
D_i	Inlet Hydraulic Diametre (m)
DW	Dry Weight
E(t)	Residence time distribution function
H	Height (m)
H_2O	Water
H_2SO_4	Sulfuric Acid

Symbol	Terminology
ha	Hectare
HCl	Hydrochloric Acid
hr	Hour
IVF	Indoor Vertical Farm
k	Turbulent kinetic energy
kW	Kilowatt
L	Length (m)
ln	Natural log
M	Molar Concentration
min	Minute
mol	Moles
mS	Milli Siemens
N	Nitrogen
n	Number
NH_4^+: NH_3	Ammonium: Ammonia
P	Phosphorus
p	Static pressure (Pa)
Pa	Pascal
Q	Volumetric flowrate ($m^3\ s^{-1}$)
Re	Reynolds Number
rpm	Revolutions per minute
s	Second
t	Tonnes
$\vec{v}$	Velocity vector ($m\ s^{-1}$)
v	Velocity ($m\ s^{-1}$)
V	Volume of aliquot / volume (m^3)
V_d	Dead volume (%)
V_f	Final volume (m^3)
Vmax	Maximum velocity ($m\ s^{-1}$)
W	Width (m)
W1	Initial biomass (g)
W2	Final biomass (g)
yr	Year
ϵ	Dissipation rate ($m^2\ s^{-3}$)
μ	Molecular viscosity (Pa s)
μ_d	Turbulent viscosity (Pa s)
ρ	Fluid density ($m^3\ kg^{-1}$)
ρg	Gravitational body force ($m\ s^{-2}$)
σ^2	Variance (s^2)
$\bar{\bar{\tau}}$	Stress tensor
τ_t	Theoretical residence time (s)
τ_m	Mean residence time (s)

1 Introduction

1.1 Background

In the face of unprecedented extreme weather, it is imperative that immediate actions are taken to address climate change. Navigating the landscape of climate breakdown is complex in nature, with the 28th Conference of the Parties (COP28) taking place in Dubai to serve as a convergence of nations in an attempt to mitigate and adapt to this global crisis. Endeavours are being made to limit the global temperature increase to 1.5°Celcius (C), but further action is required (Moosmann et. al., 2022). In a recent study published in Nature, Lamboll et al., (2023) have estimated that for a 50% chance of keeping global temperature rise to 1.5°C, the remaining carbon budget is equivalent to only 6 more years of CO_2 emissions at the current rate.

According to the 2018 Co-ORdinated INformation on the Environment (CORINE) landcover inventory, 67.6% of land use in Ireland is dedicated to agriculture (EPA, 2018). Agriculture is an intrinsic part of Irish society, but also serves as the greatest contributor to Irish Greenhouse Gas Emissions (GHG) depicted in Figure 1. Notably out of the 27 member states within the European Union (EU), Ireland has the largest agriculture emission contribution towards the national total emissions (EPA, 2023). A radical change is needed within the Irish agriculture sector to reduce GHG emissions and keep in line with global climate targets. According to the 2023 Climate Action Plan (CAP23), emissions in the Irish agriculture sector must be reduced by 25% by 2030 (Department of the Environment, Climate and Communications, 2022).

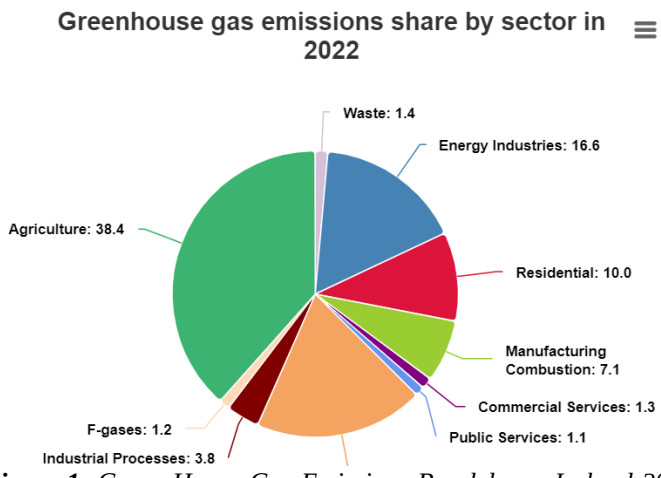

Figure 1: *Green House Gas Emissions Breakdown, Ireland 2022 (EPA, 2023)*

With global concerns around meeting climate targets heightening, laws are being introduced at both European and Irish levels to ensure all industries are meeting their targets. The Fifth Nitrates Action Programme 2022-2025 was published by the Irish

Government in March 2022. The goal of this programme is to strengthen current measures that serve to protect surface water and groundwater from nutrient pollution arising from agricultural sources (Department of Housing, Local Government, and Heritage, 2022).

Soiled water as defined by the Nitrates Directive is water from any farmyard areas "where such water is contaminated by contact with livestock faeces or urine, silage effluent, chemical fertilisers, or washings" (The Council of European Committees, 2008 as cited in Teagasc, 2021). To be described as 'soiled water', there must be a biological oxygen demand of less than 2500 m L^{-1} or less than 10 mg L^{-1} dry matter. Previously farmers had 10 days in December where the spreading of soiled water was prohibited. Now in 2023, that has increased to 21 days. In 2024, the spreading of soiled water will be prohibited for the entire month of December. This means that farmers will need access to 31 days soiled water storage capacity (The Department of Food, Agriculture, and the Marine, 2023). This will incur significant cost to farmers with no monetary gain. Solutions are needed to greatly reduce the emissions associated with Irish agriculture in its current state. There are many projects currently being funded by the Department of Agriculture, Food, and the Marine (DAFM) to reduce the negative environmental impact of the sector.

1.1.1 The Duck-Feed Project

Duck-Feed is a collaborative project between four different organisations, namely UCC, Teagasc, Technical University Dublin (TUD), and Devenish Nutrition Ltd. This research is funded by the DAFM to address key bottlenecks in the production, processing, use, and social acceptance of duckweed as a local, novel source of protein for Irish agriculture.

This project is led by Principal Investigator (P.I.) Professor Marcel Janssen of UCC and is made up of an interdisciplinary team of academics and industry professionals. The objective of Duck-Feed is to foster the expertise and experience required for the successful roll-out of duckweed cultivation across Ireland, in close collaboration with the agriculture industry. This requires the development of small-scale outdoor growth systems, consistent growth on agricultural waste streams, enhanced technology for protein extraction, feed quality assessments, process life

cycle assessments, and the assessment of social acceptance of duckweed as a protein source.

This project serves as one potentially useful intervention in the context of tightening laws surrounding nutrient spreading in Ireland. Duckweed can be utilised as a remediation tool for high-nutrient waste, while simultaneously producing a high value product.

Duck-Feed is a successor to earlier projects that focused on duckweed's role in the circular bioeconomy. BRAINWAVES was funded by the Ireland-Wales cooperation programme and NEWTRIENTS was funded by the Environmental Protection Agency (EPA), each of which provided key insights to duckweed's role as both a tool and an input for Irish agriculture.

1.1.2 Duckweed

1.1.2.1 The Plant

Duckweed (*Lemnaceae*) is a small aquatic plant that floats on top of water bodies. The Lemnaceae family consists of five genera: *Lemna*, *Landolitia*, *Wolffia*, *Wolffiella*, and *Spirodela* (Leng, 1999). Currently, thirty-six species across the genera have been identified worldwide. It is a highly resilient plant and has been found to grow in all geographical locations except for polar areas (Bhanthumnavin and McGarry, 1971).

Lemnaceae are exceptionally fast-growing and have reported doubling times of two to three days in outdoor systems (Said et al., 2009), and as little as 1.24 days when grown optimally indoors (Coughlan et al., 2022b). *Lemnaceae* biomass has high protein content, making up to 45% of its dried weight. This makes it an attractive biomass for both human and animal consumption (Coughlan et al., 2022b, Xu et al., 2021). It is a complete protein and contains all nine essential amino acids (Xu et al., 2021). The *Lemna Minor (L. minor)* species, also known as common duckweed, is native to Ireland (Paolacci et al., 2018), but is also widespread across the globe. The 36 species of duckweed, and their five genera can be seen in Figure 2.

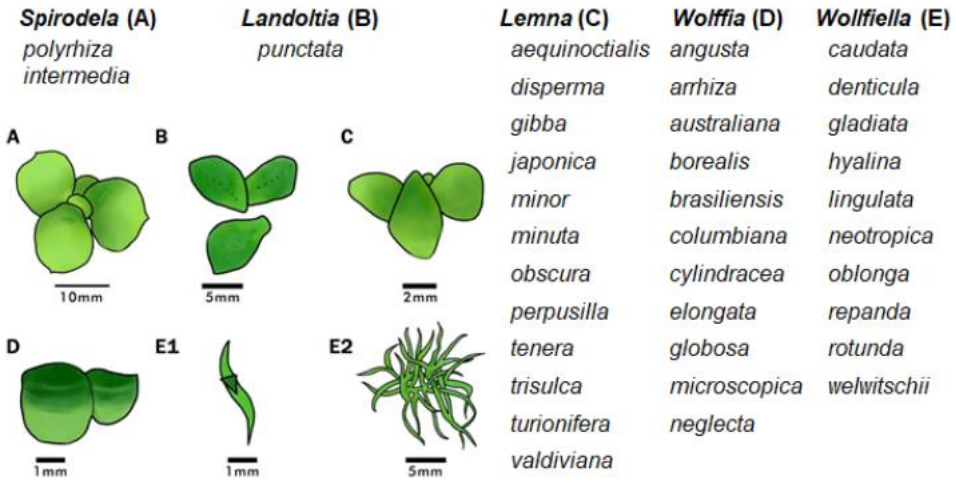

Figure 2: *Adapted from Zhou et al., (2023), the Lemnaceae plant family*

1.1.2.2 Duckweed Growth Factors

Duckweed is quite a robust plant that has been found in many different habitats. However, when looking at optimal growth conditions there are several key parameters to keep in mind. Temperature, pH, water depth, flow rate, wind, and nutrient concentration should all be considered when designing cultivation systems:

Temperature: Duckweed can grow at water temperatures of 6-33°C, with growth rates increasing with increasing temperature. However, once temperatures exceed 30°C, growth slows and eventually stops entirely due to plant stress (Leng, 1999). In Ireland, the optimal months for growing duckweed outdoors are April through September.

pH: The optimal pH range for duckweed growth is between 6.5-7.5, but duckweed can survive in the pH range of 5-9. Duckweed grows more readily at a lower pH due to the NH_4^+: NH_3 equilibrium. At lower pH, ammonia is predominantly present in the ionised form, at which nitrogen is readily absorbed by duckweed, resulting in increased growth rates. At higher pH levels, ammonia is the predominant form, which can be toxic (Leng, 1999). A recent study in Wales has shown that the acidification of nutrient-rich waste streams like dairy effluent using H_2SO_4, can not only increase the growth rates of *L. minor*, but also allows the species to grow at higher concentrations of effluent (Jones et al., 2023). This is particularly relevant in terms of duckweed's

remediation abilities. Decreasing the pH of the medium can also be achieved at a low cost.

Water Depth: Increased water depth can reduce nutrient mixing and diffusion, slowing the growth of duckweed. This also has implications for remediation capacity as the duckweed is inclined to assimilate nutrients closer to the surface. Therefore, increased depths over time can have a negative impact on nutrient removal abilities. For the treatment of wastewater, Zhao et, al., found water depths of 0.5 metres (m) to be optimal for both nutrient removal as well as duckweed growth (Zhao et al., 2014a). In both hotter and cooler climates, lower water depths can cause problems with temperature regulation. When looking at duckweed in a remediation capacity, harmony must be achieved between the surface area of the system and the total volume. An increased surface area to volume ratio can aid in the remediation (Leng, 1999).

Flow rate of Water: On indoor stacked systems, duckweed growth and remediation abilities were compared at flow rates of 0.5, 1.5, and 3.0 litres minute^{-1} (L min^{-1}), with medium depths of 25 millimetres (mm) and 50 mm. The optimal conditions for L. minor were a flow rate of 1.5 L min^{-1} at a water depth of 50 mm (Coughlan et al., 2022a). According to their findings, duckweed grew best when flow rates were low to minimise disturbance but high enough to promote nutrient mixing.

Wind Effect on Duckweed: Wind can have a very negative impact on duckweed growth, as it prevents the formation of duckweed mats, and can cause the plant to accumulate in sections of the surface water. This would impact both remediation but also growth yields. Floating rings can be employed to act as barriers for the duckweed as well as to provide wind shelter (Stejskal et al., 2022), but more permanent solutions should be considered when designing outdoor systems.

Impact of Mineral Concentrations: Nitrogen and phosphorus concentrations are critical factors in both growth rates and resulting protein content of the duckweed biomass. Reduced growth has been seen when phosphorus concentrations go below 0.017 mg L^{-1} and when total organic and ammonia nitrogen goes below 20 to 30 mg

L^{-1}. Going below this range also reduces the crude protein content of duckweed (Hassan et al., 2009). Using hydroponics growth medium, FloraGro and FloraMicro, duckweed was found to absorb nitrogen and phosphorus from the medium at approximately a rate of 500 and 50 milligrams metre^{-2} surface area day^{-1} (mg m^{-2} d^{-1}) respectively (Coughlan et al., 2023). This shows the importance of balancing nutrient concentration with the available surface area when looking at remediation solutions.

1.1.2.3 Duckweed as an Industrial Resource

Duckweed has been proven to serve as a multi-functional plant, benefitting a variety of industries. Key areas that are looked at below include human nutrition, animal feed, biofuel production, domestic wastewater treatment, agriculture, and aquaculture.

Human Nutrition: Duckweed is very tolerant of extreme weather conditions and grows well under harsh environmental conditions including limited nutrient availability, reduced light intensity, and temperature extremes (Femeena et al., 2023b). Its resilience to external environmental changes will be very important amidst the current climate breakdown. Weather patterns are becoming increasingly unsettled globally, which will affect food scarcity. Duckweed can be produced at a low environmental and economic cost. In the coming years, it may begin to replace less sustainable food types on the market.

Duckweed is a complete protein and contains all nine essential amino acids that are required for the growth and development of humans. *W. Globose* was found to contain vitamin B12, which is typically lacking from plant-based foods and needs to be supplemented in vegan diets (Xu et al., 2021). Duckweed has long been produced for human consumption in rural Asia and India (Bhanthumnavin and McGarry, 1971). Yahaya et al., completed metabolic analysis of *L. minor*, and *W. globosa.* They found that adding duckweed to food like ice cream greatly increased the nutritional value and deemed duckweed a good candidate for suitable food additive (Yahaya et al., 2022). Feed studies have also been undertaken in mice to compare duckweed protein with tradition casein for growth and development. Through the study it was deduced that the replacing 25% dietary casein with duckweed protein has no negative affect growth and development of mice (Roman et al., 2021).

Animal Feed: In Ireland there is a heavy reliance on imported soya and maize to supplement tillage as a feed for livestock. According to Crops 2030, Ireland's self-sufficiency for animal concentrate feeds was just 21% in 2018 (Teagasc, 2020). The replacement of soya and maize with a native feedstock could greatly reduce the GHG emissions associated with the agriculture sector. It would also greatly improve food security.

Due to its rich nutritional composition, duckweed has been used successfully as a form of animal feed. It could play a key role in revolutionising the Irish feed market, creating a more environmentally friendly option as a feedstock. In 2018, Sońta et al., (2018) found that due to duckweed accumulating toxic metals from the aquatic environment where it grew it may not be suitable as a sole feed for livestock. However, it was found that partially replacing soya with duckweed was beneficial. More studies are needed to fully understand the role duckweed could play as a livestock feed.

Biofuel Production: The use of duckweed as an energy source has many advantages. Its short doubling times, low cellulose content, and low environmental impact make it an attractive feedstock for the energy industry (Yang, 2022). Certain duckweed species Dry Weight (DW) has been found to contain 75.9% of starch. *L. punctata* has been investigated for its use as a feedstock for bioethanol production. With a conversion of 0.38 grams $gram^{-1}$ (g) it is a highly efficient process (Guo et al., 2023). This could be very suitable for duckweed that is not deemed suitable for human/animal consumption. Due to increased food insecurity, the ethics around using a food resource to generate biofuels can be problematic.

Other studies have also shown that altering the growth conditions of duckweed can increase starch accumulation, namely inducing plant stress. Increasing light intensity, lowering temperatures, and reduced nutrients have all been found to favour the production of starch (Cui and Cheng, 2015, Cui et al., 2011).

Domestic Wastewater: Duckweed is also being used as a form of domestic wastewater treatment, but it is not without limitations. In a non-optimal system, duckweed death can increase organic load in the tank, increase suspended solids, and the nutrient load can be too high for effective removal (Al- Hashimi and Joda, 2010). pH control, species selection, and system design were determined to be key

contributors to a successful system. Regarding system design, increasing hydraulic retention time and having shallower liquid depths greatly increased the success of duckweed in domestic wastewater treatment. Liquid depths of less than 50 cm and plug-flow conditions are most favourable. This was evaluated through influent and effluent concentration of 6 studies (Körner et al., 2003). Research by Chen et al., also found that the use of polycultures for wastewater treatment increased overall nutrient removal. The polyculture had a removal efficiency of 99.1% of total nitrogen compared with 95.6 to 98.8 % for the monocultures. Additionally, the polyculture had a removal efficiency of 90.8 % for total phosphorus, greater than 86.2 to 90.2 % for the monocultures (Chen et al., 2018).

Agriculture: Large amounts of nutrient-rich waste effluent are produced from agricultural activity every year. Swine and dairy waste are two of the biggest culprits, with discharge into waterways causing eutrophication in waterways, harming local ecosystems. Duckweed is being investigated as a low-cost, energy-efficient technology to deal with the wastewater produced by these intensive industries.

Beyers et al., (2023) undertook a life cycle assessment of the "tertiary treatment of liquid fraction pig manure", which focused on duckweed ponds as a final remediation step for the swine waste. Duckweed ponds were found to be less environmentally harmful than constructed wetlands or direct land application of the swine waste. However, concerns were raised over issues with potassium recycling and mineral loss. Another study focused on the impact of specific duckweed species on nutrient remediation and biomass production with swine wastewater. A mixture of *Landoltia punctata* OT, and *L. minor* OT was found to have increased nutrient recovery and greater biomass production than the monocultures of both species. Using a mixture of species also increased the starch and protein content in the resulting biomass (Zhao et al., 2014c). This method greatly increases the overall efficiency of the system and could be an attractive option for the treatment of agricultural waste streams.

In America, growing alfalfa using wastewater from the dairy industry is a common practice. A study was carried out comparing duckweed to alfalfa for both reduction of N and P loads, and spatial efficiency (Femeena et al., 2023a). The footprint of the duckweed cultivation systems could be 40% of that of the alfalfa land

cultivation, but still result in a reduction of "12.8% N and 9.2% P loads". Duckweed also offers another advantage, with an almost seven times increase in revenue than alfalfa because of the high protein content of the biomass.

For any type of processing technology using duckweed, strain selection should be undertaken to select the most important traits. Species with the highest relative growth rates usually have lower protein content and importantly, nutrient uptake rate tended to decrease in strains that had high biomass and protein contents (Walsh et al., 2022). This is particularly relevant in terms of wastewater remediation, as regulations will be in place for the treated water.

Aquaculture: Duckweed has been used on an industrial scale in tandem with aquaculture facilities. It is a low-cost solution to remediate aquaculture wastewater. These recirculating aquaculture systems use duckweed to prevent anoxia and fish death. A successful example of this was the site Mount Lucas in Co. Offaly, Ireland. The resulting effluent from four fishponds flowed through a sixteen-canal treatment system, with approximately 2 hectares (ha) of duckweed growth (Stejskal et al., 2022). Nutrient concentration studies at the site have shown that duckweed can sustain good water quality in a recirculated aquaculture system. Tests carried out to analyse the nutrient concentration of the wastewater pre and post-processing revealed that Lemnaceae removed '0.78 and 0.38 tonnes (t) year^{-1} (yr^{-1}) of total nitrogen and total phosphorus' (Paolacci et al., 2022a). As well as the remediation success, the site produced high yields of duckweed, of approximately 30 t yr^{-1} Dry Weight (DW) (Stejskal et al., 2022). The production of high-value biomass from a waste stream, with the added benefit of remediation makes this a very attractive option for aquaculture going forward.

1.1.3 The Role of Duckweed in the Circular Economy

The circular economy as stated by the European Parliament in 2023 is a "model of production and consumption" that extends the life cycle of products (European Parliament, 2023). This process involves minimising waste through the reuse, recycling, and repairing of materials. By doing so, the monetary value of the product is increased, and the negative environmental impact of the supply chain is reduced. The European Green Deal was set out in late 2019, with a focus on accelerating the

continent towards climate neutrality by 2050. The circular economy is central to the EU's transition towards sustainable growth within the Green Deal (Fetting, 2020).

This project involves two key pillars, the remediation of nutrient rich agricultural waste streams and the valorisation of duckweed as a high protein crop. Duckweed removes available nitrogen and phosphorus through a surface absorption process. It floats on a water body, and takes up the nutrients it requires for growth, cleaning the water (Leng, 1999). This can be employed for agricultural waste streams like run-off from a dairy parlour (Jones et al., 2023). It is a nutrient rich source that is often discarded. Due to duckweed multiplying every two to three days, in the right environment it can be used to efficiently remediate nutrients from the wastewater. The duckweed crop can then be used to provide a protein rich feed for the animals (Demann et al., 2022). This regeneration of value from the waste stream is key to creating a circular process within Irish agriculture.

1.2 Research Aims and Objectives

The primary objective of this thesis is the design, construction, and testing of a pilot-scale system and the design of a medium-scale optimised system for duckweed production. The resulting design must be suitable for use in farmyard conditions. The overarching theme of the thesis is the circular bioeconomy and is part of the DAFM funded project Duck-Feed. This work has been informed by literature, interdisciplinary academic knowledge, and close collaboration with stakeholders. The outcome of this work will aid in the promotion of duckweed as a solution to Irish farmers. Duckweed has the potential to clean wastewater produced on farms and produce a high value protein crop.

The goal of this thesis encompasses several specific objectives, each contributing to the achievement of an optimal design for the duckweed cultivation systems as well as an assessment of duckweed growth in a variety of operating conditions in such systems:

- An extensive literature review focused on the design of duckweed cultivation systems. Following this survey, it was evident that there was no comparative system design analysis for optimal duckweed production. Typically, in the western hemisphere large scale 'raceway' designs were found to be favoured, while simple ponds were the common choice in Asia. The design aspects will be further discussed in Section *2.3*.
- The design and construction of three pilot-scale systems. These were used to analyse the effect of hydrodynamics on relative growth rate and nutrient remediation ability of duckweed. The three systems compared were a stagnant tank, a tank with recirculated flow, and a tank with baffles that had recirculated flow. This was to cover all scenarios presented individually in literature. Section *3.2* has further information on the construction of the growth systems.
- Basic testing of the pilot systems. This included tracer response experiments for mixing and residence time. It also involved looking at duckweed growth within the systems and comparing them for relative growth rate and nutrient remediation. The results are highlighted in Section *4.3* and *4.4* respectively.
- CFD Modelling using ANSYS Fluent® software. Models were constructed using ANSYS Spaceclaim for both the system with baffles and system without

baffles, which can be found in Section *3.1.2.* This provides key insights on mixing, dead zones, and surface velocities.

- Validation of the CFD model simulations using transient models and the tracer response experiments, Section *4.2.1*.
- Design of the medium-scale outdoor system for the next phase of the project, Section *4.5.*
- Integration of plant biology and engineering. Liaise closely with project partners in BEES to have a plant biology informed approach to the experimental design, Section *3.3*.

Through the successful completion of these objectives, this thesis endeavours to contribute invaluable insights into the future design and construction of duckweed growth systems. This work will encourage and foster the development and use of duckweed as a tool for Irish agriculture and the circular economy.

1.3 Structure of Thesis

The thesis consists of five chapters and five appendices.

This first chapter, Chapter One, provides an outline of the Master's thesis and the structural layout. It includes background information on the Duck-Feed project, as well as the premise for this research.

Chapter Two contains a literature review on duckweed growth systems, highlighting the need for research on the difference between pond and raceway style systems.

Chapter Three provides the methodologies used throughout this research project.

Chapter Four offers a discussion and critical analysis of the results.

The thesis concludes with Chapter Five, where recommendations for future work are provided.

2 Literature Review

A review of system design for duckweed cultivation systems.

2.1 Introduction

Duckweed cultivation has been an integral part of human society for over two millennia. Sources have revealed that duckweed played a key role in ancient rituals and was also used in ancient medicinal practices (Edelman et al., 2022). In recent years, the cultivation of duckweed has garnered increasing attention due to global environmental and agricultural challenges. Crippa et al., (2021) had an article published by Nature which highlighted that one third of global GHG emissions are linked to food-systems, namely food production, food consumption, and food waste. Food-systems need to radically adapt in order to reduce the environmental impact of this sector. Duckweed production provides one potential intervention which can mitigate the GHG emissions of this sector. In south-east Asia, duckweed is already commonly found in the human diet (de Beukelaar et al., 2019). It contains all nine essential amino acids, and its dry weight consists of up to 30% protein (Appenroth et al., 2017). Alongside its potential in nutritional value, ongoing research is focusing on duckweed as a feedstock for biofuel production. Its high starch content is suitable for bioethanol production by fermentation (Faizal et al., 2021). Another common industrial use of duckweed is its phytoremediation ability. It can remove excess nutrients and pollutants from waterways (Liu et al., 2021). Therefore, duckweed will play a multi-functional role as the world adapts towards more sustainable technologies.

With heightened interest in the plant and its cultivation, optimising the design of growth systems must be a priority. This review aims to provide a comprehensive overview of the current research and intelligence surrounding system design for duckweed cultivation. Understanding the optimal design for these systems is key to increasing their productivity, feasibility, and efficiency. This review will positively contribute to the current discourse on innovative and sustainable cultivation practices.

The primary objective of this review is to collate the distinct styles for duckweed cultivation systems documented in literature. This undertaking is motivated by a noticeable gap in the literature, with limited research conducted on a laboratory

scale. There are no comparative studies that have been carried out at a large scale. The absence of clear information on optimal system design places future cultivation endeavours at a disadvantage. Consequently, this review will serve as a valuable resource for both current design considerations and future work in this field. The research question guiding this review is the effect of system design for duckweed cultivation systems. The methodology involved a detailed search strategy, screening process, paper selection, with the results being grouped by system type.

2.2 Methodology

For the selection of papers, the inclusion criteria focused on system design, residence time, and mixing with the system. If a paper did not mention any of the above, it was not selected. This is due to the research question being focused on design consideration rather than plant biology, microbiology, and genetic engineering.

The databased used for this review were Scopus, PubMed, and Web of Science. The primary searches were "duckweed bioreactor", "duckweed system", "duckweed agriculture", "*lemna* bioreactor", "*lemna* system", and "*lemna* agriculture". The secondary searches were "duckweed bioreactor AND outdoor", "duckweed system AND outdoor", "*lemna* bioreactor AND outdoor", and *lemna* system AND outdoor". Figure 3 contains a flow diagram of the search strategy (BMJ, 2021).

A total of 6300 records were generated through the primary and secondary searches. After the duplicates were removed, 2593 remained for screening. The records were first screened by title, followed by abstract analysis. After this 2539 were removed. 28 papers could not be accessed as they were behind a paywall. 26 papers were read in full, after which 16 were excluded. Details of exclusion criteria can be found in Figure 3. Ten papers are included in the review.

2.2.1 PRISMA Flow Diagram of Search Strategy

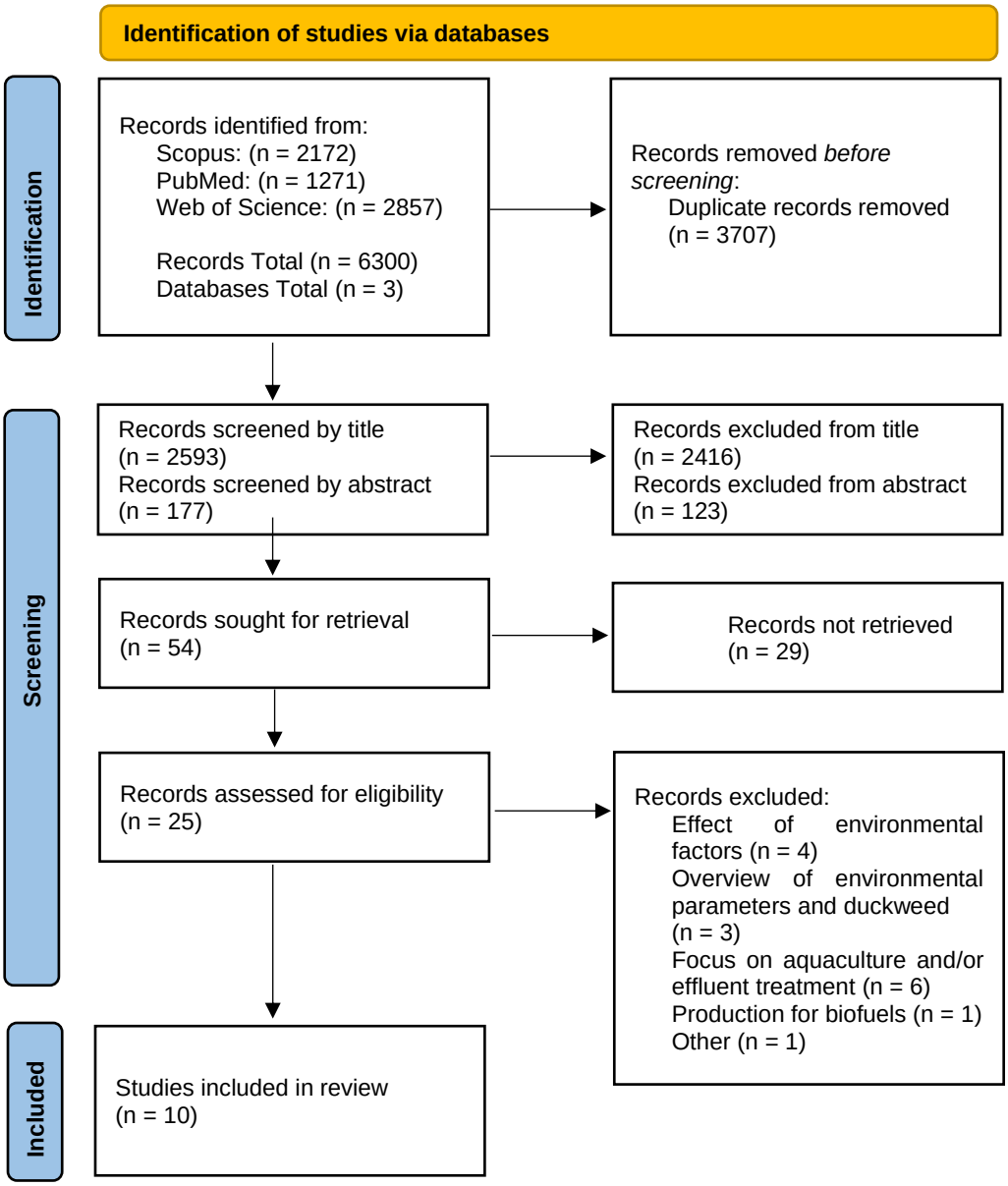

Figure 3: *Adapted from the PRISMA 2020 flow diagram for search strategy of databases (BMJ, 2021)*

2.3 Results

Following an extensive search of literature pertaining to duckweed cultivation and system design, ten papers were selected for analysis. This review focuses on both indoor and outdoor systems for ducked production. Additionally, it references the positive impact of pretreatment steps on the growth rate of duckweed.

2.3.1 Indoor Systems for Duckweed Cultivation

Due to the nature of indoor cultivation systems, they provide a means of duckweed production that is not weather-dependent. This is particularly advantageous for countries that have a short season that is suitable for outdoor cultivation. Indoor cultivation provides many benefits including controlled light intensity, spectrum, photoperiod, and temperature (Petersen et al., 2022a). Moreover, cultivation indoors using tiered systems decreases the footprint of the system while increasing the surface area for duckweed growth (Coughlan et al., 2022b). These factors enhance the economic viability of indoor duckweed systems.

2.3.1.1 Tiered Systems (Vertical Farms)

Indoor stacked systems for duckweed cultivation provide a new method for duckweed cultivation, having only recently been described in detail in literature. It improves the efficiency of land usage dramatically. Hydroponics have been used in other industries for growing crops including tomatoes. Duckweed has the potential to utilise this method. Indoor systems offer complete control over the environmental conditions so it can be used to the advantage of the grower. These are closed-loop systems which involve the recirculation of media and demonstrate remarkable water and fertiliser conservation. Notably it can prevent loses "of up to 90% of irrigation water and 85% of fertilisers" (Petersen et al., 2022b, Rosa-Rodríguez et al., 2020).

A study published in 2022 focused on the effect of flow rate and depth on the Relative Growth Rate (RGR) of *L. minor* and nutrient removal from a tiered indoor system (Coughlan et al., 2022a). It consists of five trays that are vertically stacked, each with a surface area of 0.295 m^2. Combined, the system had 1.48 m^2 for plant growth. The nutrient medium was pumped from a sump tank to the top tray, and the remaining trays were gravity fed. This kept the medium in constant recirculation. A

photoperiod of 16:8 h (light: dark) and light intensity of 150 μmoles metre^{-2} second^{-1} (μmol m^{-2} s^{-1}) were applied.

Six scenarios were investigated, with three flow rates and two liquid depths. The details can be found in Table 1 and shows the resulting system velocities. The run time was seven days. The RGR was calculated from days 0-3, and day 3-7. A mean value was then determined. From the experiments it was found that duckweed growth was best at the intermediate flow rate of 1.5 L min^{-1} with a liquid depth of 5 cm. This resulted in a RGR of 0.13 d^{-1}. This allowed for adequate nutrient mixing without too much disturbance to the duckweed. No details of the production rate of duckweed or protein % was provided (Coughlan et al., 2022a).

Table 1: *Adapted from (Coughlan et al., 2022a) detailing the experimental setup*

Experimental Setup	Flow rate (Lm^{-1})	Liquid Depth (cm)	Velocity (ms^{-1})
1	0.5	2.5	0.0008
2	1.5	2.5	0.0024
3	3	2.5	0.0048
4	0.5	5	0.0004
5	1.5	5	0.0012
6	3	5	0.0024

Petersen et al., (2022b) also investigated the use of indoor stacked systems for *L. minor* cultivation, calling it an Indoor Vertical Frgr

arm (IVF). This IVF had nine vertically stacked basins, each 195 cm x 145 cm x 10 cm, and a sump tank which can be seen in Figure 4. A liquid height of 5 cm was used. The total surface area for duckweed growth was 25.5 m^2. This cultivation system ran for a period of forty days. A photoperiod of 12:12 h was maintained, with a light intensity of 105 μmol m^{-2} s^{-1}. The maximum flow rate of the medium recirculating in the system was 10 L min^{-1}. Harvesting was carried out at irregular intervals. When the duckweed fronds were visually overlapping, the duckweed was harvested. After harvesting the system was always restored to 80% surface area coverage.

Based on the 40-day growth period the following data was extrapolated. The system had the potential to provide dry biomass at a rate of 7.54 t yr^{-1} ha^{-1} DW,

equivalent to 2.07 g m^{-2} d^{-1}. Additionally, the biomass produced was of high quality and contained 32% crude protein.

Figure 4: *Vertical stacked system for duckweed cultivation in use (Petersen et al., 2022)*

2.3.2 Semi-Outdoor Systems for Duckweed Cultivation

Ruekaewma et al., (2015) explored the effect of different styles of production systems on growth production of *W. globosa* in small semi-outdoor systems in Thailand. This is one of the few studies published that compared the effects of different agitation methods on duckweed growth. Five distinct systems were trialed (Table 2), and these are depicted in Figure 5. Each system consisted of a black plastic tank with a surface area of 0.152 m^2 for duckweed growth and were 0.4 m in height.

The experiments were run outdoors but were covered by a plastic roof to avoid interference from the rain. A medium depth of 0.3 m was used, with the water topped up regularly to compensate for evaporation. The total cultivation time was twenty-one days. The production rate for each system is detailed in Table 2. The system with horizontal surface agitation had the greatest yield with a production rate of 1.52 ± 0.04 g m^{-2} d^{-1} DW. After proximate analysis it was found to contain 48.2% protein (Ruekaewma et al., 2015).

Table 2: *Each of the five culture systems and their mechanisms, adapted from the text (Ruekaewma et al., 2015)*

System Type	Method	Production Rate ($g\ m^{-2}\ d^{-1}$) DW
static culture	no circulation	0.94 ± 0.04
vertical aeration culture	400 L $hour^{-1}$ (hr) vertical flow created using an air stone	0.96 ± 0.27
horizontal surface agitation	paddle wheel at 3500 revolutions per minute (rpm)	1.52 ± 0.04
top water spraying system	900 L hr^{-1} top spraying with water from the bottom of the system	1.18 ± 0.17
layer culture system with top water spraying	same top water spraying but plankton net placed over water surface	0.86 ± 0.09

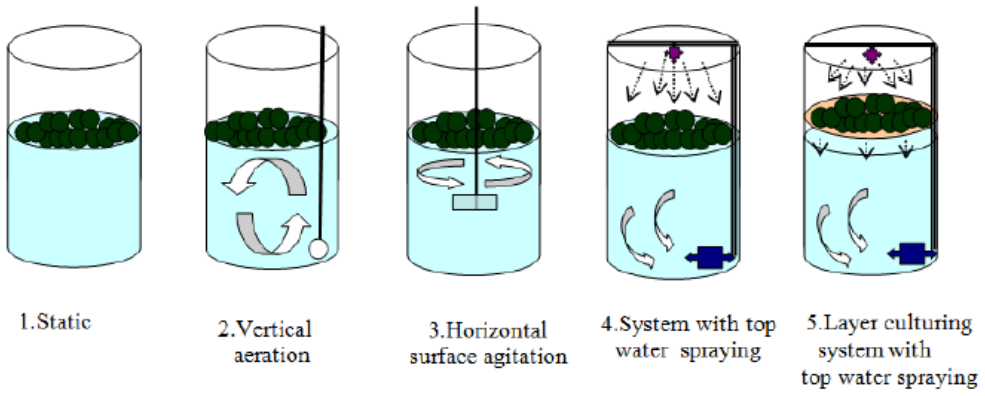

Figure 5*: The different growth systems for W. globosa (Ruekaewma et al., 2015)*

2.3.3 Outdoor Cultivation Systems

Unlike indoor cultivation of duckweed, outdoor systems are not in controlled environments. The growing season differs in each country depending on the climate. As discussed in Section *1.1.2*, duckweed growth is dependent on temperature, and wind. Despite this, there are many successful examples of outdoor duckweed cultivation globally. This review looks at a variety of outdoor systems based in Ireland, Belgium, China, and Brazil. The outdoor cultivation of duckweed in Europe is limited by the climate. The typical production rate is estimated to be between 7 and 22 t ha^{-1} yr^{-1} (Landolt and Kandeler, 1987, Devlamynck et al., 2021a) for realistic less than

optimal conditions. However, under optimal conditions, it can reach yields of 73 t ha^{-1} yr^{-1} (Leng, 1999, Landolt and Kandeler, 1987). This demonstrates the commercial potential of duckweed regardless of geographical location. Limited literature was found on the comparison of outdoor systems for duckweed production. This section of the review will focus on raceways, tanks, ponds, and cascading systems.

2.3.3.1 Raceways

Stejskal et al., (2022) examined the use of an Integrated MultiTrivf

ophic Aquaculture (IMTA) system in Co. Offaly, Ireland. It was a self-contained system that allowed for the production of perch and trout while using duckweed to control the water quality. It involved a mixed culture of *L. gibba* and *L. minor*. The system utilised a cutaway bog that was previously used for peat harvesting. The water surface area available for duckweed growth was 10,901 m^2, approximately 1 ha. This was divided into sixteen channels, 8 m in width and 16 m in length which created a raceway shape that can be seen in Figure 6. There was variation in water depth in the channels, but it remained between 0.5 m and 0.8 m. They utilised floating foam rings to provide wind shelter, while also reducing movement of the duckweed mat. It was a recirculated system and fluid flow through the system was maintained by four paddlewheels, two at the outflow point and two at the inflow point. Notably, the system was powered by a wind turbine and unused peat from the old bog. The maximum surface velocity recorded was next to the paddlewheels, 0.16 m s^{-1}. However, the mean surface velocity was 0.022 m s^{-1}.

The system produced in excess of 30 t of duckweed biomass (dry weight), 30 t $year^{-1}$ ha^{-1} DW, which is the equivalent to an average production rate of 8.2 g m^{-2} d^{-1} DW (Stejskal et al., 2022). This shows the capability of an outdoor system in an Irish climate to produce satisfactory yields of duckweed.

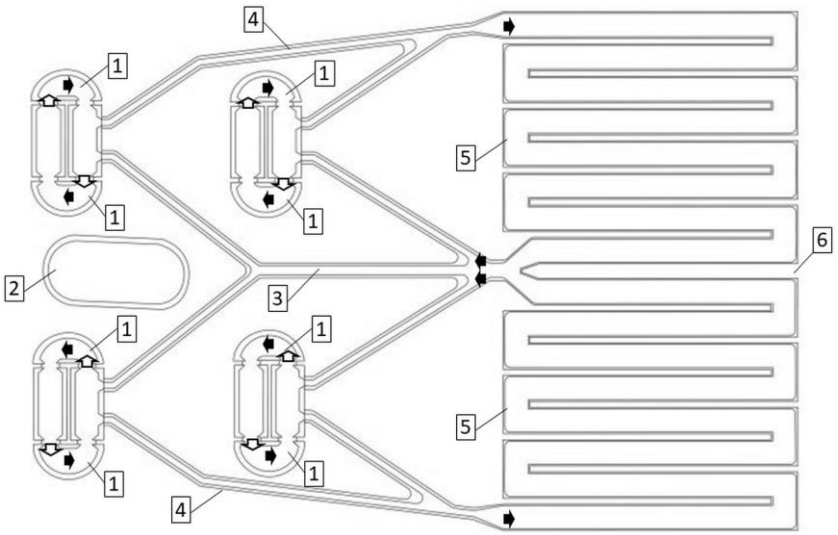

Figure 6: *Schematic of the system taken from (Stejskal et al., 2022). The black arrows note the location of paddlewheels, while the open arrows are airlifts.*

A second paper published about the same site focused on biomass production and nutrient removal (Paolacci et al., 2022b). During the summer a biomass production experiment was carried out over the course of five weeks. In this period of optimal growth conditions, the site was found to produce 19.22 g m^{-2} d^{-1}. This was significantly higher than the average production rate. The growing period is quite short in Ireland. After analysis, the duckweed biomass produced was found to have a protein content of 21.84 ± 2.45% (Paolacci et al., 2022b).

2.3.3.2 Tanks

The effects of operation parameters on nutrient removal from wastewater and high-protein biomass production in a duckweed-based (*Lemma aequinoctialis*) pilot-scale system Zhao et al., (2014b) were examined in China. The effect of water depth, coverage rate, and harvest regime were all considered. *L. aequinoctialis*, a local duckweed species, was selected for the experiments. This involved 12 individual systems, the details of which can be found in Table 3. Each had dimensions of (24 m x 0.5 m x 0.6 m) and were 12 m^2.

To prevent wind disturbance to the duckweed, the surface of each basin was divided in two by a partition. The experiments lasted a period of 84 days. On day 0, each tank was filled with local lake water. From day 1, 1 m^3 of wastewater was added to each system daily via a submersible pump at a flow rate of 0.00014 m^3 s^{-1}. The optimal conditions were determined to be a coverage rate of 150%, a medium depth

of 50 cm, and a harvest regime of 4 days. Under these conditions, production rates of 6.65 g m^{-2} d^{-1} DW were achieved. The duckweed was found to contain 36.16% crude protein (Zhao et al., 2014b).

Table 3: *Experimental parameters of each duckweed basin, adapted from (Zhao et al., 2014)*

Experiment	Water Depth (cm)	Coverage Rate %	Harvest Regime (d)	Volume (m^3)	Turbulent kinetic (d)
1	20	150	4	2.4	2.4
2	30	150	4	3.6	3.6
3	40	150	4	4.8	4.8
4	50	150	4	6	6
5	50	75	4	6	6
6	50	150	4	6	6
7	50	225	4	6	6
8	50	300	4	6	6
9	50	150	2	6	6
10	50	150	4	6	6
11	50	150	6	6	6
12	50	150	8	6	6

2.3.3.3 Ponds

A study was published in 2012 evaluating the efficiency of duckweed ponds for nutrient removal and biomass production using swine waste. This work was completed in Brazil, and native species *L. punctata* was chosen. Two ponds were constructed DP1 and DP2, and their dimensions were 20.5 x 7.5 x 0.8 m, and 15 x 6.0 x 0.4 m respectively. Both ponds were initially filled with rain and river water. The design can be seen in Figure 7. Low concentrations of swine waste were pretreated using a biodigester, this waste was then held in a storage pond. The effluent was applied in batches, so that 1 m^3 d^{-1} entered DP1 for each 15-day batch. DP2 was supplied with nutrients from DP1 by gravity. Each pond was inoculated with a fresh weight of 220 g m^{-2} of duckweed. To combat the impact of wind on duckweed growth, bamboo dividers were used and left to float on the surface of the ponds. Duckweed

was harvested every two days. DP1 had a biomass production of 18 g m^{-2} d^{-1} DW, and a crude protein of 35%. The biomass production rate of DP2 was 8.3 g m^{-2} d^{-1} DW, and the crude protein was 28%. The lower yield and protein of 28% can be explained by the lower nutrient concentration of DP2 (Mohedano et al., 2012).

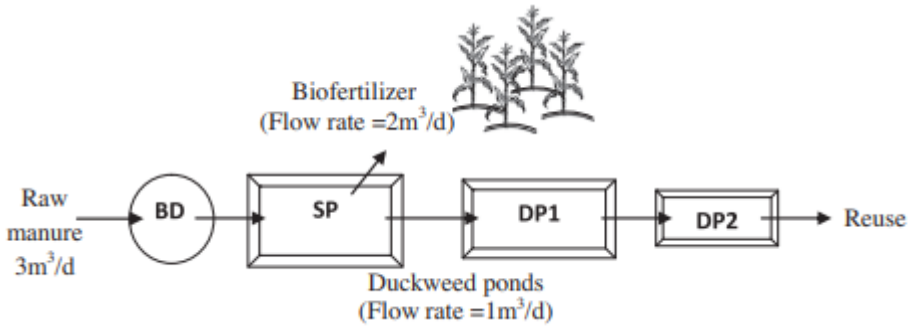

Figure 7: *Experimental design taken from (Mohedano et al., 2012). BD = Biodigester; SP = Storage Pond; DP1 and DP2 = Duckweed ponds 1 and 2*

2.3.3.4 Cascading Systems

Devlamynck et al., (2021a) investigated the use of a cascading system for the production of *L. minor* using swine manure. The experiments were carried out in Belgium, beginning on the 28th of August, for a period of 55 days. The experimental setup can be seen in Figure 8. Each cascade used three Intermediate Bulk Cimtaontainers (IBCs). The IBCs used for cultivation and for effluent had an area of 0.9 x 1.1 m removed to expose the surface. The nutrient medium used at the beginning in the influent and cultivation IBCs contained rainwater, biological effluent, and the liquid fraction of pic manure. The system was set up so that 800 L of media from the influent IBC would be pumped into the cultivation IBC with a dosing pump. This would replenish nutrients taken up by the duckweed. The effluent IBC would be filled from the cultivation IBC using an overflow mechanism. Every 7 days, the duckweed was harvested, and the cultivation tank would be inoculated with 500 g of fresh weight again. The average growth rate experienced in the system was 4.5 ± 1.7 g m^{-2} d^{-1} DW, with an average protein content of 35 ± 2%.

Figure 8: *Experimental setup from (Devlamynck et al., 2021a). The IBC on the left is used for storage and mixing of the influent. It is pumped into the middle IBC where duckweed is cultivated. The lower IBC is filled with effluent by an overflow mechanism*

Devlamynck et al., (2021b) also carried out a second cascading style cultivation experiment in April 2018. Three pilot-scale systems were used, Figure 9 depicts the setup of one of these systems. Like the previous experiment there is an influent tank and an effluent tank, but this system contains three cultivation tanks that are fed by an overflow cascade. On day 0 the tanks were filled with rainwater. Each subsequent day, wastewater was pumped from the influent tank to cultivation tank B.1 by a flow pump. B.2, and B.3 were fed by the overflow mechanism. Each system had a different nutrient medium: aquaculture effluent, swine wastewater, and a synthetic medium.

The system with swine waste had the highest growth productivity of 6.1 ± 2.5 g m^{-2} d^{-1}, with aquaculture and synthetic medium being significantly lower, 5.2 ± 1.7 and 4.7 ± 1.7 g m^{-2} d^{-1} DW respectively. The protein content of the duckweed produce in synthetic medium was the highest at 35%, with swine and aquaculture containing 32% and 29% respectively (Devlamynck et al., 2021b).

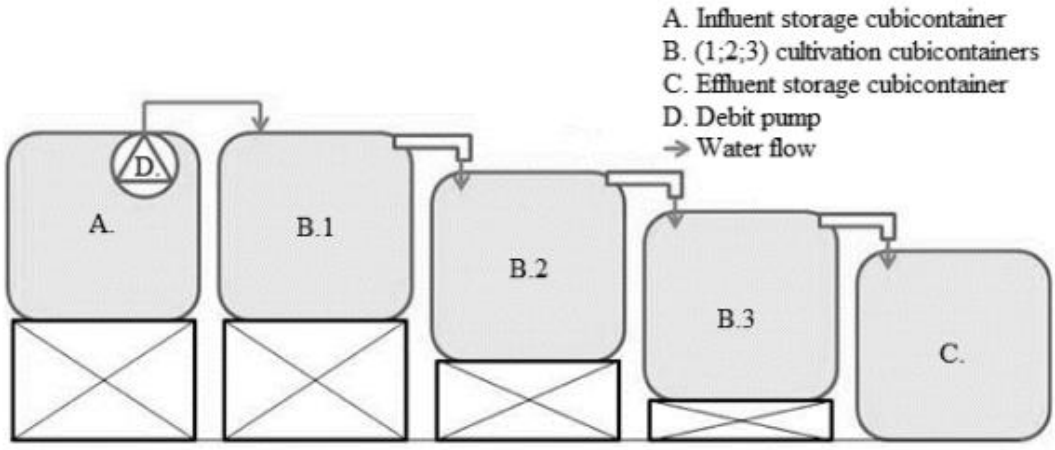

Figure 9*: Experimental setup of the cultivation system (Devlamynck et al., 2021b)*

2.3.4 Effect of Design on Protein Production

A recently published comparative study from Thailand, aimed to investigate the effect of different aquaculture conditions on the nutritional quality of *W. arrhiza* biomass. Thirteen different systems, and one control were compared for their protein content after cultivation. The details of each can be found in Table 4. Each vertical tray (Systems 1-5 and 7-9) was 0.9 x 1.0 x 0.4 m in dimension. For System 6, a cylindrical horizontal system was used. This had a propeller and had a volume of 0.01 m^3. Systems 10-13 were a cement pond, 1.0 x 0.4 x 0.4 m in dimension. The commercial control was shop bought duckweed. After each sample, it was concluded that the outdoor pond with hydroponics and an electrical conductivity of 0.5 milli Siemens (mS) cm^{-1} was the optimal environment for protein production. The sample contained 41.91 ± 3.40% (Prosridee et al., 2023). No details on the production rate of duckweed in each system were provided.

Table 4: *Summary of experimental design from (Prosridee et al., 2023)*

System	Location	Type	Method	Light Intensity (µmol m^{-2} s^{-1})	Electrical Conductivity (mS cm^{-1})
1	indoor	vertical tray	fluorescent white LEDs	200	-
2	indoor	vertical tray	white LED light	250	-
3	indoor	vertical tray	white LED light	200	-
4	indoor	vertical tray	blue + red LED light	200	-
5	indoor	vertical tray	white + blue + red LEDs	200	-
6	indoor	horizontal stirrer	concentration light	200 - 600	-
7	indoor	vertical tray	water supply	-	-
8	outdoor	vertical tray	hydroponics	-	0.5
9	outdoor	vertical tray	reverse osmosis water	-	-
10	outdoor	cement pond	pig manure	-	-
11	outdoor	cement pond	chemical fertiliser	-	-
12	outdoor	cement pond	hydroponics	-	0.5
13	outdoor	cement pond	hydroponics	-	1
14	n/a	commercial sample	n/a	-	-

2.3.5 Pretreatment Steps for Enhancing Growth Rate

For the design of an optimal system for duckweed production, it is important to consider pretreatment steps that would improve the growth rate of the plant. In a study lead by Ma et al., it was found that the pre-aeration of influent waste promotes nutrient removal in a pilot-scale duckweed-based pond by influencing the duckweed growth and bacterial community (Ma et al., 2023). This work directly examined the effects of pre-aeration using two parallel systems in China. It involved two pilot-scale 12 m^2 ponds, one received pre-aerated wastewater (Pond 1), and one did not (Pond 2). The dimensions for each were 24 m x 0.5 m x 1.7 m.

The systems were run for 268 days from March to November. It was a semi-continuous setup and had a hydraulic retention time (HRT) of 6 days. On day 0, mixed wastewater was added to both ponds to achieve a water depth of 0.5 m. Each pond was inoculated with 550 g fresh duckweed m^{-2}. Every two days, 2 m^3 of mixed wastewater was pumped into the ponds, and 2 m^3 of pondwater was removed. This ensured the liquid depth remained the same. Before any wastewater was added to Pond 1, it was aerated in a pre-aeration pond for two hours. This was achieved using a 0.75 kilo Watt (kW) submerged aerator. The wastewater was added directly to Pond 2 with no aeration. Duckweed was harvested every four days to maintain a density of 550 g fresh duckweed m^{-2}. Pond 1 had a production rate of 9.2 g m^{-2} d^{-1} and a crude protein of 33.18%. Pond 2 had a production rate of 6.88 g m^{-2} d^{-1} and a crude protein of 32.88%. Pre-aeration was found to increase the growth rate of duckweed by 33% but had no significant effect on protein content (Ma et al., 2023).

2.3.6 Summary of Findings

2.3.6.1 Indoor Systems

Table 5: *Summary of Indoor Systems*

Reference	System Type	Species	Surface Area (m^2)	Light Intensity (μ mol m^{-2})	Photoperiod (h)	Depth (m)	Flow rate (L min^{-1})	Growth Rate (DW) (g m^{-2} d^{-1})	Crude Protein (%)
(Coughlan et al., 2022a)	IVF	*L. minor*	1.48	150	16:08	0.05	1.5	not stated	not stated
(Petersen et al., 2022b)	IVF	*L. minor*	25.5	105	12:12	0.05	10	2.07	32
(Prosridee et al., 2023)	vertical tray	*W. arrhiza*	0.9	200 (LED white)	not stated	0.4	0	not stated	49.3 ± 0.4
(Prosridee et al., 2023)	vertical tray	*W. arrhiza*	0.9	250 (LED white)	not stated	0.4	0	not stated	51.7 ± 0.5
(Prosridee et al., 2023)	vertical tray with horizontal stirrer	*W. arrhiza*	0.9	200 - 600	not stated	0.4	not stated	not stated	54.9 ± 0.7
(Prosridee et al., 2023)	vertical tray	*W. arrhiza*	0.9	no light	not stated	0.4	0	not stated	15.9 ± 0.9

2.3.6.2 Indoor Systems

Table 6: *Summary of Semi-Outdoor Systems*

Reference	System Type	Species	Nutrient Medium	Surface Area (m^2)	Depth (m)	Flow rate (L hr^{-1})	Growth Rate (g m^{-2} d^{-1})	Crude Protein (%)
(Ruekaewma et al., 2015)	Static Culture	*W. globosa*	Hutner's	0.152	0.3	0	0.94 ± 0.04	not stated
(Ruekaewma et al., 2015)	Vertical Aeration	W. globosa	Hutner's	0.152	0.3	400	0.96 ± 0.27	not stated
(Ruekaewma et al., 2015)	Horizontal Surface Agitation	W. globosa	Hutner's	0.152	0.3	not stated	1.52 ± 0.04	48.2
(Ruekaewma et al., 2015)	Top Water Spraying System	W. globosa	Hutner's	0.152	0.3	900	1.18 ± 0.17	not stated
(Ruekaewma et al., 2015)	Layer culture system with top water spraying	W. globosa	Hutner's	0.152	0.3	900	0.86 ± 0.09	not stated

2.3.6.3 Outdoor Systems

Table 7: *Summary of Outdoor Systems*

Reference	System Type	Species	Nutrient Medium	Surface Area (m^2)	Wind Protection	Flow rate ($L\ hr^{-1}$)	Growth Rate ($g\ m^{-2}\ d^{-1}$)	Crude Protein (%)
(Stejskal et al., 2022)	IMTA Raceway	*L. minor* + *L. gibba*	Aquaculture Effluent	10901	Foam Rings	not stated	8.2	21.84 ± 2.45
(Zhao et al., 2014b)	Tanks	*L. aequinoctialis*	Wastewater	12	Divided Tank with Partition	8.4	6.65	36.16
(Mohedano et al., 2012)	Ponds	*L. punctata*	Biodigested Swine Waste	DP1: 154	Bamboo Dividers	0.69	18	35
(Mohedano et al., 2012)	Ponds	*L. punctata*	Biodigested Swine Waste	DP2: 90	Bamboo Dividers	gravity fed	8.3	28
(Devlamynck et al., 2021a)	Cascading IBC System	*L. minor*	Biological effluent + pig manure	not stated	not stated	4.8 + gravity fed	4.5 ± 1.7	35 ± 2
(Devlamynck et al., 2021b)	Cascading IBC System	*L. minor*	Swine waste	not stated	not stated	4.8 + gravity fed	6.1 ± 2.5	32
(Prosridee et al., 2023)	vertical tray	*W. arrhiza*	Hydroponics	0.9	not stated	0	not stated	43.9 ± 0.6
(Prosridee et al., 2023)	vertical tray	*W. arrhiza*	Reverse osmosis water	0.9	not stated	0	not stated	25.5 ± 0.5

Reference	System Type	Species	Nutrient Medium	Surface Area (m^2)	Wind Protection	Flow rate (L hr^{-1})	Growth Rate (g m^{-2} d^{-1})	Crude Protein (%)
(Prosridee et al., 2023)	cement pond	*W. arrhiza*	Pig manure	0.4	not stated	not stated	not stated	61.7 ± 1
(Prosridee et al., 2023)	cement pond	*W. arrhiza*	Chemical Fertiliser	0.4	not stated	not stated	not stated	45.5 ± 0.5
(Prosridee et al., 2023)	cement pond	*W. arrhiza*	Hydroponics (1 mS cm-1)	0.4	not stated	not stated	not stated	49.1 ± 0.3

2.3.6.4 Effect of Pretreatment on Duckweed Cultivation

***Table 8**: Effect of Pretreatment on Production rates of Duckweed*

Reference	System Type	Species	Nutrient Medium	Surface Area (m^2)	Wind Protection	Flow rate (L hr^{-1})	Growth Rate (g m^{-2} d^{-1})	Crude Protein (%)
(Ma et al., 2023).	Pond 1	not stated	Aerated wastewater	12	not stated	42	9.2	33.18
(Ma et al., 2023).	Pond 2	not stated	wastewater (not aerated)	12	not stated	42	6.88	32.88

2.4 Discussion and Future Implications

This review of duckweed cultivation systems encompasses both indoor and outdoor approaches in production methods. It revealed a nuanced understanding on the influence of design on the growth and productivity of duckweed. The chosen papers provide a comprehensive overview of current designs, including the environmental conditions and pretreatment steps that improve and optimise duckweed biomass cultivation.

2.4.1 Indoor Systems for Duckweed Cultivation

Indoor cultivation systems offer the unique advantage of controlled environmental parameters. They are emerging as viable alternatives to outdoor cultivation systems, particularly for regions with less suitable climates. IVFs are an innovative approach to maximise land usage efficiency and water conservation. Using IVFs, Coughlan et al., (2022a) further emphasised the importance of flow rate and depth analysis in duckweed cultivation. The study provided valuable insights into system velocities that enhance nutrient mixing but do not disturb the duckweed.

The investigation by Petersen et al., (2022b) further showcased IVFs as a viable option for duckweed cultivation. The setup with nine stacked basins demonstrates the potential for sustained duckweed growth over a 40-day period. The reported biomass production rate of 7.54 t yr^{-1} ha^{-1} DW underscores the economic viability of indoor systems, contributing to the development of high-quality biomass with 32% crude protein. While there are costs associated with the lighting and temperature regulation of indoor systems, pairing them with on-site renewable energy sources would reduce the costs and environmental footprint.

2.4.2 Semi-Outdoor Systems for Duckweed Cultivation

The exploration of semi-outdoor systems in Thailand by Ruekaewma et al., (2015) provides valuable insights into the effect of production methods on duckweed production rate. The study's focus on comparing five distinct systems, including static culture, vertical aeration culture, horizontal surface agitation, top water spraying, and layer cultures, offers a comprehensive understanding of the varied production rates and protein content associated with each method. The system with horizontal surface

agitation stands out with the highest yield and protein content of all the systems, 1.52 g m^{-2} d^{-1} DW and 48.2% respectively Ruekaewma et al., (2015). Further work should be carried out to investigate these findings at a larger scale, with a focus on surface agitation.

2.4.3 Outdoor Cultivation Systems: Raceways, Tanks, Ponds, and Cascading Systems

Outdoor systems, while weather-dependent, exhibit substantial success in various global contexts. The examination by Stejskal et al., (2022) of an integrated multitrophic aquaculture (IMTA) system in Ireland, utilising a raceway design, presents a holistic approach to sustainable duckweed cultivation. The reported biomass production exceeding 30 t, equivalent to 8.2 g m^{-2} d^{-1} DW, showcases the capability of outdoor systems to achieve satisfactory yields. This is particularly noteworthy given the Irish climate.

The study of Zhao et al., (2014b) in China explores the use of tanks for high-protein biomass production. After trialing many combinations of operational parameters, a coverage rate of 150%, a medium depth of 50 cm, and a harvest regime of 4 days were identified as the optimal regime. This achieved a production rate of 6.65 g m^{-2} d^{-1} DW with 36.16% crude protein and reinforces the importance of operational parameters on yields.

Studies in Brazil, Mohedano et al., (2012), and Belgium, Devlamynck et al., (2021a), delve into the efficiency of duckweed ponds and cascading systems, respectively, demonstrating diverse approaches to outdoor cultivation. The use of biodigester effluent as a nutrient source for two ponds in series had an impressive production rate of 18 g m^{-2} d^{-1} DW. Moreover, the cascading system's potential to achieve an average growth rate of 4.5 g m^{-2} d^{-1} DW and a protein content of 35% highlights the adaptability and productivity of such systems.

2.4.4 Effect of Design on Protein Production

A comparative study by Prosridee et al., (2023) in Thailand evaluated the effect of different aquaculture conditions on the nutritional quality of *W. arrhiza* biomass. The outdoor pond with hydroponics was found to be the optimal environment for protein production. This emphasises the importance of system design for influencing

the nutritional content of duckweed. Notably, the system with the 2nd highest protein content was the vertical indoor tray with a horizontal stirrer. This compliments the findings by Ruekaewma et al., (2015), which found horiztontal surface agitation to positively influence the growth rate of duckweed.

2.4.5 Pretreatment Steps for Enhancing Growth Rate

Ma et al., (2023) investigated the impact of pre-aeration on duckweed production rates in a pilot-scale duckweed pond in China. The 33% increase in growth rate in the pre-aerated system underscores the significance of considering pretreatment strategies in the overall design of duckweed cultivation systems.

2.4.6 Future Implications

The insights gained from this review on duckweed cultivation offer promise on duckweed as an integral part of sustainable agriculture. The success of both indoor and outdoor cultivation methods provides an opportunity to overcome the limitations of climate and land availability. Promising outdoor production rates globally emphasises the adaptability of duckweed in a variety of environments and additionally, it increases the likelihood of widespread adoption.

The optimisation of duckweed cultivation systems holds implications not only for biomass production but also for addressing global challenges. As discussed in Chapter One, the high protein content of duckweed positions it as a valuable resource for food and feed production (Yahaya et al., 2022, Sońta et al., 2018). The development of efficient systems, considering design parameters and pretreatment steps, could pave the way for a sustainable, nutrient rich protein.

Moreover, integrating duckweed cultivation with wastewater treatment highlights its potential in mitigating environmental issues (Chen et al., 2018, Al-Hashimi and Joda, 2010). Duckweed removes nutrients from the wastewater, acting as a biological filter. Systems like this could play a crucial role in water quality improvement. These integrated approaches to duckweed cultivation are inextricably linked to the circular economy.

2.5 Concluding Remarks

In conclusion, this review provides an overarching perspective of the current research on duckweed cultivation systems. The diversity of indoor and outdoor systems ranging from IVFs to raceways reflects the versatility of duckweed and its ability to thrive in many environmental contexts. The design of a system has been found to affect both the production rate and nutrient composition of the plant, underpinning the importance of the review.

Indoor cultivation systems provide a controlled environment that is weather independent. Further work is required to optimise indoor systems to match the production rates of duckweed cultivation outdoors. However, indoor systems are advantageous as they maximise land usage (IVFs) and can be used year-round. Outdoor systems, despite their dependence on weather have exhibited significant success globally. Integrating production with aquaculture and waste-water remediation systems further increases the sustainability of these systems.

Future advancements in technology and automation may further enhance the efficiency of duckweed cultivation. Efforts are required to ensure continuous research and development is sustained. This is essential to address gaps in knowledge and further optimise system design.

The implications of this review extend beyond duckweed cultivation to both the environment and global nutrition. Duckweed will play an integral role in the sustainable use of natural resources. Lastly, the cultivation of duckweed will contribute to food security, environmental conservation, and the circular economy. The review contributes to harnessing the full potential of duckweed through system design and highlights the importance of using duckweed as both a crop and tool for global good.

3 Methodology

The third chapter includes a detailed account of the tools, techniques, and procedures utilised for conducting this research. Section *3.1* focuses on CFD Modelling. This was carried out using ANSYS Fluent®, a commercially available software. Modelling is used to complement experimental analysis and shouldn't be used as a replacement for laboratory testing. Section *3.2* involves the construction of the pilot-scale growth systems and tracer response studies. Section *3.3* consists of duckweed relative growth rate experiments. These were carried out in three distinct systems and at three inlet velocities to provide insights into the effect of system design and flow rate on duckweed production. Lastly, Section *3.4* contains total nitrate and total phosphorus experimental methods. These were used to understand the impact of system design and inlet velocity on nutrient uptake rates.

3.1 CFD Modelling

3.1.1 Governing Equations

The governing equations for the Fluent simulations in this Master's thesis are the Navier-Stokes equations for the transport of mass and momentum (ANSYS, 2002). The Navier-Stokes equations are Newton's equations of the motion of fluid flow. They follow the principle of conservation for energy, mass, and momentum of fluid flow (Dhont, 1996). The density of water within each system is considered constant, meaning the flow can be considered incompressible (Chin, 2017). When dealing with incompressible Navier Stokes equations, since the fluid in the system is isothermal, the energy equation does not have to be solved. Equations 1, 2, 3, and 4 describe the conservation of mass generally and for incompressible flow, momentum, and stress tensor respectively (ANSYS, 2002).

The Conservation of Mass Equation:

The mass flow rate of the fluid entering the system is equal in magnitude to the mass flow rate exiting.

$$\frac{\partial \rho}{\partial t} + \nabla . (\rho \vec{v}) = 0 \quad (1)$$

Where ρ is density of fluid, *t* is time, ∇ is a vector differential operator, and $\vec{v}$ is a velocity vector.

As the fluid in the system is incompressible, the equation can be reduced to:

$$\nabla . (\vec{v}) = 0 \quad (2)$$

The Momentum Equation:

Equation 3 describes the transport of momentum in the *i*th direction in a non-accelerating reference frame.

$$\frac{\partial}{\partial t}(\rho\vec{v}) + \nabla . (\rho\vec{v}\vec{v}) = -\nabla p + \nabla . (\bar{\bar{\tau}}) + \rho\vec{g} + \vec{F} \quad (3)$$

Where *p* is static pressure, $\bar{\bar{\tau}}$ is stress tensor (see below equation 4), gravitational body force is $\rho\vec{g}$, and other source terms that arise are $\vec{F}$.

The Stress Tensor Equation:

$$\bar{\bar{\tau}} = \mu\left((\nabla\vec{v} + \nabla\vec{v}^{T}) - \frac{2}{3}\nabla . \vec{v}I\right) \quad (4)$$

Where molecular viscosity is given by μ, and $\left((\nabla\vec{v} + \nabla\vec{v}^{T}) - \frac{2}{3}\nabla . \vec{v}I\right)$ represents the effect of volume dilation.

3.1.2 Simulation Description

3.1.2.1 Model Geometry

The 3D model geometry for both the IBC with baffles and IBC without baffles were constructed on ANSYS Spaceclaim®. Both models were simplified versions of the physical tanks, with smooth walls and 90° corners. The resulting dimensions can be seen in Figures 10, and 11. This is a limitation of the CFD models as IBCs typically have rounded corners due to the manufacturing process.

Using sketch mode in Spaceclaim®, the models were first constructed. Then, as the goal was to analyse fluid flow within the tanks, the volume extract tool was employed to extract the volume within the enclosed bounds of the tank. The solid

structure was 'suppressed for physics', so the resulting model would pertain to the volume of the system.

System with No Baffles

The IBC tank is 116 cm in length (L), 98 cm in width (W), and the water depth which is what is accounted for in the computational domain was selected to be 15 cm, here referred to as height (H). Both the inlet and outlet have a diameter of 2 cm. This height was chosen as it was the original water depth desired for experiments involving duckweed. Lower water depth, and higher surface area is more effective for nutrient remediation as discussed in Chapter One (Zhao et al., 2014a).

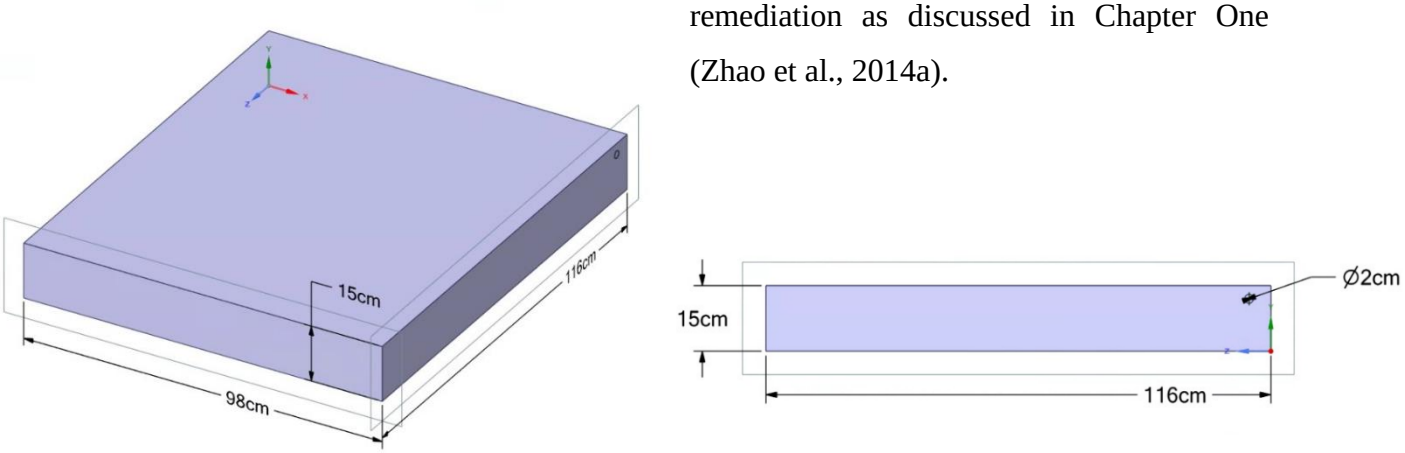

Figure 10: *Volume geometry with dimensions, system with no baffles a) Isometric view b) Y-Z plane*

System with Baffles

The tank is 116 cm in L, 98 cm in W, and 15 cm in H, with similar analogy to the non-baffled system. It has 6 baffles, each 70.5 cm in L, 0.6 cm in W, and 15 cm in H. The first and last baffle are each 21 cm from the walls of the tank. The remaining baffles are evenly spaced 15 cm apart. The inlet and outlet are both 2 cm in diameter.

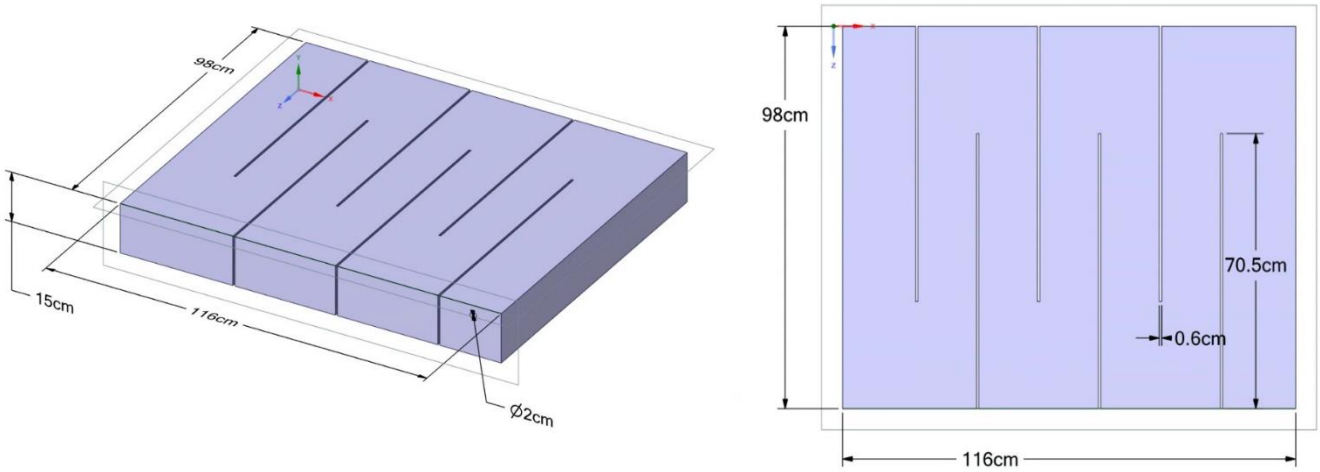

***Figure 11**: Solid geometry with dimensions, system with baffles a) Isometric view b) Z-X plane*

3.1.2.2 Mesh Independence Studies

The mesh for tank volumes was generated using ANSYS Meshing®. Creating a suitable mesh for the simulation is very important. The resulting mesh influences the reliability, accuracy, and stability of the model (ANSYS, 2009). Appendix 2 has further information on the element quality, aspect ratio, skewness, and orthogonal quality of the mesh. As the geometry of the tanks were asymmetrical, symmetry could not be used to reduce computational power demand of the models. Using the sizing tool, smaller mesh was employed for the open boundary (interface of water and air) of each model. Additionally, the mesh refinement tool was used at tank edges. This was carried out to achieve a more accurate solution for these areas of potentially problematic flow. Capture curvature was active for all models, this increases mesh refinement at both the inlet and outlet.

Mesh independent studies involve systematically refining the mesh until the solution is deemed independent of mesh size/number. It allows for the selection of a mesh model that is a good representation of the physical phenomenon being modelled. Carrying out mesh independence studies increases confidence in the simulation, and the subsequent results. The method used for this study involved monitoring the area-

weighted average velocity at numerous points on the model. Once the monitored parameters did not change with increasing mesh density, the solution was deemed independent of the mesh. Figure 12 shows the area of inspection for the non-baffled system as an example.

The area-weighted average velocity of the inlet, outlet, line 1, and line 2 were recorded for each consecutive model. The graphic results of the mesh independence studies can be found in Appendix 3.

System with No Baffles

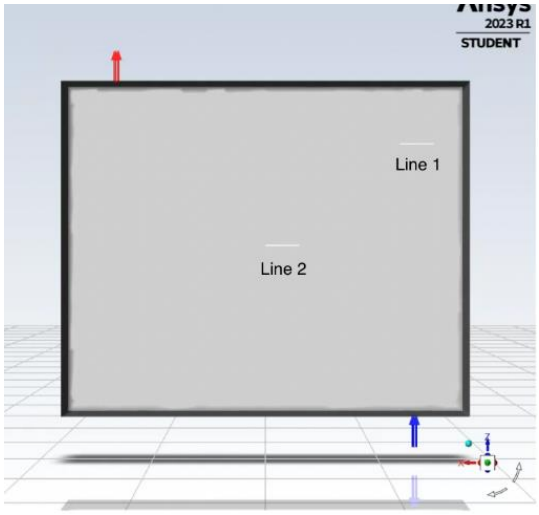

Figure 12: *Z-X plane view of model with line 1 and line 2, system with no baffles.*

The coordinates for line 1 and line 2 are as follows:

Coordinates for line 1: $x_1 = 0.2$, $y_1 = 0.1$, $z_1 = 0.8$; $x_2 = 0.1$, $y_2 = 0.1$, $z_2 = 0.8$

Coordinates for line 2: $x_1 = 0.6$, $y_1 = 0.1$, $z_1 = 0.5$; $x_2 = 0.5$, $y_2 = 0.1$, $z_2 = 0.5$

The location of these lines in relation to the model can be seen in Figure 12.

The details of the 7 mesh models that were examined for the system with no baffles can be seen in Tables 5, and 6. The mesh deemed independent of the solution was mesh number 6, with an element count of 218,506 cells.

Table 9: *Mesh Models generated during mesh independence studies with final element count for system with no baffles.*

Mesh Number	Element Size (m)	Open Boundary Face Sizing (m)	Mesh Refinement at 12 edges	Element Count (cells)
1	0.08	0.065	1	42834
2	0.052	0.042	1	57363
3	0.043	0.035	1	72011
4	0.032	0.028	1	84900
5	0.03	0.02	1	142741
6	0.03	0.015	1	218506
7	0.015	0.015	1	353382

Table 10: *Area-weighted average velocity at named monitoring points for system with no baffles.*

Mesh Number	Average Velocity at Inlet ($m\ s^{-1}$)	Average Velocity at Outlet ($m\ s^{-1}$)	Average velocity at Line 1 ($m\ s^{-1}$)	Average Velocity at Line 2 ($m\ s^{-1}$)
1	0.05	0.059	0.0051	0.00034
2	0.05	0.058	0.0051	0.00030
3	0.05	0.058	0.0061	0.00029
4	0.05	0.059	0.0585	0.00080
5	0.05	0.059	0.0067	0.00063
6	0.05	0.058	0.0068	0.00027
7	0.05	0.058	0.0065	0.00024

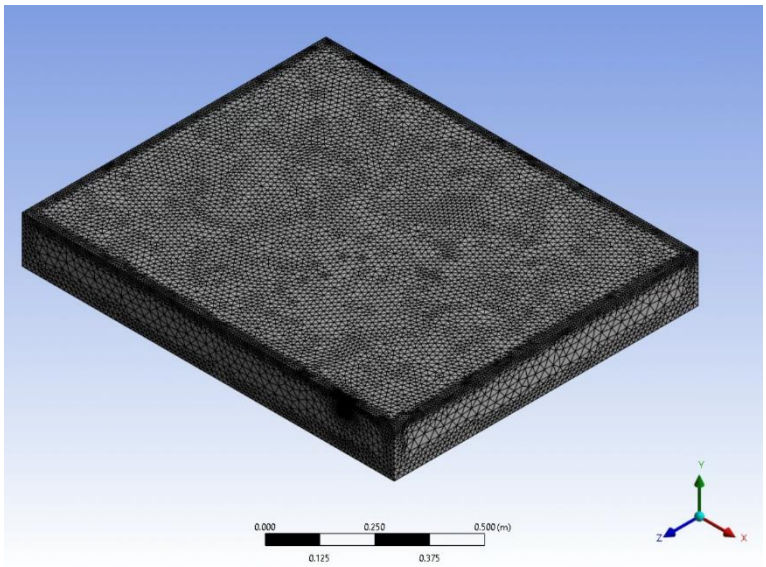

Figure 13: *Mesh number 6, system with no baffles*

System with Baffles

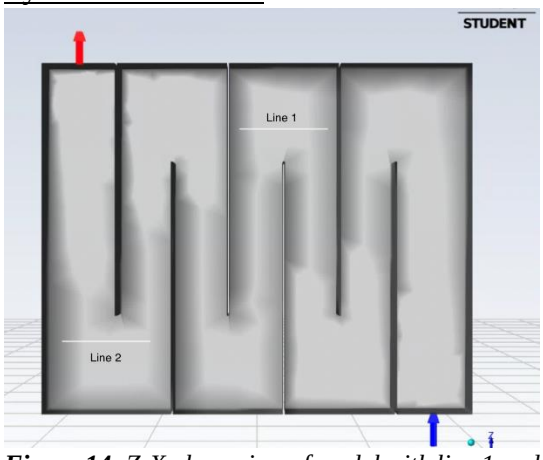

Figure 14: *Z-X plane view of model with line 1 and line 2, system with baffles.*

The coordinates for line 1 and line 2 are as follows:

Coordinates for line 1: $x_1 = 0.65$, $y_1 = 0.1$, $z_1 = 0.8$; $x_2 = 0.4$, $y_2 = 0.1$, $z_2 = 0.8$

Coordinates for line 2: $x_1 = 0.9$, $y_1 = 0.1$, $z_1 = 0.2$; $x_2 = 1.15$, $y_2 = 0.1$, $z_2 = 0.2$

The location of these lines in relation to the model can be seen in Figure 14. The details of the 8 mesh models that were

examined for the system with baffles can be seen in Tables 7, and 8. The mesh deemed independent of the solution was mesh number 7, with an element count of 421,697 cells.

Table 11: *Mesh Models generated during mesh independence studies with final element count for system with baffles.*

Mesh Number	Element Size (m)	Mesh Refinement at 72 edges	Element Count (cells)
1	0.2	1	44717
2	0.09	1	53394
3	0.06	1	77821
4	0.04	1	129827
5	0.055	2	180371
6	0.09	3	272577
7	0.06	3	421697
8	0.05	3	495528

Table 12: *Area-weighted average velocity at named monitoring points for system with baffles.*

Mesh Number	Average Velocity at Inlet (m/s)	Average Velocity at Outlet (m/s)	Average velocity at Line 1 (m/s)	Average Velocity at Line 2 (m/s)
1	0.03	0.035	0.00035	0.00043
2	0.03	0.035	0.00035	0.00045
3	0.03	0.035	0.00035	0.00042
4	0.03	0.035	0.00030	0.00039
5	0.03	0.035	0.00026	0.00038
6	0.03	0.035	0.00034	0.00047
7	0.03	0.035	0.00026	0.00042
8	0.03	0.035	0.00027	0.00041

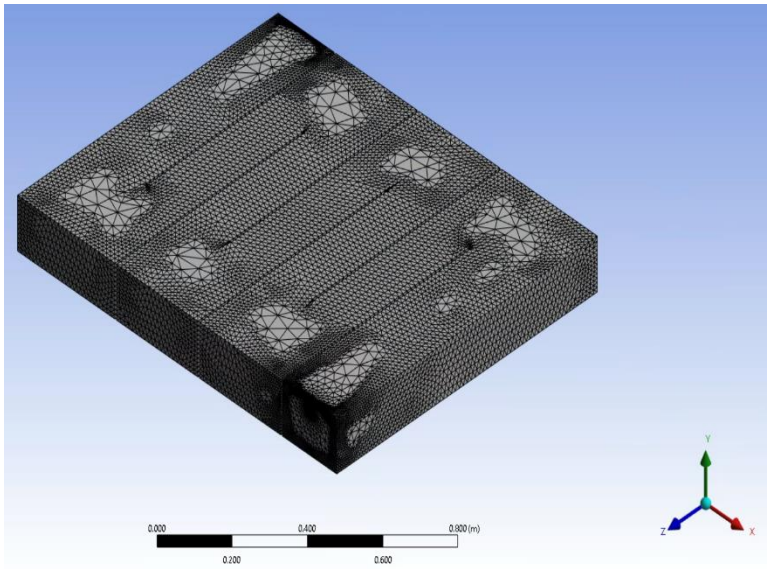

Figure 15: *Mesh number 7, system with baffles.*

3.1.2.3 Selection of Boundary Conditions (BC)

Accurate selection of the boundary type and conditions are critical for a successful solution. For the inlet, the velocity BC was selected. The pressure outlet was selected as the outlet BC. The walls of the system were set to 'no slip', following from the 'no slip condition' for surface fluid flow. The open boundary was set as a wall with zero specified shear stress, as it is a free surface. The simulation was modelled as single-phase, due to the assumption that there is minimal interaction between air and water at the open boundary.

3.1.3 Setup and Solution of Models

Both models, the system with no baffles and the system with baffles have the same selected simulation settings. These are all listed in Appendix 1. For the systems viscosity model, two different models were selected. For the mesh independence studies, the laminar model was chosen. For the remaining models the turbulent realizable kϵ model was selected. This selection was influenced by the Reynold's Number (Re) of the inlet in each scenario. This is discussed further in Section *3.1.5.* Equations 5 and 6 represent the k (turbulent kinetic energy) and ϵ (dissipation rate) transport equations respectively (ANSYS, 2009). This model has been validated for a wide range of situations, and out-performs the standard kϵ model (ANSYS, 2006).

k*:*

$$\frac{\partial}{\partial t}(\rho k) + \frac{\partial}{\partial x_j}(\rho k u_j) = \frac{\partial}{\partial x_j}\left(\left(\mu + \frac{\mu_t}{\sigma_k}\right).\frac{\partial k}{\partial x_j}\right) + G_k + G_b - \rho\epsilon - Y_M + S_k$$

(5)

ϵ:

$$\frac{\partial}{\partial t}(\rho\epsilon) + \frac{\partial}{\partial x_j}(\rho\epsilon u_j) = \frac{\partial}{\partial x_j}\left(\left(\mu + \frac{\mu_t}{\sigma_\epsilon}\right).\frac{\partial_\epsilon}{\partial x_j}\right) + \rho C_1 S_\epsilon - \rho C_2 \frac{\epsilon^2}{k+\sqrt{v\epsilon}} + C_{1\epsilon}\frac{\epsilon}{k}C_{3\epsilon}G_b + S_\epsilon$$

(6)

where the following conditions were met

$$C_1 = \max\left(0.43, \frac{n}{n+5}\right), \qquad n = S\frac{k}{\epsilon}, \qquad S = \sqrt{2S_{ij}S_{ij}}$$

3.1.3.1 Steady State

For the analysis of fluid flow with each system, only steady state simulations were used. Liquid H_2O was selected as the fluid for the volume region from the Fluent Database. The full simulation setup can be found in Appendix 1.

3.1.3.2 Transient State

The transient state involved running the models for a specified period of time, allowing for changes of conditions with time. The purpose of the transient simulation for this research is the verification and validation of the CFD model with the physical tanks. The transient solution was not used for fluid flow analysis.

The key difference between the steady state and transient state settings is that the species model is selected for the transient model. The species model is employed to track the concentration of tracer injected over time. These results are then used to validate the models.

Species Transport Equation:

When this equation is solved, ANSYS Fluent predicts Y_i, the local mass fraction of each species. This occurs through the solving of a convection-diffusion equation for the *i*th species.

$$\frac{\partial(\rho Yi)}{\partial t} + \nabla.(\rho\vec{v}Yi) = -\nabla.\vec{J}_i + R_i + S_i$$

(7)

Where the w1 production of *i* is R_i. The rate of creation by addition from the dispersed phase as well as any user-defined sources is S_i (ANSYS, 2009).

The solution is first solved in a steady state, with water as the only feed. The equations being solved at this stage are flow, turbulence, and energy. Once the solution is solved, it is switched from steady state to transient state. The previous equations do not need to be solved in transient state so are de-selected to reduce computational power requirements. The tracer equation is now selected. The mass fraction of the tracer is set to 1 at the inlet BC species setting. This ensures that only tracer is injected into the tank during the chosen time frame. The solution runs for 0.3 seconds, which results in an injection of 100 ml tracer for an inlet velocity of 1.1 m s^{-1}, to mimic a pulse tracer injection. The mass fraction of the tracer is then set to zero, so only water enters the system after that time step. This method is called a pulse injection. As the species transport model is activated, the molar concentration at the outlet can be tracked over time. The solution then runs until the concentration of tracer reaches 0 moles $litre^{-1}$. These simulations are replicated experimentally and are later used comparatively to validate the CFD model.

3.1.4 Solver

The solution was deemed converged when the residuals of each variable had fallen below $1x10^{-3}$. However, while a solution may converge, it may not be an accurate representation of the real-life model. The accuracy of a solution is dependent on the physical model, computing power available, and mesh refinement. The simulation must be set up to match the real-life problem as closely as possible. This is why experimental validation of the CFD model is important. The % accuracy required for the solution depends on the problem being modelled (van Hooff et al., 2017).

3.1.5 Inlet Reynolds Number

Reynolds Number (Re) is dimensionless. It denotes the ratio of inertial and viscous forces experienced by a fluid (Rehm et al., 2008). The Re of each model's inlet was calculated using Equation 8. This equation was chosen as water is a Newtonian fluid (Alexander, 2017). As the experiments utilised synthetic hydroponics, the fluid characteristics for calculating Re were that of water, acquired from literature.

Density, ρ was 997 kg m^3. D_i represents the inlet hydraulic diameter in (m). The fluid viscosity μ utilised was 1.002 x 10^{-3} Pascal seconds (Pa s). Table 13 contains the calculated parameters for each modelled scenario. The calculation of Re at the inlet for each scenario influenced the decision of the chosen viscous model for that problem. Section *4.2* contains the outputs from the CFD modelling. For the mesh independence studies, as the Re at the inlet was < 2100, the laminar model was chosen. For all other studies, the turbulent model was selected as the Re > 4000.

$$\mathrm{Re} = \frac{\rho v D_i}{\mu} \tag{8}$$

Laminar flow: Re < 2100

Transient Flow: 2100 < Re > 4000

Turbulent Flow: Re > 4000

Table 13: *Determination of Reynolds Number for the Inlet of each Simulated Model*

	Type		Flow rate ($m^3 s^{-1}$)	Fluid Depth (m)	Inlet Velocity ($m s^{-1}$)	Inlet Diameter (m)	Inlet Area (m^2)	Reynolds Number at Inlet
1	Baffles		0.0000094	0.15	0.03	0.02	0.000314	597
2	Baffles		0.0000094	0.15	0.03	0.02	0.000314	597
3	Baffles		0.0000094	0.15	0.03	0.02	0.000314	597
4	Baffles		0.0000094	0.15	0.03	0.02	0.000314	597
5	Baffles		0.0000094	0.15	0.03	0.02	0.000314	597
6	Baffles		0.0000094	0.15	0.03	0.02	0.000314	597
7	Baffles	Mesh	0.0000094	0.15	0.03	0.02	0.000314	597
8	Baffles	Independence	0.0000094	0.15	0.03	0.02	0.000314	597
9	Baffles		0.000094	0.55	0.3	0.02	0.000314	5970
10	Baffles	Effect of	0.00020	0.55	0.65	0.02	0.000314	12935
11	Baffles	Flow rate	0.00031	0.55	1	0.02	0.000314	19900
12	No Baffles		0.000016	0.15	0.05	0.02	0.000314	995
13	No Baffles		0.000016	0.15	0.05	0.02	0.000314	995
14	No Baffles		0.000016	0.15	0.05	0.02	0.000314	995
15	No Baffles		0.000016	0.15	0.05	0.02	0.000314	995
16	No Baffles		0.000016	0.15	0.05	0.02	0.000314	995
17	No Baffles	Mesh	0.000016	0.15	0.05	0.02	0.000314	995
18	No Baffles	Independence	0.000016	0.15	0.05	0.02	0.000314	995
19	No Baffles		0.000094	0.55	0.3	0.02	0.000314	5970
20	No Baffles	Effect of	0.000094	0.55	0.65	0.02	0.000314	12935
21	No Baffles	Flow rate	0.000094	0.55	1	0.02	0.000314	19900

Table 13 depicts each simulated model used for this analysis, and the resulting Reynold's number at each inlet. A fluid depth of 0.15 m was chosen for the mesh independence experiments as this was the liquid height used in the wet-lab residence time experiments (Section *3.2.4*). The fluid depth was increased to 0.55 m for analysis of the effect of flowrate as this corresponds to the fluid depth in the growth systems during the relative growth rate experiments (Section *3.3.2*).

3.2 Tracer Response Experiments

3.2.1 Background

Mixing is an operational process, resulting from three types of motion: molecular, eddy and bulk motion. Molecular mixing occurs due to concentration differences within a system and is more commonly known as molecular diffusion. Eddy motion occurs when a system is operating under turbulent conditions (Nere et

al., 2003). Eddies are swirling fluid structures, with flow that is directionally different from bulk fluid (Doran, 2013). The principal motion of fluid in a vessel is known as bulk motion (Baker et al., 2015). Molecular diffusion and eddies can also influence bulk fluid flow in a system (Nere et al., 2003). An understanding of mixing and fluid flow can also provide information on dead zones within the vessel. Design alterations can be implemented if necessary to minimise these areas of limited mixing. Another method for understanding fluid flow within a vessel is tracer response experiments. The volume of tracer injected is minimal to ensure limited effect on fluid flow within the system. Monitoring the behaviour of tracer within the vessel can reveal information about fluid flow including mixing and residence times within the system (Zhang et al., 2018).

3.2.2 Construction of Growth Systems

For the pilot-scale growth systems, IBCs were selected as they are cheap, durable, and ubiquitous in the farming community. From the literature review, there was no clear answer as to which style of system is best for duckweed production. IBCs provided flexibility to examine the difference between a stagnant tank, a recirculated tank, and a recirculated baffled tank. Each IBC had the top cut off which left the tank exposed, making them suitable for these experiments. On two of the IBCs, an inlet and outlet of 2 cm diameter were added. These were 14 cm from the bottom of each tank. An inlet/outlet size of 2 cm was chosen for its compatibility with the available pumps, Oase Optimax 4000. The use of only one inlet was selected because of the number of available pumps in BEES. This is a limiting factor of the experiments and further work could investigate the effect of both the number of inlets, and inlet diameter on duckweed growth in these systems. The influence of the number of inlets and inlet position on hydrodynamics of growth systems were investigated by (Maguire et al., 2024). While the study found that increasing the number of inlets reduced the stagnant volume of the tank, it did not investigate the relationship between the number of inlets and duckweed growth.

Yellow tubing approx. 320 cm in length was used to connect the inlet to the outlet in both systems. Figure 16 shows the setup of the two recirculated tanks. For the baffles six sheets of PVC were ordered, they were 70.5 cm in L, 60 cm in H, and 0.6 cm in W. The baffles were set in place using marine grade sealant, Sikaflex 291i

sealant. This was used to ensure the baffles were flush with the tank, removing any unwanted leakage amongst the channels to ensure fluid flow was controlled. The walls of the IBC were no longer rigid with the top removed, so to prevent the baffles moving two iron bars were used to reinforce the structure. To reduce leaks at the inlets and outlet thread seal tape was wrapped around the thread to make them watertight.

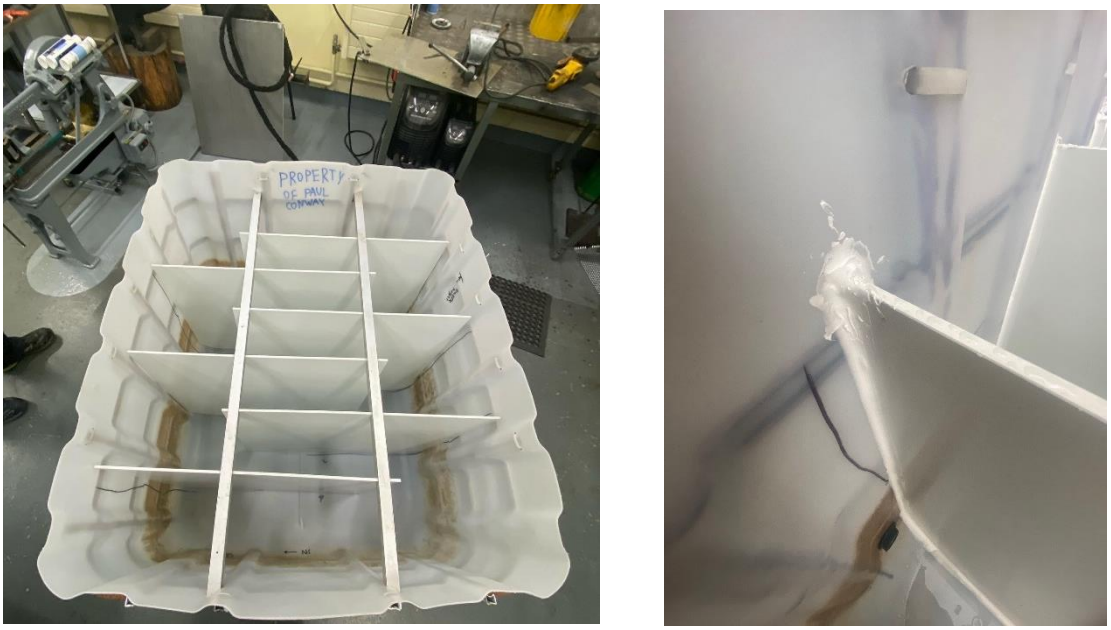

***Figure 16**: Photographs of the IBC with baffles a) overview of tank with the baffles inserted b) baffles flush with thank walls using sealant*

3.2.3 Tracer Concentration Standard Curve

First, 2 Molar (M) HCl was made in the lab. This was carried out under the fume hood. The recipe used was 2 M HCl = 167 mL HCl (37% w/v) with 1 L of water. This is based on Equation 9 below. First the water was measured and added to the reagent flask. The acid was measured with volumetric flasks and then added to the reagent flask after the water.

$$37\%\,\frac{w}{v}\,\mathrm{HCl}, \qquad \rho = 1.19\,\frac{\mathrm{kg}}{\mathrm{L}}, \qquad \text{Molecular weight } (Mw) \text{ of HCl} = 36.5\,\frac{\mathrm{g}}{\mathrm{mol}}$$

$$37\%\ \frac{w}{v}\,\mathrm{HCl}\ x\ 1.19\,\frac{\mathrm{kg}}{\mathrm{L}} = 0.44\,\frac{\mathrm{kg}}{\mathrm{L}}\,\mathrm{HCl} \qquad (9)$$

$$37\%\ \text{HCl solution} : 12\ M\ \text{HCl}$$

Therefore,

$$1\ M\ \text{HCl} = 83\ \text{ml HCl (37\%)}, \qquad 2\ M\ \text{HCl} = 167\ \text{ml HCl (37\%)}$$

Using Equation 10, a series of concentrations were chosen and made up from the stock solution. The conductivity of each concentration was recorded using the Cond 315i from WTW. This data can be found in Table 10.

$$\frac{\text{Volume of Aliquot (V)}}{\text{Final Volume } (V_f)} = \frac{\text{Final Concentration } (C_f)}{\text{Stock Concentration } (C_i)} \quad (10)$$

Table 14: *Data for Standard Curve*

Conductivity (on meter) mS cm^{-1}	**Concentration** moles $litre^{-1}$
0.236	0
3.67	0.01
17.36	0.05
36.6	0.1
68.9	0.2
166.3	0.5
311	1

A graph of this data, mapping conductivity in (mS cm^{-1}) to known concentrations in (mol L^{-1}) was plotted. This can be seen in Figure 17. The graph had an R^2 value of 0.9987 which shows the graph is a good fit. From the graph the equation of the curve was generated using excel, namely Equation 11. This equation was then used to map recorded conductivities during the tracer response experiments to their concentrations.

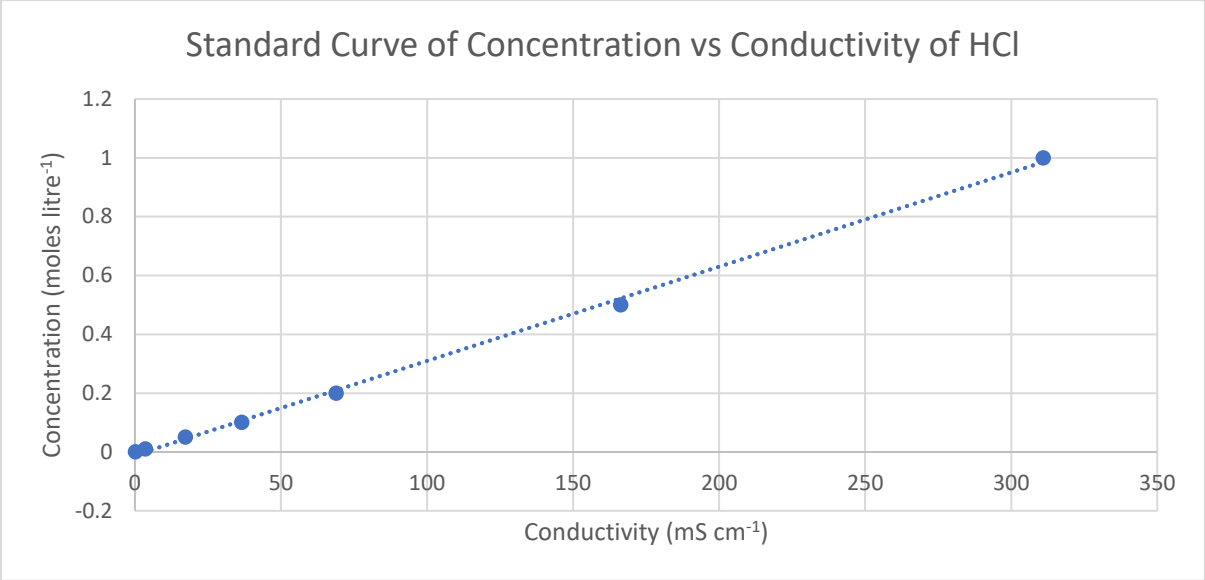

Figure 17: *Standard Curve Mapping Concentration to Conductivity*

$$\text{Tracer Concentration } (M) = 0.003 * \text{Conductivity } \left(\frac{\text{mS}}{\text{cm}}\right) + 0.0108 \quad (11)$$

3.2.4 Experimental Mixing Time Characterisation

Mixing time experiments are used to better understand mixing within the vessel and are an important indicator of system performance. Experimental mixing time is the length of time needed for an injected tracer to achieve homogeneity (typically 95%) in a bioreactor (Ascanio, 2015). Mixing time infers information on mixing and flow within a system that can be used to inform optimisation and scale-up (Hadjiev et al., 2006). In industrial fermentation processes, it is favourable to have low mixing times for the reaction vessel. Lower mixing times aid rapid and uniform distribution of nutrients (Nadal-Rey et al., 2022). However, in the instance of nutrient remediation, an increase in contact between biomass and nutrients can be beneficial. Tracer studies provide data on this contact time (Patel et al., 2021).

There is a multitude of techniques used to experimentally determine mixing time, including colorimetry, conductivity and pH, thermography, and electrical resistance tomography (Cabaret et al., 2007, Fitschen et al., 2021, Mann et al., 1997, Lee and Yianneskis, 1997, Ascanio, 2015). They are categorised based on the amount of disturbance to flow, and the kind of data collected. Depending on the level of flow disturbance, they are further categorised as non-intrusive and intrusive. While both are

accurate, intrusive methods cause disturbance to flow patterns due to the addition of probes to the system. Regarding the type of collected data, they can be categorised as Eulerian (direct) or Lagrangian (indirect) data. A Eulerian approach typically requires less processing as it uses real-time results. The use of conductivity and pH is an example of an intrusive, direct method (Ascanio, 2015).

3.2.4.1 Method

The experiments were performed with both the IBC and the IBC with baffles. Each tank was filled with water to a liquid height of 15 cm. The volume of liquid in the tank was approximately 0.17 m^3. The pump was located at the outlet of each tank and set to a flow rate of 0.001 $m^3 s^{-1}$. A pipe was fitted from the inlet to the outlet, so the fluid was constantly being recirculated through the system.

The 2M HCl solution was utilised as the tracer. The recipe for the 2 M HCl and details of the standard curve can be found in Section *3.2.3*. For each system, baffled and non-baffled, 3 replicates of the tracer pulse injection were completed so the average mixing time of the system could be determined. The data was recorded using a TC-08 thermocouple data logger from Pico Technology. This allowed the conductivity to be recorded over time at a selected interval of 5 s.

The system was allowed to run for a period of time before the tracer was added. 10 ml of 2 M HCl was added at the inlet of the tank at 'time 0 s', and the conductivity was recorded at the outlet. The final conductivity recorded for Run 1 was used as the initial conductivity for Run 2, so the tanks did not need to be emptied and refilled for each run. Using the standard curve and the data recorded, a graph of concentration vs time of HCl in the system was plotted. From this data the experimental mixing time was recorded. Once the values reached within 5% from the final concentration, the solution can be considered homogenous. This value is the experimental mixing time.

In future work it is advised that the system runs for three theoretical residence times to ensure the system is in steady state before addition of the tracer.

3.2.5 Experimental Residence Time Characterisation

3.2.5.1 Method

The residence time experiments were carried out to validate the computational models generated with ANSYS Fluent. For the experimental setup, a pump at the inlet

was connected to a sump tank with a flow rate of 0.00035 $m^3 s^{-1}$. This ensured there was a fresh water supply for the inlet for the duration of each run. A pump was also setup at the outlet, also at 0.00035 $m^3 s^{-1}$ to removed water from the IBC at this rate. This ensured the liquid height in the tank remained constant at 15 cm. The volume of liquid in the tank was approximately 0.17 m^3. Again, the conductivity was measured using a handheld conductivity meter, Cond 315i from WTW. For each system, 3 identical pulse tracer injection experiments were completed. The data was recorded using a TC-08 thermocouple data logger from Pico Technology.

At time 0 s, 20 ml of 2 M HCl was added to the system at the inlet of the tank. The conductivity of the system was recorded at the outlet, and the experiment ran until the conductivity reached a constant level. The conductivity curve was converted to concentration of HCl using the standard curve. Each of the 3 runs for both systems were compared to the simulation data to validate the CFD models, to ensure they were an accurate representation of each system. This method was adapted from (Fogler, 2006). Results from the tracer experiments are discussed in Section *4.1*.

3.3 Relative Growth Rate of Duckweed

Experiments were carried out to understand the growth of duckweed in each cultivation system. The strain of duckweed used was Lemna minor *L. "Blarney"*, number 5500 in the Rutgers Duckweed Stock Cooperative database.

3.3.1 Location-Focused Growth Rate Experiments

For the first set of relative growth rate experiments, 2 recirculated systems were compared: a system with no baffles and a system with baffles. These experiments were carried out at a fixed inlet velocity of 0.3 m s^{-1}. To gain a greater understanding of the individual systems, rings were allowed floating a specific area on the top of each tank. These rings corresponded to specific points of interest from the velocity contours produce from the CFD models. This is looked at more closely in Section *4.3.1*. A limitation of this experiment is the absence of a ring (point of interest) in the center of the system with no baffles. In trials of the experiment, the ring was found to move over the course of the run so this was omitted. 5 rings were used in the system with no baffles, and 4 in the system with baffles. They were secured in place by plastic string. Each ring floats on the surface of water in the tank and does not interfere with duckweed growth. The position of these rings can be seen in Figure 18 below. The focus of these experiments was to understand the effect of system design and mixing

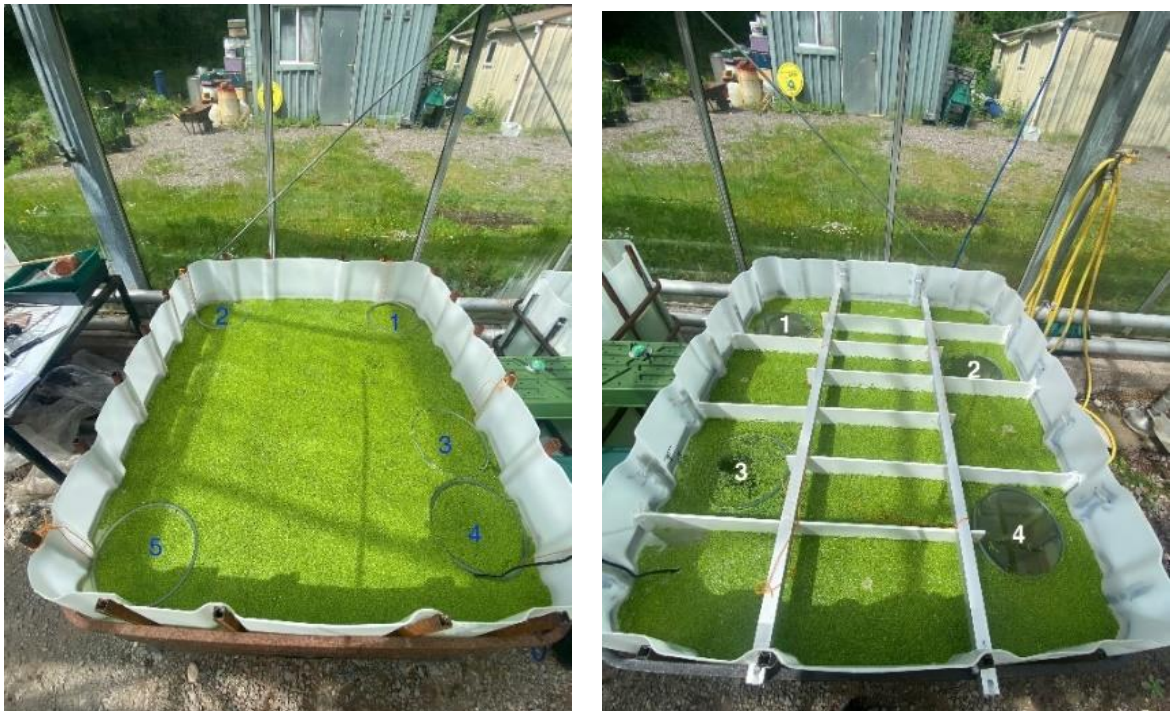

***Figure 18**:* Overview of ring locations in each system a) system with no baffles, b) system with baffles

on duckweed growth. 1/6 of the recommended optimal hydroponics were added to each system. 18.75 mL of FloraGro 3-1-6 and 18.75 mL Terra Aquatica TriPart NPK 5-0-1 was used per system for each run. More information on the composition of the hydroponics used can be found in Appendix 4.

Four runs were carried out and each run lasted 7 days. Based on the surface area of each system, for 60% coverage 290 g of duckweed was added at the beginning of each run. Each ring had 7.8 g of duckweed added to it on day 0, and the remainder of the 290 g was added outside of the rings. Each tank was recirculated using a pump, Oase Optimax 4000, set to an inlet velocity of 0.3 m s^{-1}. At the end of each run (7^{th} day), the weight of duckweed biomass in each ring, and the overall system was recorded. The relative growth rate is then calculated for each system.

3.3.2 Relative Growth Rate Experiments- Three Systems

The three systems that the relative growth of duckweed was calculated in were 1. an IBC with no recirculation, 2. an IBC with recirculation, and 3. an IBC with baffles that is recirculated. All three systems are examples of batch processes. Notably, the IBC that was not recirculated had no inlet velocity. The tests on the recirculated IBCs were carried out at three inlet velocities, 0.3 m s^{-1}, 0.65 m s^{-1}, and 1 m s^{-1}. This was undertaken to explore the effect of flow rate and system design on growth rate. Recirculation was used as a tool to add agitation in the system to see if there would be a change in duckweed growth and nutrient uptake. Nine runs were carried out. This is detailed in Table 15 for clarity. The fresh duckweed biomass for each experiment was collected from the Gibba System which is discussed in Section *3.3.3.*

Table 15: *Experimental design*

Effect	Run	Triplicate	System	Inlet Velocity m s^{-1}
Low velocity	1	1.1	IBC with no recirculation	n/a
		1.2	IBC with recirculation	0.3
		1.3	IBC with baffles and recirculation	0.3
	2	2.1	IBC with no recirculation	n/a
		2.2	IBC with recirculation	0.3
		2.3	IBC with baffles and recirculation	0.3
	3	3.1	IBC with no recirculation	n/a
		3.2	IBC with recirculation	0.3
		3.3	IBC with baffles and recirculation	0.3
High velocity	4	4.1	IBC with no recirculation	n/a
		4.2	IBC with recirculation	1
		4.3	IBC with baffles and recirculation	1
	5	5.1	IBC with no recirculation	n/a
		5.2	IBC with recirculation	1
		5.3	IBC with baffles and recirculation	1
	6	6.1	IBC with no recirculation	n/a
		6.2	IBC with recirculation	1
		6.3	IBC with baffles and recirculation	1
Medium velocity	7	7.1	IBC with no recirculation	n/a
		7.2	IBC with recirculation	0.65
		7.3	IBC with baffles and recirculation	0.65
	8	8.1	IBC with no recirculation	n/a
		8.2	IBC with recirculation	0.65
		8.3	IBC with baffles and recirculation	0.65
	9	9.1	IBC with no recirculation	n/a
		9.2	IBC with recirculation	0.65
		9.3	IBC with baffles and recirculation	0.65

The goal of the experiment was to look at the effect of fluid flow within each system and the impact of system design on relative growth rate. 1/3 of the optimal hydroponics strength was used. This was to highlight the specific effect of each system on duckweed growth. By limiting the nutrients available for growth, it was hoped that any effect of system type would more visible. 37.5 mL of FloraGro 3-1-6 and 37.5 mL Terra Aquatica TriPart NPK 5-0-1 was used per system for each run. This equated to 1/3 of the optimal strength for a system of 116 cm x 98 cm x 55 cm (L x W x H). This was increased from 1/6 optimal nutrients in Section *3.3.1* as the extremely low nutrients resulting in very poor growth of duckweed and inconsistent results.

A liquid depth of 55cm was chosen as the height of the baffles were 60 cm. At a lower depth, the difference in light intensity the duckweed would experience between the system with baffles and without would be too great. Therefore, for a more comparable experiment the higher depth was chosen. The pump used for both recirculated systems was the Oase Optimax 3000. It has a maximum flow rate of 2800 L h^{-1} and a maximum head height of 3 m. The lowest flow rate on the pump (measured experimentally), 338 L h^{-1}, corresponded to an inlet velocity of 0.3 m s^{-1}. The higher inlet velocities of 0.65 m s^{-1} and 1 m s^{-1} were chosen after analysis of the CFD models.

These experiments were carried out in a glasshouse, for semi-outdoor conditions. The light intensity and temperature for the duration of the experiments were recorded using a HOBO connect meter. The difference in light and temperature during each run is discussed further in Section *4.3.* Muslin cloth was draped over the tanks to reduce the light intensity experienced by the duckweed as during summer months, as high light intensity can result in plant stress. Bamboo sticks were used the prevent the muslin falling into the tanks. This setup can be seen in Figure 19. Each run was 5 days in length. On day 0, 250 g of fresh biomass from the Gibba System was added to each tank with fresh water at a depth of 55 cm, and 1/3 hydroponics strength. The day 5 biomass was recorded for each system over 3 replicates for each flow rate.

Figure 19: *IBC setup in the glasshouse a) ensuring the IBCs are level b) muslin draped across the IBCs to reduce light intensity*

3.3.3 Calculation of RGR

The RGR was calculated using Equation 12 (Connolly and Wayne, 1996). This formula utilises the natural logarithm of the weights to account for exponential plant growth and to normalize growth rates across plants of different sizes. The initial biomass was harvested from the Gibba system, and the duckweed was lightly patted dry with a paper towel to have an accurate weight. The same process was carried out before weighing the final biomass at the end of each run.

$$\mathrm{RGR} = \frac{\ln \frac{W_2}{W_1}}{\Delta T} \quad (12)$$

Where ΔT number of days of the experiment, ln is the natural log, W_1 is the initial biomass in g, and W_2 the final biomass in g.

3.3.4 The Gibba System

For the experiments in Section *3.3.2*, the Gibba system was used to provide fresh duckweed biomass. Previously, duckweed was collected from outdoor IBCs, but this didn't provide a consistent and replicable starting point for each run. The Gibba was seeded with L. minor that was grown in a controlled, sterile environment. This ensured that the duckweed had no external contaminants.

The Gibba is made up of 5 stacked trays (72 cm x 41 cm x 11 cm), and a sump tank (60 cm x 41 cm x 41 cm). The setup can be seen in Figure 20. The water is fed to Tray 1 using a pump (Rio Pump 1700) and the rest of the trays are gravity fed. As it is an indoor system, LED strip lighting is used. This is operated on a 16:8 hour day (light:dark) (Coughlan et al., 2022a). Including the sump, the total system volume is approximately 500 L. On day 0, 125 mL of FloraGro 3-1-6 and 125 mL Terra Aquatica TriPart NPK 5-0-1 is added. Each tray is seeded with 250 g fresh duckweed which is about 60% surface coverage. Every seven to ten days, the system is emptied and cleaned down. After fresh water and nutrients have been added, each tray is filled with 250 g of duckweed again. This was carried out for the duration of the experiments.

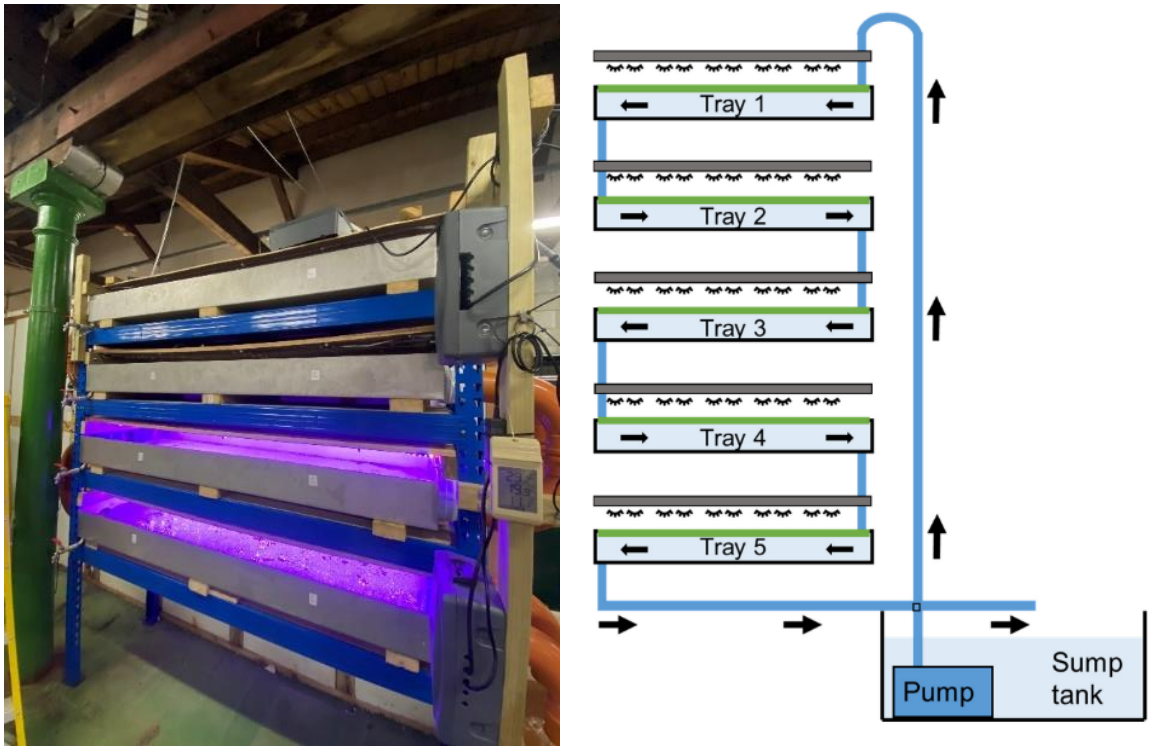

***Figure 20**: The Gibba System a) Photo of system b) Schematic of the Gibba System (Coughlan et al., 2022a)*

3.4 Nutrient Uptake by Duckweed

The analysis of nutrient uptake by duckweed within each system provides novel information on system design and remediation rates. This input is very important due to tightening restrictions in spreading soiled water which was discussed in Chapter One (Department of Food, 2023). The tests referred to in Section *3.4.1* and *3.4.2* below are commonly used to determine the total nitrate and total phosphorus content of soiled water in research and industrial settings.

Samples were collected at the end of each five-day run for the series of duckweed growth experiments in Section *3.3.2*. This allows for the comparison of duckweed growth between the systems, but also determines if there is a difference in remediation rates. Total nitrate and total phosphorus were calculated using the blow method for the IBC with no recirculation, the recirculated IBC, and the recirculated IBC with baffles at inlet velocities 0.3 m s^{-1}, 0.65 m s^{-1}, and 1 m s^{-1}. The samples from all the experiments were stored in the cold room at 4°C. They were then inverted before the tests were carried out to ensure that the solution was homogenous and allowed to reach room temperature. The spectrophotometer used in these experiments was the DR3900 Laboratory Spectrophotometer from Hach. Figure 21 depicts the reaction tubes in the water bath used for both total nitrate and total phosphorus experiments, as well as the spectrophotometer.

Figure 21: *a) Reaction tubes in the water bath b) Spectrophotometer and the reaction cuvettes*

3.4.1 Total Nitrate

The LCK 138 Laton test from Hach was used to measure the total nitrogen in each sample. The referenced manufacturer's guide was followed for this experiment (Hach, 2017).

3.4.2 Total Phosphorus

The test used for the detection of total phosphorus in each sample was from Hach, LCK348 Phosphorus total. The referenced manufacturer's guide was followed for this experiment (Hach, 2020).

4 Results and Discussion

4.1 Tracer Response Experiments

Tracer response experiments were conducted to enhance understanding of the mixing within each system and to validate the CFD models. For these experiments, the tracer HCl was utilised. The movement and dispersal of HCl within the system was quantified to gain further insights into fluid behaviour in the system. HCl was selected as a tracer as it has similar physical properties to water to avoid altering flow dynamics.

4.1.1 Experimental Mixing Time Characterisation

To determine the experimental mixing time, data was collected from three runs within each system. The conductivity in (mS cm^{-1}) was tracked at the outlet of each IBC (with and without baffles). These conductivity values were subsequently correlated with concentrations using the standard curve for HCl. The average of the three runs for each system was then plotted. Figure 22a and 22b depict the plots for Runs 1-3 in the system with no baffles and system with baffles respectively. The graphs represent concentration (mol L^{-1}) against time (minutes).

The experimental mixing time was defined as the value within 5% of the final detected concentration. This indicates when the system has achieved a homogenous concentration (Ascanio, 2015). Each run was concluded when the conductivity meter displayed a steady reading. However, as this was monitored visually, some runs may have ended prematurely. Notably, Run 3 in the system with no baffles is considerably shorter than Runs 1 and 2. As a result, Run 3 was not included when finding the average mixing time. The average mixing time was calculated for both systems as well as the standard error for the replicates. For the system with no baffles, this was determined to be 3.4 ± 2.2 minutes, whereas the system with baffles exhibited a significantly longer mixing time of 7.3 ± 0.2 minutes. The system with baffles had a far lower standard error than the system with no baffles. This shows that the system behaved predictably.

In industries or applications where lower mixing times are advantageous, increased mixing efficiency and reduced costs, the findings are particularly relevant (Yang et al., 2022). As these experiments were typically a period of five to seven days

in length with continuous recirculation, the time taken to reach homogeneity was less critical. Originally intended for validating CFD models, the mixing time experiments were of a lesser focus when ANSYS fluid could not successfully model the recirculated transient system.

4.1.1.1 Plots for Experimental Mixing Time

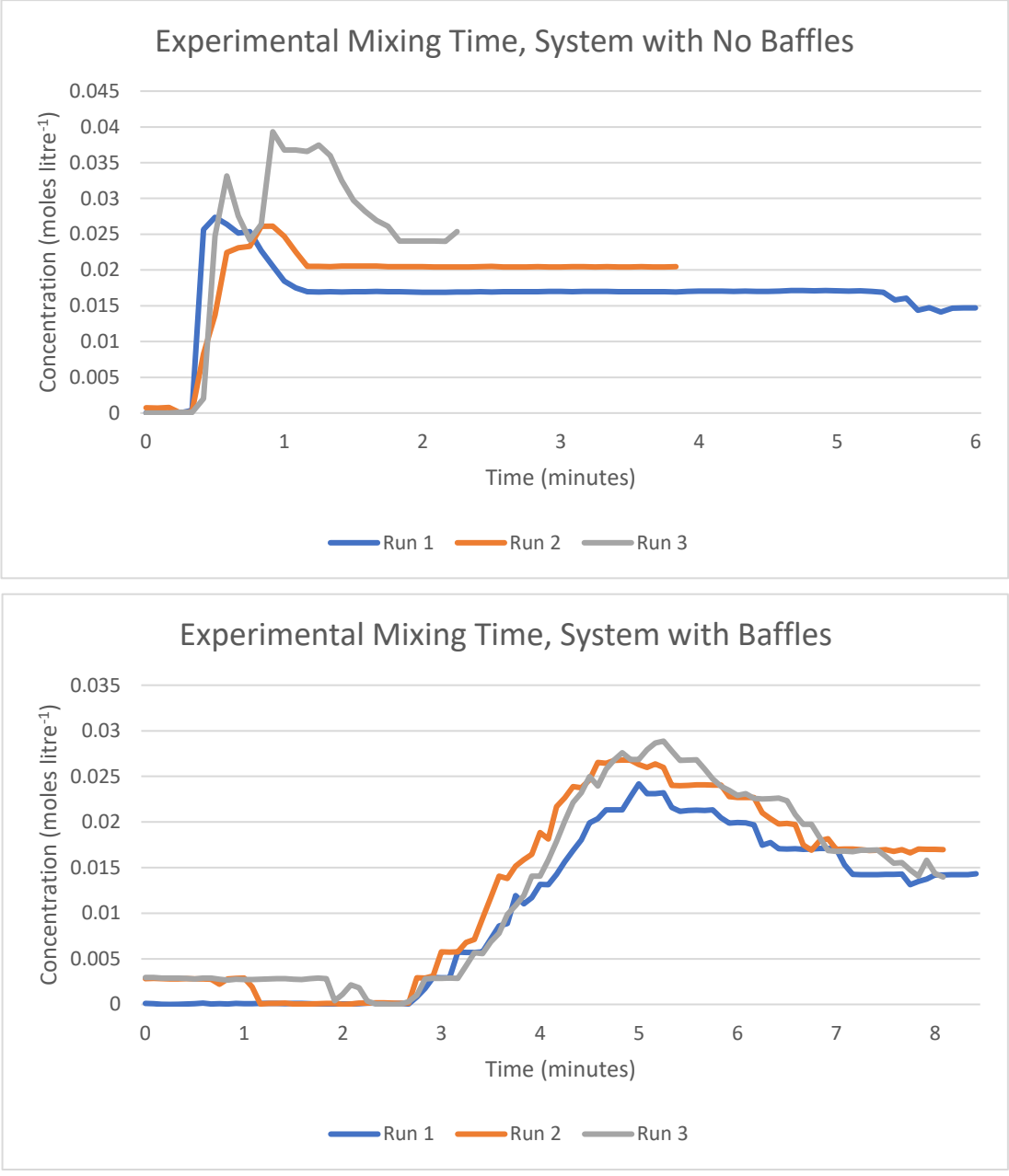

Figure 22: *Experimental Mixing Time Data a) System with no baffles, b) System with baffles*

4.1.2 Experimental Residence Time Characterisation

The residence time of a system, as defined by (Viitanen, 2005), represents the average time that a fluid remains it. In terms of reactor design, experimental residence time holds a particular significance. System design typically accounts for residence time to ensure it is compatible with reaction kinetics. This consideration ensures that sufficient time is allocated for reactions to occur within the system (Hui et al., 2023).

To quantify the residence time of each system, the conductivity at the outlet was continuously monitored over time. Again, employing the standard curve, the conductivities were correlated with their corresponding concentrations. The resulting concentration graphs for the system with no baffles and system with baffles are illustrated in Figures 24 and 25, respectively. Three runs were executed for each system. Given there is a single injection of tracer into the system at the beginning of each experiment, they are categorised as pulse reactions (Fogler, 2006). This influences the shape of the concentration (C) curves depicted in Figure 23. Unlike pulse injections with a single input of tracer, step injections consist of the continuous addition of tracer to the system.

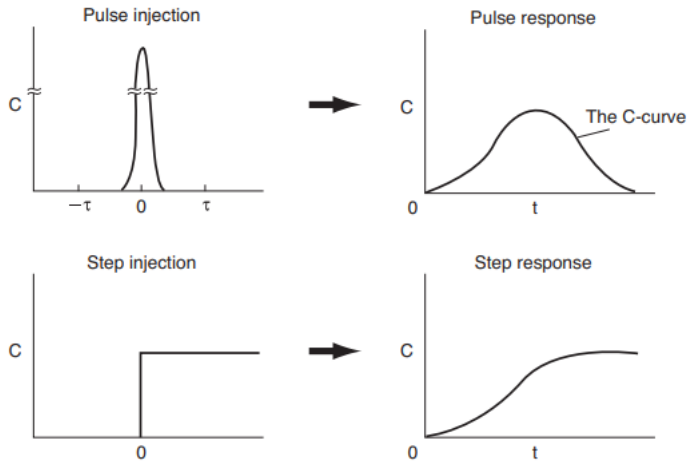

Figure 23: *C(t) Curves for both pulse and step injections (Fogler, 2006)*

To determine the mean residence time τ_m, of the system, a series of calculations must be completed using the data from the concentration curves. Equation 13 defines *E(t)* as the residence time distribution function. Equation 14 defines τ_m, the mean residence time, and Equation 15 defines the variance, σ^2 (Fogler, 2006). MATLAB

was employed to find the area under the curve for each integral. Details of the calculated τ_m, and σ^2 for each system can be found in Tables 15 and 16.

$$E(t) = \frac{C(t)}{\int_0^\infty C(t)\,dt} \quad (13)$$

$$\tau_m = \int_0^\infty t.E(t)\,dt \quad (14)$$

$$\sigma^2 = \int_0^\infty (t-\tau_m)^2 E(t)\,dt \quad (15)$$

The average residence time for both systems was determined to be 756 seconds. However, upon closer inspection of the graphs, it was observed that the tracer concentration in the system with no baffles did not return to 0 mol L^{-1}. This would suggest that the actual residence time of the system may be higher than the experimentally determined value. Equation 16 defines the theoretical residence time, τ_t, where volume (V) is in m^3, and volumetric flow rate (Q), is in $m^3\,s^{-1}$. V is 0.17 m^3, and Q is 0.00035 m^3 s^{-1}. The theoretical residence time for both systems is 486 seconds, a significant deviation from the experimentally determined value.

$$\tau_t = \frac{V}{Q} \quad (16)$$

The addition of a conductivity probe at another position in each tank (for example in the centre), would provide a more holistic view of the residence time in each system. This may explain the difference between the theoretical residence time and the experimentally determined value.

4.1.2.1 System with No Baffles

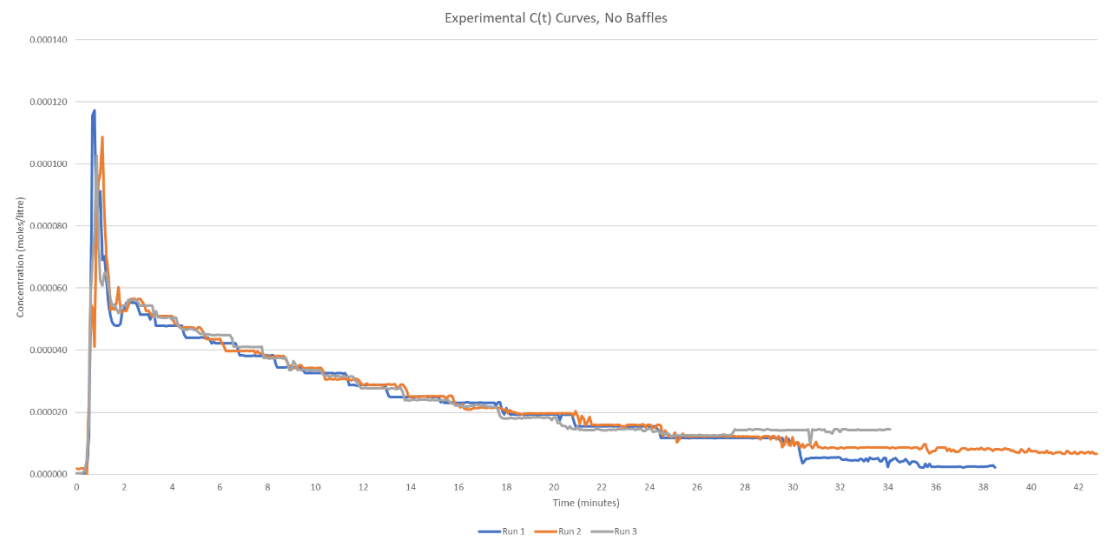

Figure 24: *Experimental C(t) Curves, system with no baffles*

Table 16: *Mean Residence Time and Variance, system with no baffles*

Parameter	Run 1	Run 2	Run 3
Mean Residence Time, τ_m (minutes)	11.9	13.6	12.3
Mean Residence Time, τ_m (s)	711	818	739
Theoretical Residence Time, τ_t (s)	486	486	486
Variance, σ^2 (s^2)	291674	429170	316973

To further refine the results, the residence time experiments could be repeated with additional time given to ensure that all the tracer in the system has been removed. As there is high variance, the runs are less likely to be uniform. Changes to experimental setup like working with higher concentrations of HCl may improve this.

4.1.2.2 System with Baffles

The C(t) acquired from the system with baffles are more consistent. They follow the expected curve reported by (Fogler, 2006) for pulse injections. Unlike the system with no baffles, the concentration of the tracer returned to 0 mol L^{-1} at the end of each replicate.

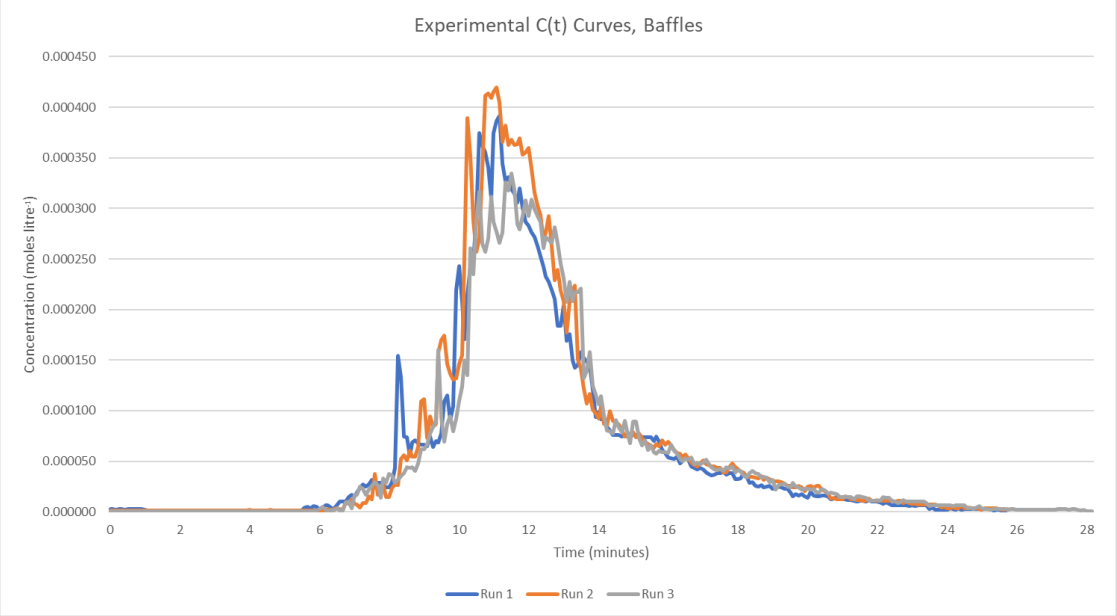

***Figure 25**: Experimental C(t) Curves, system with baffles*

There is close agreement between the mean residence times in each replicate, as depicted in Table 17. This highlights the reproducibility and reliability of the data. The variance values are relatively low, which suggests a tight distribution of residence times around the mean. This indicates that the system will behave in a more uniform manner over a series of replicates in comparison to the system with no baffles.

***Table 17:** Mean Residence Time and Variance, system with baffles*

Parameter	Run 1	Run 2	Run 3
Mean Residence Time, τ_m (minutes)	12.4	12.5	12.9
Mean Residence Time, τ_m (s)	745	752	773
Theoretical Residence Time, τ_t (s)	486	486	486
Variance, σ^2 (s^2)	31555	32612	32683

4.2 CFD Modelling

In this thesis, CFD Modelling was served as an important tool to comprehend fluid flow within each experimental setup. A comprehensive exploration involved 21 models in the steady state. This included 15 models in the mesh independence study. Each model yielded a range of data, encompassing critical parameters such as the velocity of the fluid interface with air (open boundary), maximum velocity at the open boundary, minimum velocity at the open boundary, and the percentage of stagnant cells in each system. Additionally, two distinct models were run in the transient state for the validation of both models.

4.2.1 Validation of CFD Models

The validation process included a rigorous comparison of data collected from the experimental residence time runs with the simulation data. The CFD model was configured to simulate species transport. This entailed a tracer with identical properties to water being injected from the outlet, which ensured there was minimal disruption to fluid flow dynamics. The concentration of the tracer was tracked at the outlet in mol L^{-1} over time. To quantify the data, the residence time distribution function was computed for each data set, and E(t) curves were generated. These are depicted in Figures 26 and 27. For comparative purposes the data was normalised using Equation 17.

$$\text{x normalised} = \frac{\text{x}-\text{x}_{\text{min}}}{\text{range}} \qquad (17)$$

Here x_{min} represents the smallest recorded value of x and the range is given by $x_{maximum}$-x_{min}. The validation procedures adopted in this study followed similar methodologies to that in literature, specifically focusing on the determined residence time of an injected tracer (Maguire et al., 2023, Upender et al., 2021).

4.2.1.1 System with No Baffles

In Figure 26, the visual comparison of the three experimental replicates with the simulation residence time data is shown. The simulation data is a noteworthy visual alignment with the experimental replicates, showcasing a close match in the four peaks and their respective tails. This visual congruence reinforces the precision of the CFD

model in accurately representing the IBC with no baffles. However, a distinctive feature is the elongated tail of the simulation curve compared to that of the experimental replicates. The velocity contour in Section *4.1.1.1*, highlights the short circuiting and dead zones present in this system. This would explain the initial spike in the graph in Figure 26, with a large portion of the tracer exiting at the path of least resistance. This bypassing present in this system is considered poor mixing and is one of the reasons the theoretical residence time was different from the experimentally determined value.

Notably, the prolonged tail in the simulation curve does not seem indicative of an overestimation of tracer dispersal in the IBC. Instead, it highlights a limitation of the experimental work. The tails of the experimental replicates do not reach 0 E(t), signalling premature endings to each replicate. Had the experiments run until all the tracer had exited the tank, it is assumed that the results would align more closely with the simulation. This premature termination of the experiments is attributed to experimental error, as conductivity readings were visually interpreted to determine when all the tracer had left the IBC.

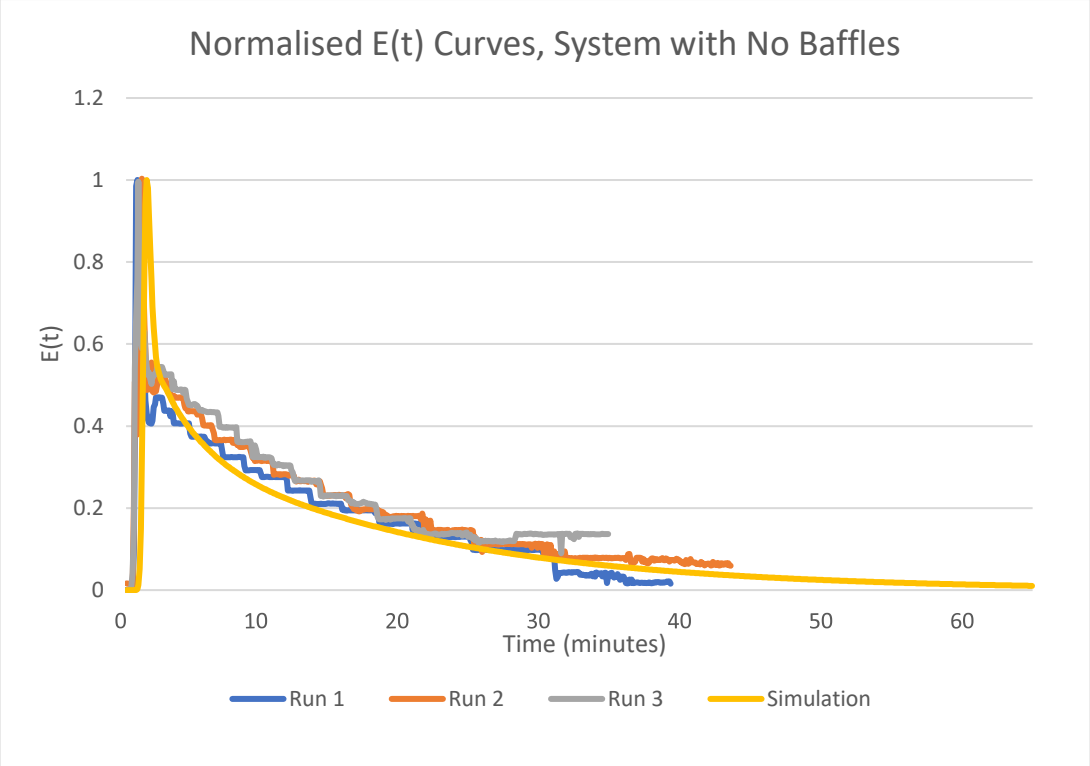

***Figure 26**: Normalised E(t) Curves, system with no baffles*

For the comparative analysis between the CFD model and experimental replicates, simulation data up to approximately 45 minutes was considered. This corresponds to the duration of the experiments. Equations 13-15 were utilised to calculate the mean residence time and variance of the simulation, and Table 18 presents a comprehensive comparison between the simulation and experimental runs.

Table 18: *System Residence Time, Variance, Deviation*

System with No Baffles				
Parameter	**Run 1**	**Run 2**	**Run 3**	**Simulation**
Mean Residence Time τ_m (s)	711	818	739	781
Deviation (%)	-8.9	4.7	-5.4	n/a
Variance, σ^2 (s^2)	291674	429170	316973	403265
Standard Deviation (s)	540	655	563	635

The deviation, ranging from -8.9% to 4.7%, falls within an acceptable range, aligning with deviations reported in the literature for similar studies (Upender et al., 2021, Zhang et al., 2014). Moreover, both variance and standard deviation values were consistent with the simulation data. Based on this comprehensive comparison, the CFD model appears to accurately represents the experimental setup, acting as a robust validation for the CFD model.

4.2.1.2 System with Baffles

The normalised E(t) Curves for the system with baffles are presented in Figure 27. The curve, especially the experimental curves highlight the plug-flow nature of the IBC with baffles. All the tracer exists the system in a similar timeframe. This is very different from the residence time distribution present in the IBC with no baffles. In contrast to the E(t) curves of the system with no baffles, the simulation curve does exhibit a close alignment with the replicate curves. Notably, there appears to be an overestimation of tracer dispersal in the system, evident in the significantly higher variance of the simulation compared to the replicates' variance. This discrepancy could be attributed to the selection of the turbulent viscous model, as discussed by (Zapata et al., 2021). Additionally, errors may have been introduced during the experimental setup, especially when working with low concentrations of HCl, where the sensitivity of the conductivity probe, and external environmental influences could impact the results. The extended tails of each curve, as noted by Fogler et al., may

introduce significant inaccuracies in both experimental and simulation data (Fogler, 2006). Despite the observed discrepancies, the deviation ranging from -14 to -17%, falls within a reasonable range found in literature for similar work (Maguire et al., 2023). For the purpose of this thesis, the model was deemed a sufficiently accurate representation of the IBC with baffles. However, acknowledging the potential for improvement, future work could be directed towards addressing the discrepancies. This may involve further refinement of the mesh, redesigning the experimental setup, and adjustments to the CFD model settings to enhance the accuracy of the validation.

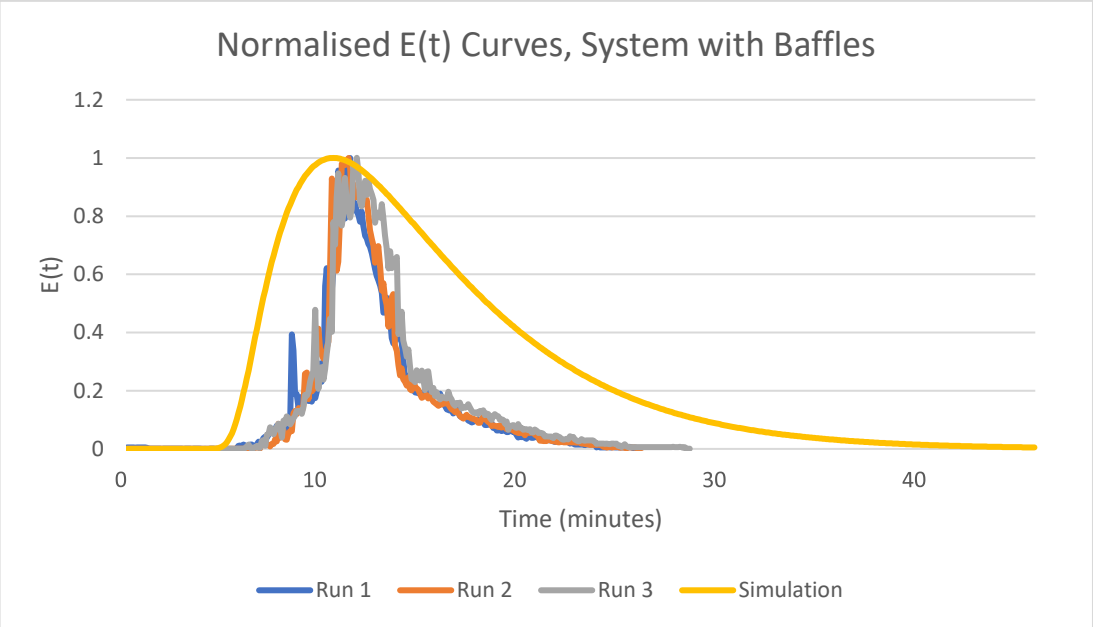

Figure 27: *Normalised E(t) Curves, system with baffles*

Table 19: *System Residence Time, Variance, and Deviation*

System with Baffles				
Parameter	**Run 1**	**Run 2**	**Run 3**	**Simulation**
Mean Residence Time τ_m (s)	745	752	773	896
Deviation (%)	-17	-16	-14	n/a
Variance, σ^2 (s^2)	31555	32612	32683	184687
Standard Deviation (s)	178	181	181	430

In conclusion, both CFD models serve as equitable representations of the IBC with no baffles and IBC with baffles. The thorough validation of these models ensures that the extracted data regarding velocities and stagnant volumes can be considered an

accurate representation of the experimental model, and meaningful conclusions can be drawn from the study.

4.2.2 Characterisation of Experimental Setups

The CFD models were employed to investigate the impact of varying inlet velocities on fluid flow within the system, specifically focusing on understanding the surface velocity experienced by duckweed. Duckweed typically is found floating on the surface of slow-moving water bodies (Leng, 1999). The CFD models facilitated the prediction of the surface velocities in each experimental setup. A field study was carried out by Janauer et al., and L. minor was found to be present in water with a velocity below 0.05 m s^{-1} (Janauer et al., 2010). The literature also indicated an upper limit of 0.1 m s^{-1} for such conditions (Giblin et al., 2014, Coughlan et al., 2022ba.

The area-weighted average velocity at the open boundary, along with the vertex maximum and vertex minimum velocities in each model, are presented in Table 20. This comprehensive analysis increases the understanding of water velocities experienced by the duckweed. Section *4.3* will delve more into the implications of water velocities on the RGR of duckweed. Notably, the presence of baffles creates a substantial reduction in the average surface velocity in the system, while the maximum velocity remains relatively consistent. The results suggest that at higher inlet velocities, the IBC with baffles may provide more favourable conditions for duckweed growth. This analysis lays the groundwork for evaluating the potential impact on duckweed growth, which is explored in Section *4.3*.

***Table 20**: Surface Velocity Analysis*

Type	Flow rate ($m^3 s^{-1}$)	Inlet Velocity (m s^{-1})	Area-weighted average velocity (m s^{-1})	Vertex Maximum (m s^{-1})	Vertex Minimum (m s^{-1})
Baffles	0.000094	0.3	0.005	0.02	7.00E-07
Baffles	0.00020	0.65	0.01	0.055	1.50E-06
Baffles	0.00031	1	0.02	0.08	1.00E-06
No Baffles	0.000094	0.3	0.01	0.02	2.00E-05
No Baffles	0.00020	0.65	0.03	0.06	2.00E-04
No Baffles	0.00031	1	0.045	0.1	2.00E-04

4.2.2.1 Dead-Zone Analysis

In the context of this analysis, the definition of a dead or stagnant zone has been derived from (Vesvikar and Al-Dahhan, 2005), as cited in (Sadino-Riquelme et al., 2022). According to this definition, a stagnant zone is characterised as a region where the velocity of fluid is less than 5% of the maximum velocity (Vesvikar and Al-Dahhan, 2005). The quantification of stagnant zones in each model was achieved using the cell register function. Employing the field variable setting, the number of cells with a velocity magnitude below 5% of the maximum velocity (Vmax) was computed. The stagnant volume is presented as the ratio of cells with a velocity of less than 5% the Vmax experienced in the volume. The results of this analysis can be seen in Table 21. Notably, the system with baffles exhibited a lower ratio of stagnant volume cells compared to the system with no baffles, which is further highlighted in Table 22. Baffles increase the turbulence of the system and promote mixing. This mixing is beneficial as it prevents nutrients settling at areas of stagnation within the tank.

Table 21: *Stagnant Volume Analysis*

Model	Type		Number of Cells Total	Number of Cells V < 0.05*Vmax	Stagnant Volume (%)
1	Baffles		44717	34450	77
2	Baffles		53394	42511	80
3	Baffles		77821	66114	85
4	Baffles		129827	116429	90
5	Baffles		180371	165705	92
6	Baffles		272577	250301	92
7	Baffles	Mesh	421697	392294	93
8	Baffles	Independence	495528	464227	94
9	Baffles		496049	415789	84
10	Baffles		496049	412313	83
11	Baffles	Effect of Flow rate	496049	389294	78
12	No Baffles		42834	27357	64
13	No Baffles		57363	36346	63
14	No Baffles		72011	51451	71
15	No Baffles		99559	76943	77
16	No Baffles		142741	110566	77
17	No Baffles	Mesh	218506	168088	77
18	No Baffles	Independence	353382	283593	80
19	No Baffles		411151	365196	89
20	No Baffles		411151	355113	86
21	No Baffles	Effect of Flow rate	411151	352874	86

Table 22: *Direct comparison of the % stagnant volume in the system with baffles and the system without baffles*

Inlet Velocity ($m\ s^{-1}$)	System with Baffles		System without Baffles	
	Model	Stagnant Volume (%)	Model	Stagnant Volume (%)
0.3	9	84	19	89
0.65	10	83	20	86
1	11	78	21	86

This detailed analysis highlights the influence of baffles in mitigating stagnant zones. This confirms their role in promoting efficient mixing. The lower percentages of stagnant zones in the system with baffles may suggest that nutrient distribution within the system is more homogenous.

4.3 Relative Growth Rate of Duckweed

The RGR experiments served as a means of understanding the relationship between system design and duckweed growth. While there is notably a scarcity of studies in the existing literature that explicitly focus on the influence of design on duckweed growth, the literature review revealed an intriguing gap regarding the impact of baffles or a raceway-style system on duckweed growth. Notably, no study identified during the literature review highlighted the specific effects of these systems on duckweed cultivation in comparison to ponds.

Contrastingly, raceway-style systems have been successfully implemented in various contexts for duckweed cultivation as evidenced by studies from (Stejskal et al., 2022), and their adoption in industrial settings. Ponds are a more conventional choice that are widely employed with similar production rates, as demonstrated by (Mohedano et al., 2012). The introduction of raceway-style systems, while potentially resulting in higher construction costs, is an intriguing prospect for the optimisation of duckweed cultivation.

Notably, academic and industrial discourse on the explicit reason behind the choice in design for a cultivation system is limited. This knowledge gap emphasises the importance of investigating and comprehending distinct design choices for duckweed cultivation. Subtle alterations in system design can have a sizeable impact on growth rates and the efficiency of a system.

4.3.1 Location-Focused Growth Rate Experiments

In order to investigate the impact of system design on RGR of duckweed, a comparative study was completed between two setups: the IBC with no baffles and the IBC with baffles. The overall results are visually represented in Figure 28. To assess the growth performance of duckweed, the RGR values were interpreted based on the following criteria:

- 0.2 to 0.3 d^{-1}, excellent growth
- 0.2 d^{-1}, good growth
- <0.15 d^{-1}, poor growth

This is based on work published in the literature regarding duckweed RGRs, specifically *L. minor* (Petersen et al., 2021, Chakrabarti et al., 2018, Ziegler et al., 2014).

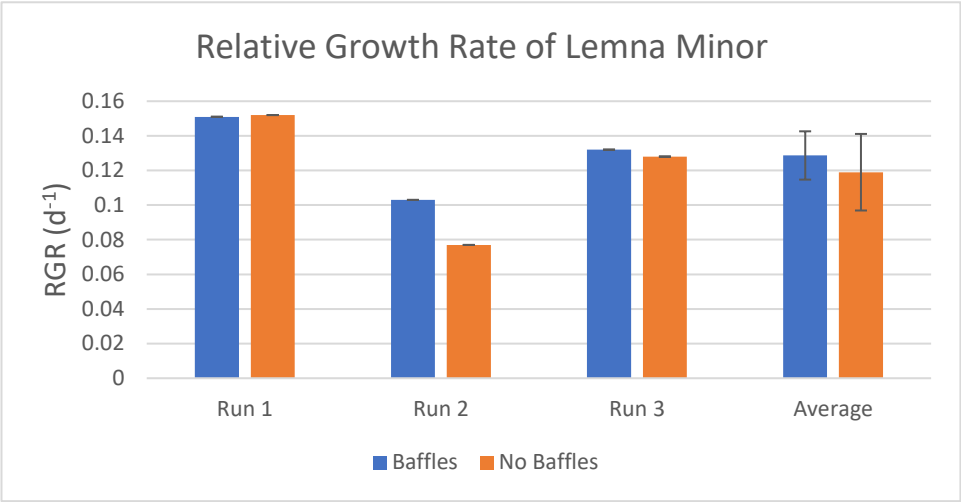

Figure 28: *Location Focused RGR Experiments*

The experiments, detailed in Figure 28, comprised of three replicates. Each replicate was a total of seven days. On day 0 the tanks were inoculated and day 7 the biomass was weighed. Additional information on how the RGR was calculated can be found in Section *3.3.3.* The two systems were run in parallel for each replicate. This ensured that in each replicate, both systems experienced the same light intensity, and temperature. This would explain trends in RGR between each run. More details on the environmental factors such as light intensity and temperature can be found in Section *4.3.1.3.* These experiments involved a liquid depth of 0.65 cm, and an inlet velocity of 0.3 m s^{-1}.

The average RGR of the system with baffles in 0.13 d^{-1}, while it was 0.12 d^{-1} for the system with no baffles. Despite both RGR values falling into the category of 'poor growth', it must be taken into consideration that only 1/6 optimal strength of hydroponics were used for the experiments. The intentional effect of limiting nutrients was in an attempt to investigate whether differences in mixing and fluid flow would affect the RGR. A standard error calculation was applied to each system, which revealed that the observed differences were not statistically significant. This outcome suggests that under conditions of limiting nutrients and low inlet velocities there is minimal difference in duckweed growth between the two systems.

4.3.1.1 System with No Baffles

In further efforts to discern any location-specific impact of fluid flow on RGRs, tools were employed to focus on the effect of location on duckweed growth. The

results of this examination are illustrated in Figure 29, providing insights into the correlation between location and RGR. Figure 30 complements these findings, depicting a velocity contour obtained from ANSYS Fluent. The red region by the inlet is the area of highest velocity. For this analysis, five small rings were positioned on the surface of the tank, and the RGR for each ring was calculated on day 5. Ring 3 had a slightly higher average RGR. Notably, Ring 1 situated directly above the inlet did not have a lower RGR even though it was subject to higher velocities.

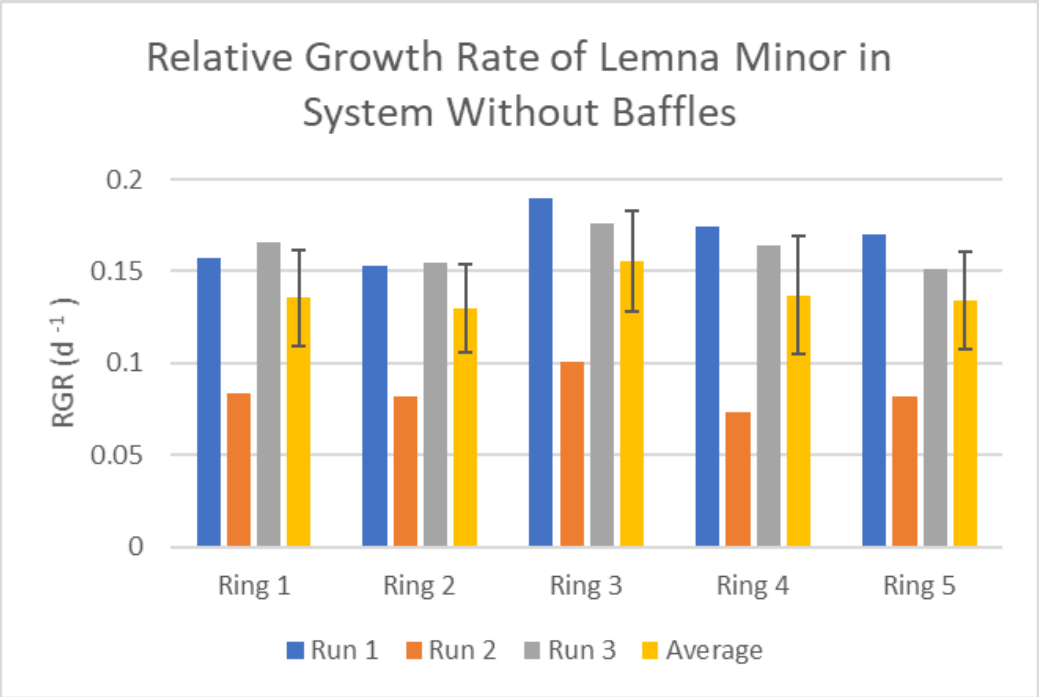

***Figure 29**: Impact of Location on RGR, System with no Baffles*

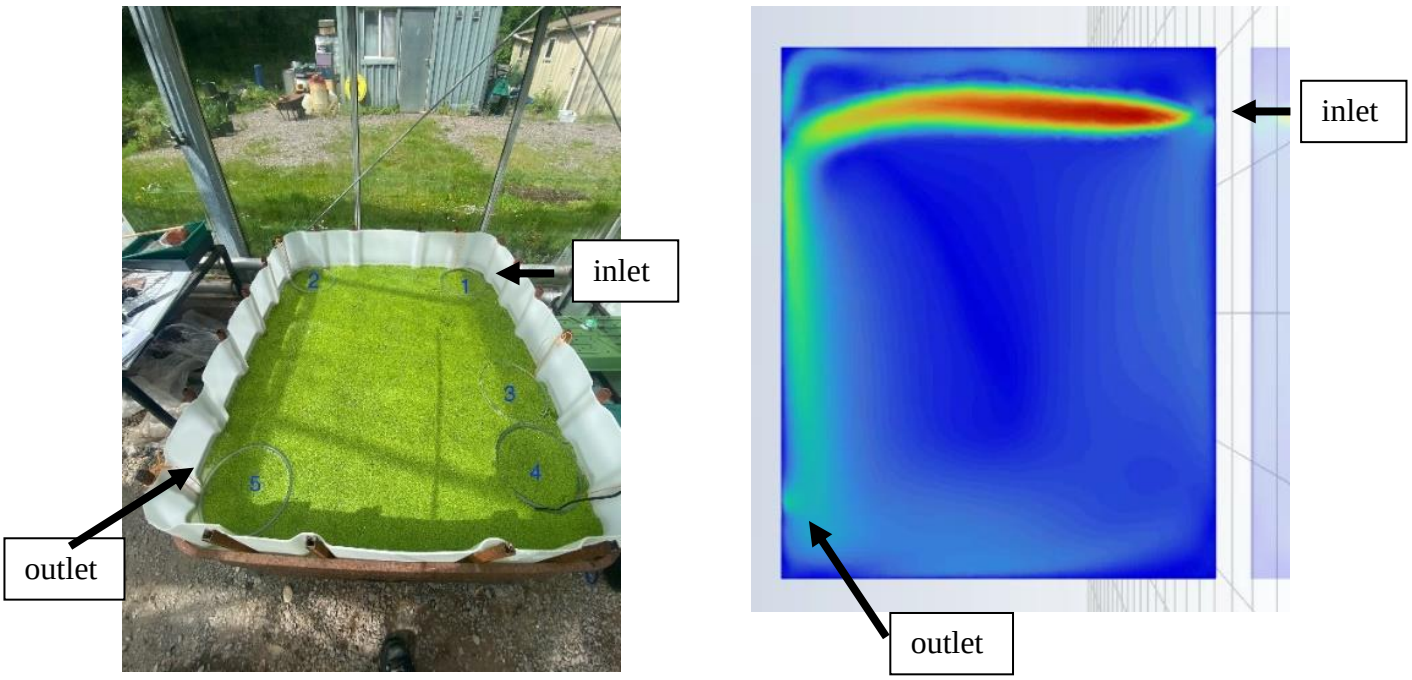

Figure 30: *a) Numbered Rings b) Velocity Contour of IBC with no Baffles (XZ Plane)*

4.3.1.2 System with Baffles

Following a similar approach, four rings were positioned on the surface of the IBC with baffles. The results are illustrated in Figure 31 revealing a noteworthy observation. Ring 2 exhibited a significantly higher RGR compared to the other rings. The surface velocity was found to be approximately 0.004 m s^{-1} using ANSYS Fluent Post-Processing. This is similar to the average surface velocity of 0.0045 m s^{-1}. Ring 1 experienced a higher surface velocity of 0.01 m s^{-1}, while rings 3 and 4 had surface velocities in the range of 0.0003 to 0.001 m s^{-1}. This suggests that duckweed prefers an intermediate velocity that allows for nutrient mixing without disruption of the plant. It could also be the case that Ring 2 is a sweet spot for higher nutrient concentrations, as RGRs appear to fall for Rings 3 and 4. Further work is required to fully understand the effect of the location of Ring 2 on RGR, but such analysis is beyond the scope of this thesis. Figure 32 provides further context and shows the location of the rings as well as the velocity contour of the system with baffles.

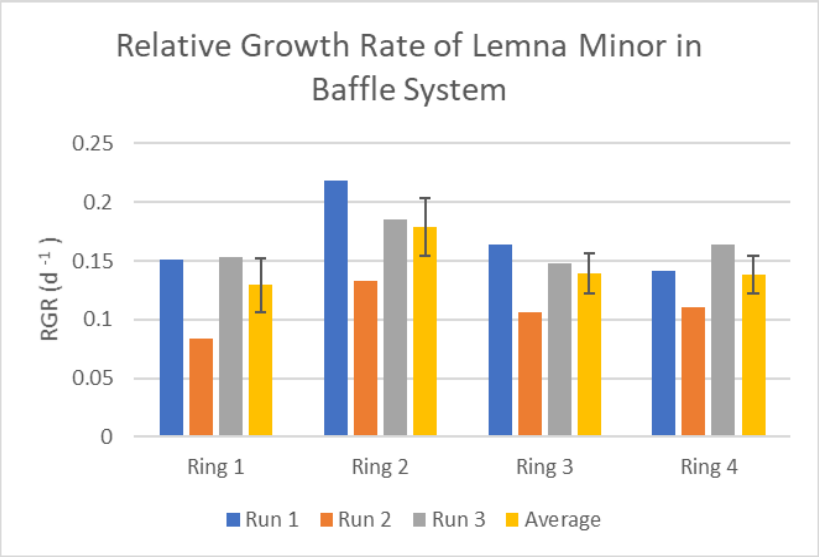

Figure 31: *Impact of Location on RGR, System with Baffles*

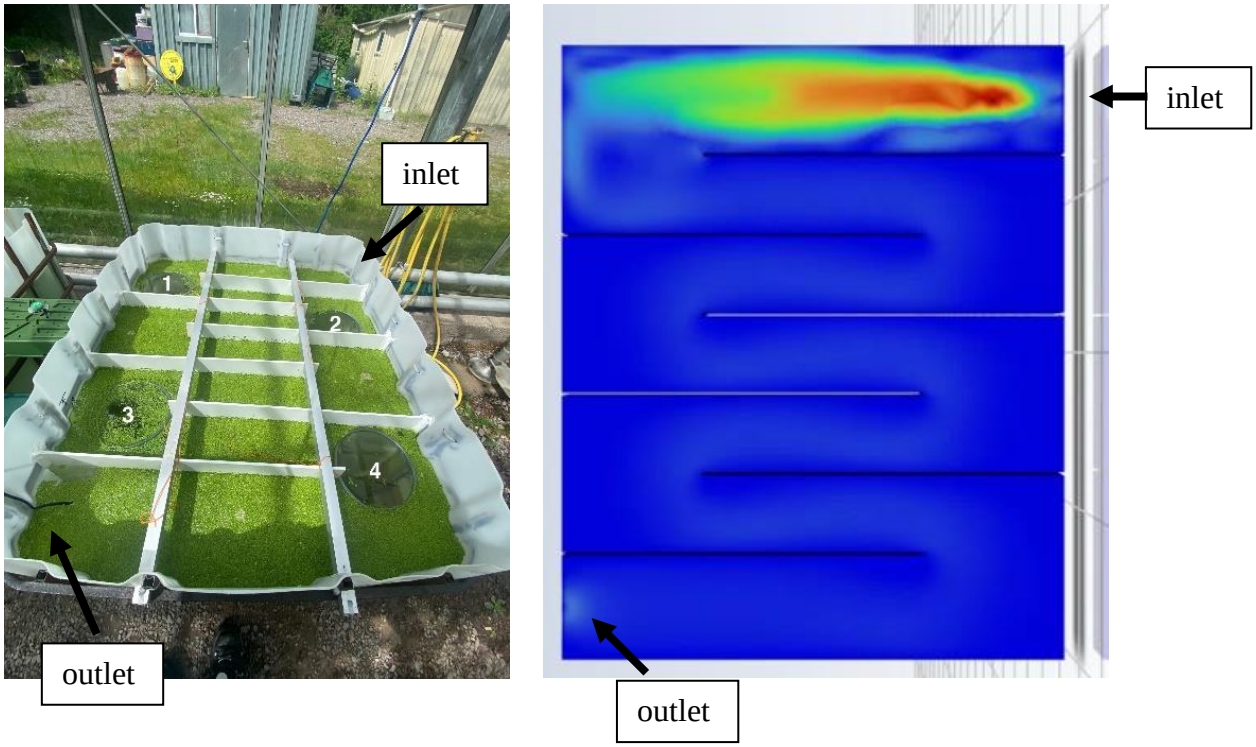

Figure 32*: a) Location of rings, b) Velocity contour of IBC with Baffles*

4.3.1.3 The Impact of Light Intensity and Temperature on RGR

The light intensity and temperature were tracked throughout the course of this research using a HOBO MX2202 Bluetooth Waterproof Temperature / Light Data Logger. The results graphs, Figures 33 and 34 illustrate the difference in these

parameters during the replicates for each set of RGR experiments. The standard error of each run was calculated and is represented by the error bars.

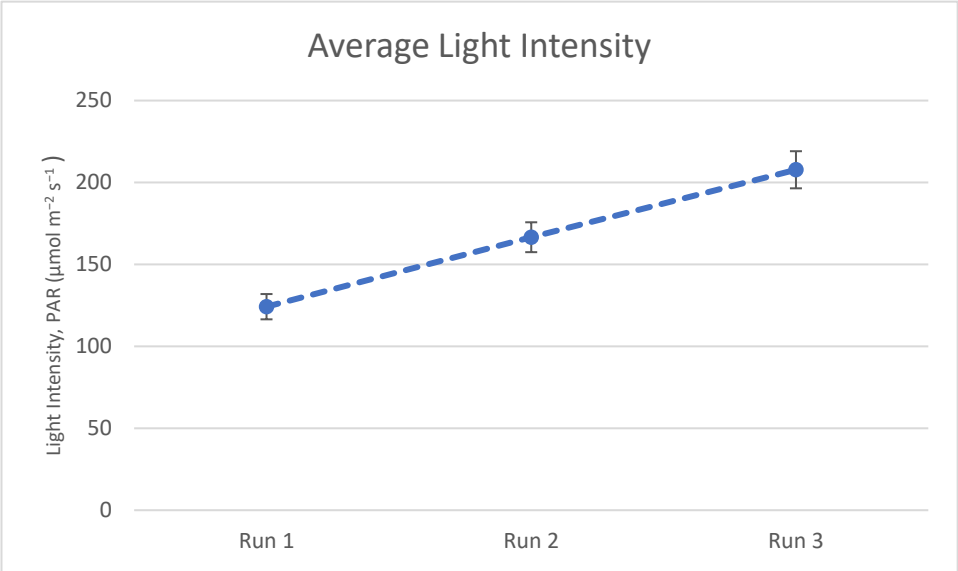

Figure 33: *Average Light Intensity - Location Focused Experiments*

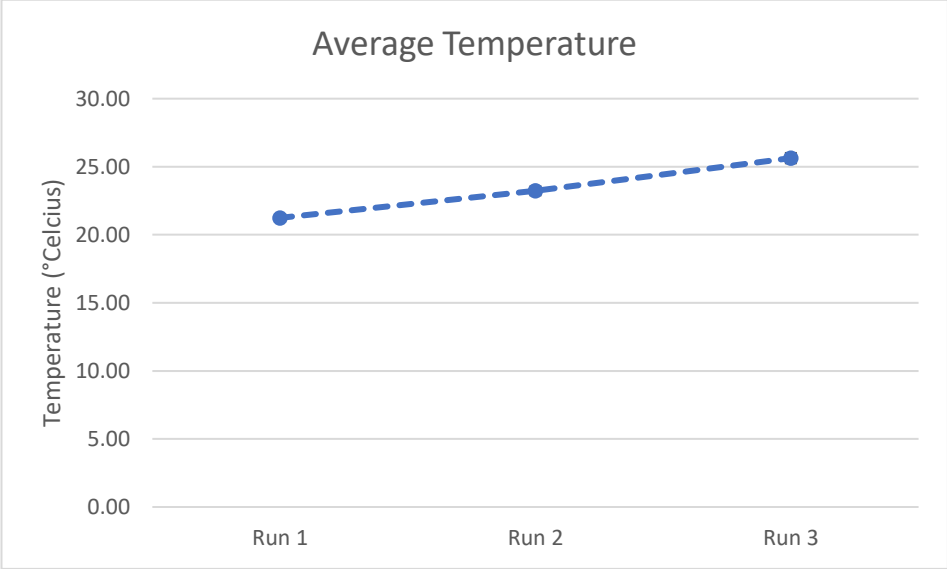

Figure 34*: Average Temperature - Location Focused Experiments*

4.3.2 Relative Growth Rate Experiments- Three Systems

The second phase of RGR experiments extended the scope to three IBCs, providing a more comprehensive understanding of the impact of fluid flow on RGRs. Two IBCs had recirculated flow, namely "recirculation (no baffles)", and "recirculation (baffles)". Additionally, a third standalone IBC was employed. This standalone IBC represented a stagnant tank with no fluid flow or mixing throughout each experiment (total of nine runs). For the purpose of this discussion, it is referred to as "no recirculation". This was used to provide a more holistic view on the effect on mixing in tanks, and its potential benefits for duckweed growth. There were 9 runs in total for this set of experiments. Refer to Table 15 in Section *3.3.2* for the experimental design and details of each run.

4.3.2.1 Raw Data

*In each set of results, the IBC with no recirculation has no inlet velocity. The inlet velocity of the two recirculated tanks is referred to in the title of each graph for clarity.

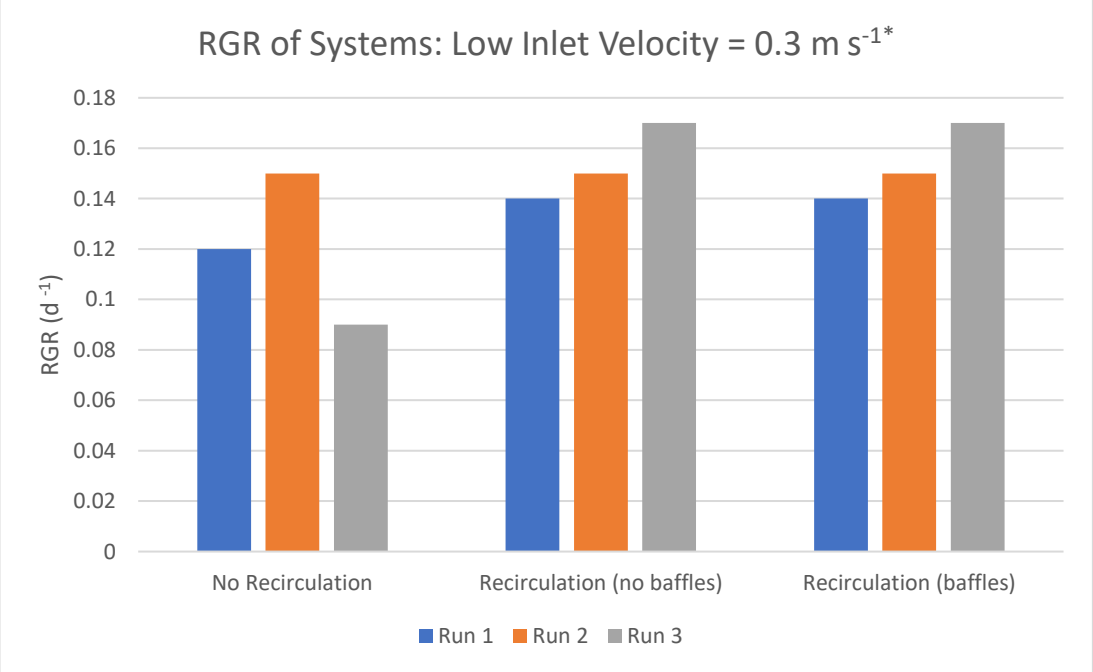

Figure 35: *RGR in each system for Runs 1 – 3 (low inlet velocity)*

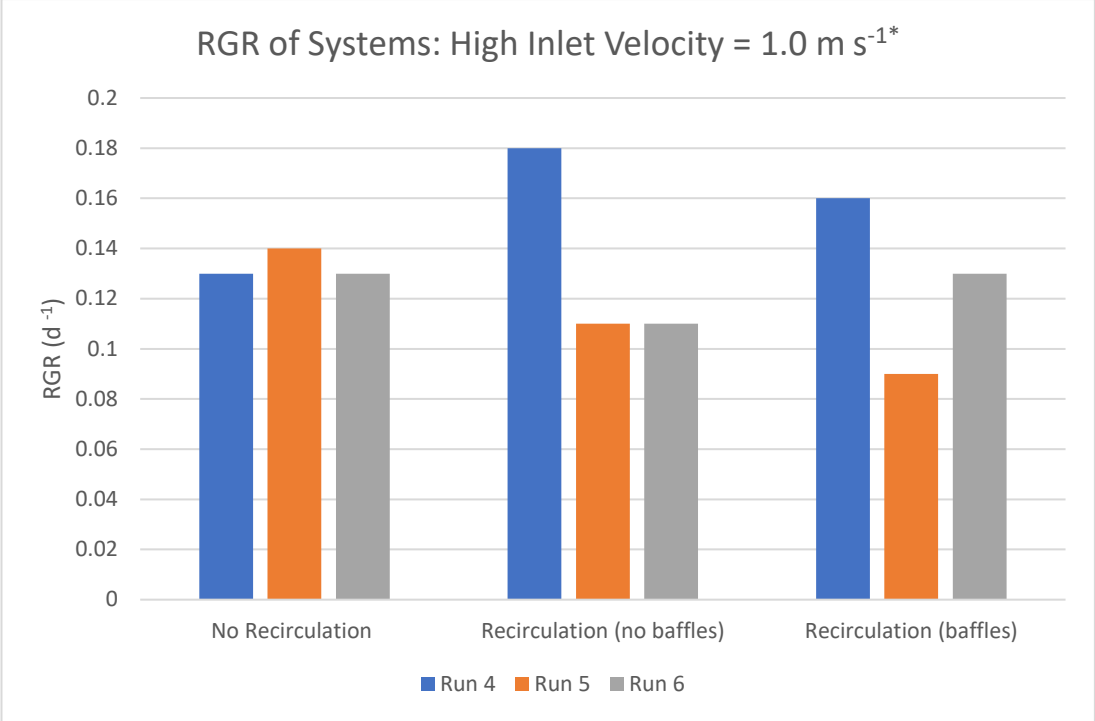

Figure 36: *RGR in each system for Runs 4 - 6 (high inlet velocity)*

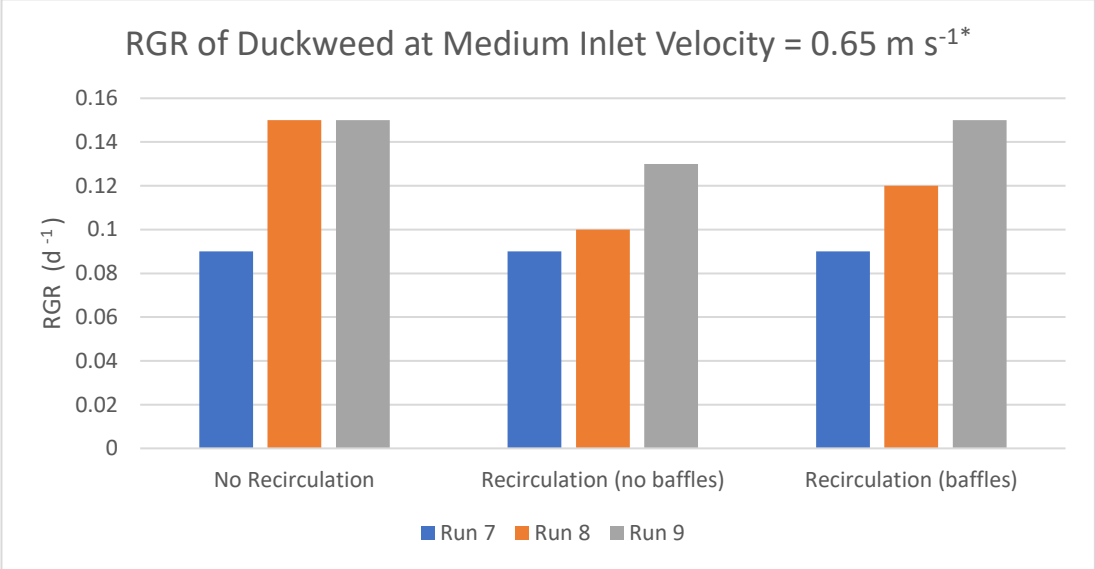

Figure 37: *RGR in each system for Runs 7 - 9 (medium inlet velocity)*

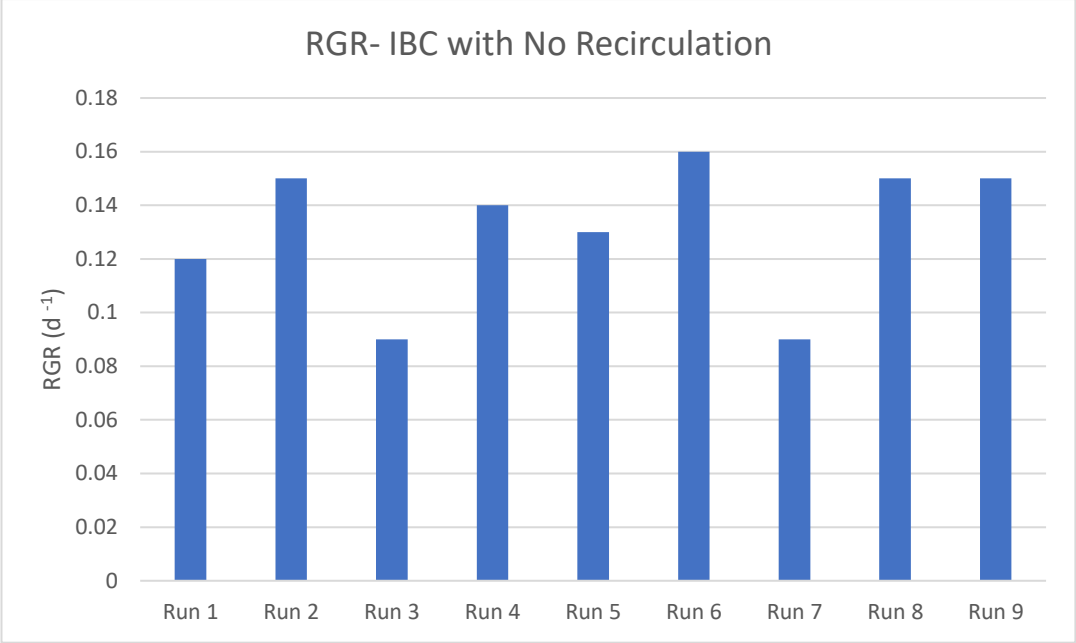

***Figure 38**: RGR in the IBC with no recirculation over 9 runs*

4.3.2.2 The Impact of Light Intensity and Temperature on RGR

These experiments run from the beginning of August 2023 to the middle of September 2023. The lower inlet velocity replicates were first (runs 1-3), followed by the high inlet velocity (runs 4-6), and medium inlet velocity replicates (runs 7-9), respectively. This is illustrated by the dip in the graphs of Figure 39, and Figure 40 for the medium inlet velocity replicates, as those took place later in the year.

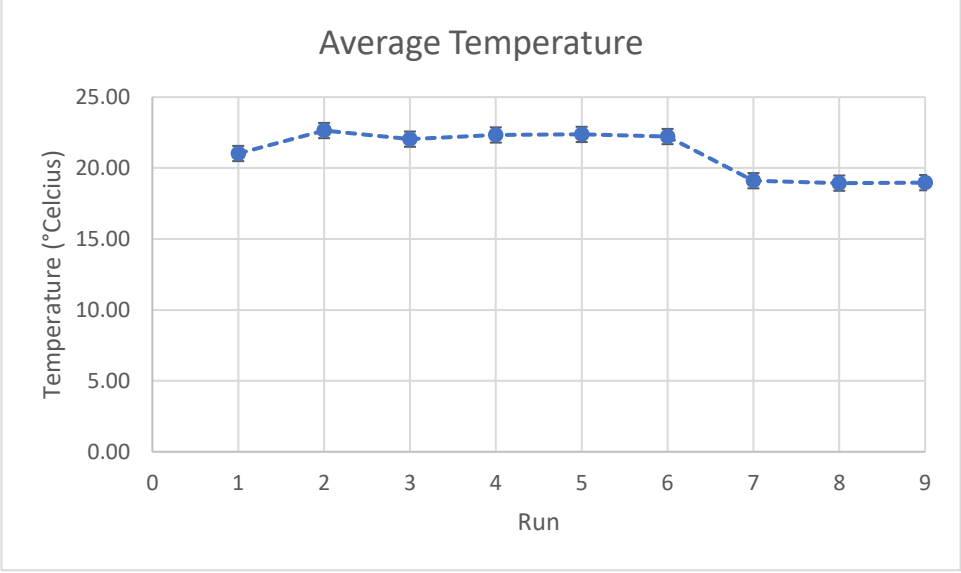

***Figure 39:** Average temperature over 9 runs*

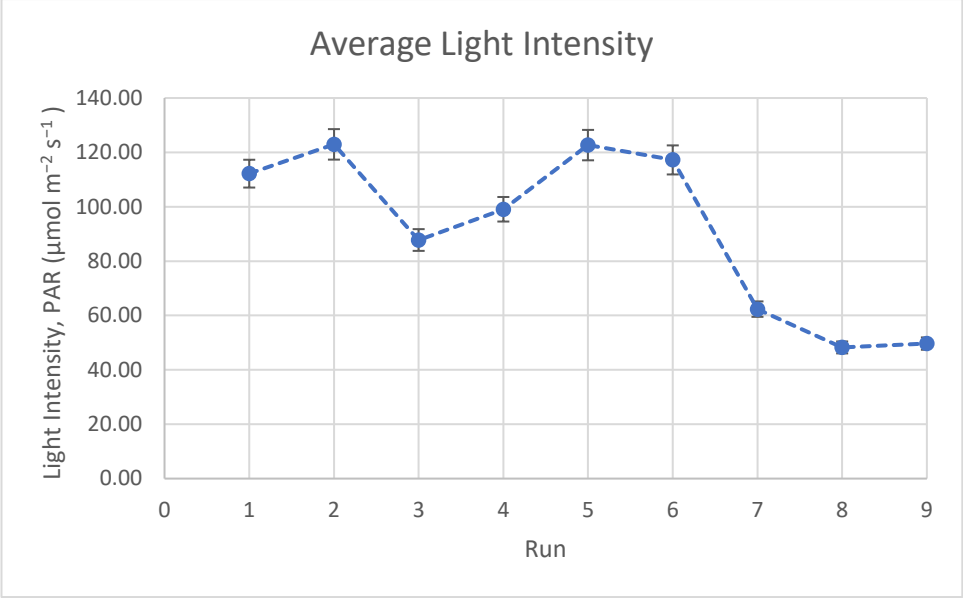

Figure 40: *Average light intensity over 9 runs*

4.3.2.3 System Comparison

The experiments were carried out at three inlet velocities (0.3 m s^{-1}, 0.65 m s^{-1}, 1.0 m s^{-1}), with three replicates conducted for each velocity. The results are depicted in Figure 42, which provides a comprehensive overview of RGRs in the three systems. As highlighted in Section *4.3.2.2*, each of the 9 runs experienced different temperatures and light intensity as they were carried out outdoors. This is a limitation of the experiments as it is difficult to draw hard conclusions from the data when the RGR of each run may have been affected by these environmental factors.

Figure 41 represents the summary of the raw data presented in Section *4.3.2.1*. It offers a more holistic picture of the impact of fluid flow and inlet velocity on the RGR of duckweed in each system. The standard error was calculated from the 3 replicates of each scenario. At the lowest inlet velocity, 0.3 m s^{-1}, there is no difference in RGR between recirculation (no baffles) and recirculation (baffles). However, the IBC with no recirculation exhibited reduced growth. Interestingly, during the runs at the higher inlet velocities, the tank with no recirculation demonstrated the highest RGR, while both recirculated tanks experienced a reduction in RGR. This shows that higher inlet velocities may have a negative impact on RGR. Notably, when comparing recirculation (no baffles) and recirculation (baffles), recirculation (baffles) had a higher RGR at higher inlet velocities of 0.65 m s^{-1} and 1.0 m s^{-1}. This observation aligns with the earlier discussion in Section *4.2.2*, where the presence of baffles was

found to significantly reduce average surface velocities, which has a positive effect on the RGR of duckweed.

At face value, the experiments highlight the positive impact of low inlet velocities the duckweed growth. At an inlet velocity of 0.3 m s^{-1}, recirculation (no baffles) and recirculation (baffles) had higher RGRs than the IBC with no recirculation that was run in parallel. This illustrates the positive impact of low levels of mixing on duckweed growth. When the tanks with recirculation experienced higher inlet velocities (0.65 m s^{-1} and 1.0 m s^{-1}), duckweed growth was negatively affected, and the stagnant tank had a higher RGR. Notably, at higher inlet velocities, the presence of baffles positively influenced RGR.

In terms of statistical analysis, multi-linear regression was carried out for each system. The goal of this was see if there was statistical significance to the relationship between inlet velocity and RGR. The results acquired from this study can be found in Appendix 5. In for each system, IBC with recirculation, and IBC with recirculation and baffles, the relationship between inlet velocity and RGR had a p value > 0.05, meaning the findings were not statistically significant. Therefore, hard conclusions cannot be drawn from the data presented in Figure 41.

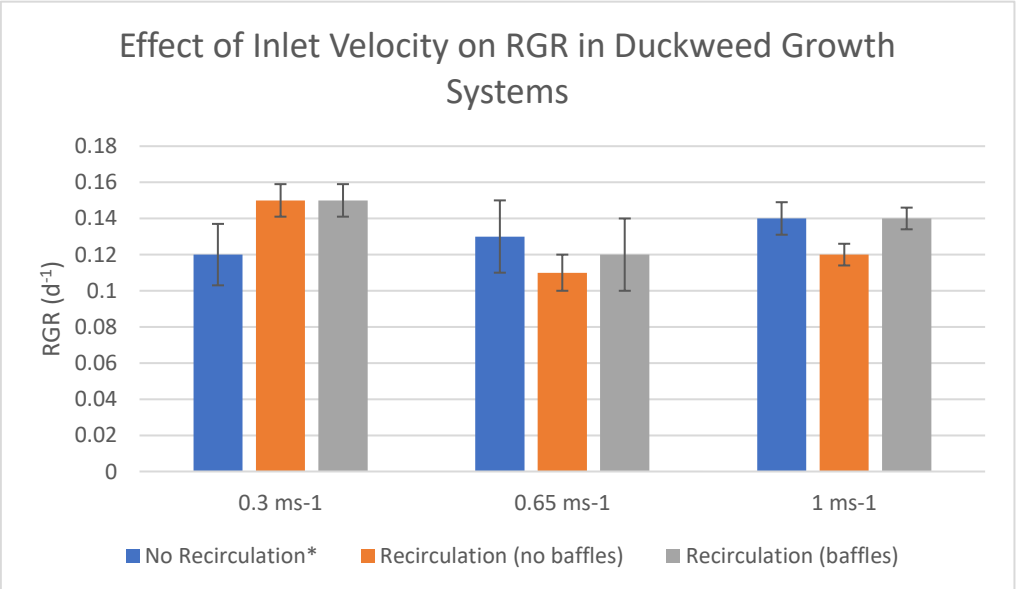

Figure 41: *Impact of Fluid Flow on RGR in Duckweed Cultivation Systems. *The no recirculation (blue bar) represents the IBC with no recirculation that was run in parallel to the recirculated systems. They are grouped by inlet velocity as the data was collected during the same run. The inlet velocity was not applied to the stagnant IBC.*

4.4 Nutrient Uptake by Duckweed

Duckweed's ability to remove nutrients and heavy metals from water makes it a valuable tool in wastewater remediation (Ali et al., 2016, Adhikari et al., 2015, Al-Hashimi and Joda, 2010). This unique capability is now being explored in the context of Irish farms as a dual-purpose solution to treat excess wastewater while simultaneously creating a monetary product (O'Mahoney et al., 2022).

At the end of each replicate during the RGR experiments, water samples were collected from each IBC. Total nitrate and total phosphorus tests were conducted on these samples to assess the potential relationship between mixing, system design, and nutrient remediation. While the tests used in this set of experiments are used for soiled water, it is important to note that the concentration of total nitrate, and total phosphorus at the beginning of each run was 10.7 mg L^{-1}, and 0.53 mg L^{-1} respectively. In 2015, a study was published on the characterisation of dairy soiled water from 60 Irish farms. It shows the high variability in total nitrate and total phosphorus concentrations between each farm. Total nitrate ranged from 70 to 479 mg L^{-1}, while total phosphorus ranged from 20 to 111 mg L^{-1} (Minogue et al., 2015). The nutrient concentration that is used for this set of experiments is significantly lower than that of typical soiled water.

4.4.1 Total Nitrate

Results from the total nitrate analysis are presented in Figure 42. The error bars indicate the standard error for three replicates. The black dotted line signifies the theoretical nitrate level in the system, based on the ratio of hydroponics used (10.7 mg L^{-1}). Notably, at lower inlet velocities, mixing and recirculation had a positive impact on nitrate removal, with over 1 mg L^{-1} more Nitrate removed in the recirculated systems. However, this influence was reduced at higher inlet velocities, where all three systems performed similarly. Again, it is important to highlight the difficulty drawing conclusions from this data as each run experienced different light intensity and temperature.

Multi-linear regression was also used as a tool to understand if there is statistical significance in the relationship between the TN values with inlet velocity for both recirculated IBCs. For the IBC with no recirculation the factors examined were light intensity and temperature for effects on TN. This work can be found in

Appendix 6. For each factor, a p value > 0.05 was acquired, meaning that the findings are not statistically significant. This may be due to the changeable environmental factors experienced by the systems over the 9 runs.

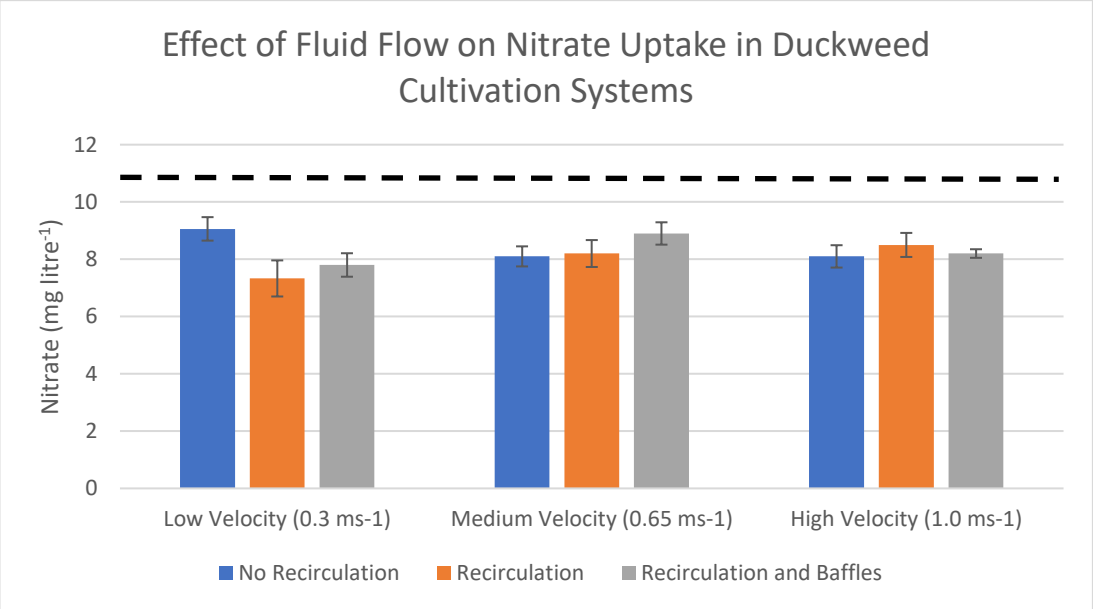

Figure 42: *Impact of Fluid Flow on Nutrient Uptake in Duckweed Cultivation Systems, Total Nitrate*

4.4.2 Total Phosphorus

Figure 43 highlights the results from the total phosphorus tests of each sample. In this case, the black dotted line represents 0.53 mg L^{-1} of phosphorus, the theoretical concentration. When comparing the IBC with no recirculation to the recirculated IBCs at a low inlet velocity, again the mixing had a positive impact on reducing phosphorus levels. However, the difference is approximately 0.05 to 0.06 mg L^{-1}. At the intermediate inlet velocity, there was minimal difference between phosphorus levels in each system. At the highest inlet velocity, the recirculated system with baffles had the lowest detected level of phosphorus, significantly lower than the IBC with no recirculation. These findings underscore the potential of duckweed cultivation systems, particularly those with recirculation and mixing to contribute to the nutrient remediation of wastewater. However, similarly to the TN results, when the TP data was analysed using multi-linear regression, each p value > 0.05. While it may appear that low inlet velocities bode best for nutrient remediation from this set of experiments, further work would benefit from being carried out in a controlled environment to mitigate external factors.

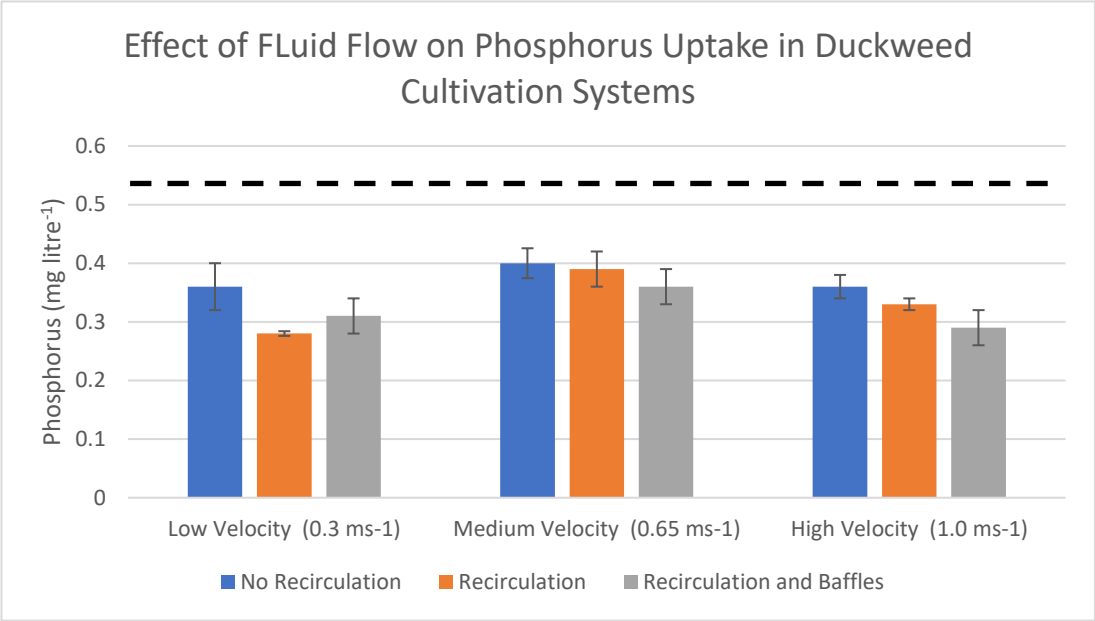

Figure 43: *Impact of Fluid Flow on Nutrient Uptake in Duckweed Cultivation Systems, Total Phosphorus*

4.5 Design of Medium-Scale Outdoor Cultivation System

The Duck-Feed Project has secured funding for the construction of outdoor ponds dedicated for duckweed cultivation within the School of BEES. A plot measuring 10 x 20 m^2 has been allotted for this purpose. The outcomes of this thesis are quite open ended. Lower levels of mixing have a positive impact on the RGR and nutrient remediation ability of duckweed. Conversely, increasing system velocities has the opposite effect. This leaves room for further exploration. The design of the medium-scale outdoor cultivation systems is an opportunity to further the knowledge of this thesis based on findings in both the literature review and the experimental work.

The final design is comprised of three ponds, each 18 m^2, as detailed in Figure 44. Crucially, the size of the ponds ensures a minimum of 2 m access on all sides, with 2.5 m spacing between each system. The three chosen designs include 1) a raceway-style system, 2) a pond with horizontal surface agitation, and 3) a pond with general recirculation (inlets and outlets at opposite ends).

Pond 1 adopts a raceway-style, commonly favoured in industrial settings. The success of a similar system at an IMTA site in Co. Offaly adds promise to the viability of raceway systems in Ireland (Stejskal et al., 2022). Pond 2 incorporates a horizontal surface agitator, a choice supported by literature. Ruekaewma et al., (2015) compared five different experimental setups and their effect on the production rate of duckweed. Horizontal surface agitation was found to greatly increase the yield of duckweed in comparison to the other setups. The benefit of this system was reinforced by Prosridee et al., (2023), who's study emphasised the benefits of horizontal surface agitation, ranking it 2nd out of 13 distinct experimental set ups for producing duckweed with the highest protein content. Pond 3, a conventional pond with recirculation, was selected for its consistent success in existing literature. Typical flow-through systems are widely used for duckweed cultivation (Mohedano et al., 2012).

These three systems will act as first of its kind, medium-scale comparison for duckweed cultivation. It will also provide valuable insights into the impact of wind on outdoor systems. The design builds on current understanding of duckweed cultivation, to provide pioneering research in the field.

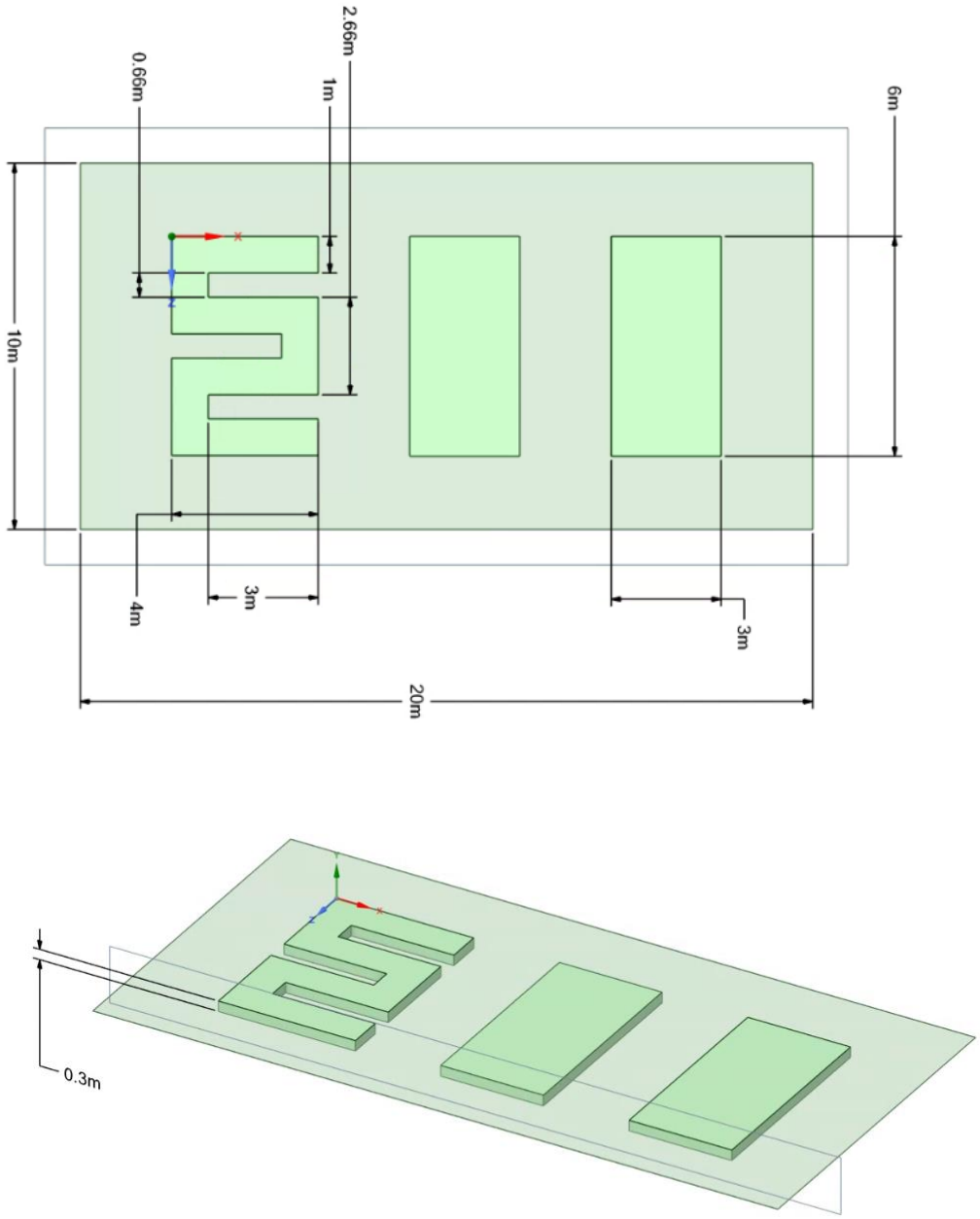

Figure 44: *a) Details of the medium-scale outdoor systems (XZ Plane) b) Isometric view of plans*

5 Conclusion

5.1 General Conclusion

This Master's thesis presents a thorough investigation into the design, construction, and testing of duckweed cultivation systems in both pilot-scale semi-outdoor and optimised medium-scale outdoor environments. While the study offers valuable insights, the primary challenge lies in interpreting the results due to the uncontrolled environmental conditions, particularly variations in light intensity and temperature. These factors, which are critical to duckweed growth and nutrient uptake, introduce significant variability, making it difficult to draw definitive conclusions regarding the impact of hydrodynamics on duckweed performance.

Despite these challenges, some general observations can be made. The results indicate that low levels of mixing, particularly with an inlet velocity of 0.3 m s^{-1}, tend to support higher relative growth rates and nutrient uptake. However, this advantage diminishes at higher inlet velocities within the range studied. It is important to note that the differences observed between system designs were subtle and overshadowed by environmental factors. This lack of stark contrast between system type suggests that design decisions may ultimately hinge on factors beyond those studied, such as wind protection and cost. Overall, the results indicate that there appears to be little difference between the various configurations and setups tested, aside from the specific instances mentioned.

Therefore, the conclusions drawn from this research must be considered within the context of these limitations. The outdoor nature of the experiments, while reflective of real-world conditions, complicates the isolation of hydrodynamic effects on duckweed growth. As a result, while some trends were observed, the findings highlight the complexity of duckweed systems and the need for carefully controlled future studies to obtain clearer insights.

Moreover, this research successfully developed a CFD model that accurately simulates the fluid dynamics within real-world duckweed cultivation systems. This model enables a detailed analysis of the effects of different inlet velocities on mixing and fluid flow in IBCs, with and without baffles. Such insights are vital for understanding how mixing influences the relative growth rate and nutrient uptake in duckweed. Additionally, the model provides crucial estimates of water surface

velocities, which are particularly relevant given that duckweed floats on the water's surface. By identifying dead zones within the system, the model further elucidates how fluid flow dynamics impact RGR and nutrient remediation in duckweed systems. These findings contribute to a deeper understanding of the interplay between hydrodynamics and plant growth, offering valuable guidance for optimising system design.

5.2 Recommendations for Future Work

Future research should aim to address the limitations encountered in this study by conducting experiments in a controlled environment where variables such as light and temperature can be tightly regulated. This would allow for a more precise assessment of the impact of system design and hydrodynamics on duckweed growth and nutrient uptake.

Additionally, further investigation into the role of external factors like wind considered when designing cultivation systems. Exploring a wider range of inlet velocities and system configurations in a controlled setting could help determine the optimal conditions for duckweed production, potentially leading to more conclusive results. However, the findings suggest that there appears to be minimal difference between the various configurations and setups examined, with the exception of specific scenarios noted earlier.

Finally, this research underscores both the need for, and value of an interdisciplinary approach, combining engineering and plant biology to develop robust duckweed cultivation systems. By addressing the gaps identified in this study, future work can contribute significantly to the advancement of sustainable agriculture and wastewater remediation practices.

Bibliography

DHONT, J. K. G. 1996. Chapter 5 - Hydrodynamics. *In:* DHONT, J. K. G. (ed.) *Studies in Interface Science.* Elsevier.

ADHIKARI, U., HARRIGAN, T. & REINHOLD, D. M. 2015. Use of duckweed-based constructed wetlands for nutrient recovery and pollutant reduction from dairy wastewater. *ECOLOGICAL ENGINEERING,* 78**,** 6-14.

AL- HASHIMI, M. A. & JODA, R. A. 2010. Treatment of Domestic Wastewater Using Duckweed Plant. *Journal of King Saud University - Engineering Sciences,* 22**,** 11-18.

ALEXANDER, D. E. 2017. Chapter 4 - Biological Materials Blur Boundaries. *In:* ALEXANDER, D. E. (ed.) *Nature's Machines.* Academic Press.

ALI, Z., WAHEED, H., KAZI, A. G., HAYAT, A. & AHMAD, M. 2016. *DUCKWEED: AN EFFICIENT HYPERACCUMULATOR OF HEAVY METALS IN WATER BODIES*.

ANSYS, I. 2002. Introductory FLUENT Notes v6.0.

ANSYS, I. 2006. FLUENT 6.3 User's Guide.

ANSYS, I. 2009. ANSYS Fluent 12.0 Theory Guide.

APPENROTH, K.-J., SREE, K. S., BÖHM, V., HAMMANN, S., VETTER, W., LEITERER, M. & JAHREIS, G. 2017. Nutritional value of duckweeds (Lemnaceae) as human food. *Food Chemistry,* 217**,** 266-273.

ASCANIO, G. 2015. Mixing time in stirred vessels: A review of experimental techniques. *Chinese Journal of Chemical Engineering,* 23**,** 1065-1076.

BAKER, R. O., YARRANTON, H. W. & JENSEN, J. L. 2015. 1 - Introduction. *In:* BAKER, R. O., YARRANTON, H. W. & JENSEN, J. L. (eds.) *Practical Reservoir Engineering and Characterization.* Boston: Gulf Professional Publishing.

BEYERS, M., RAVI, R., DEVLAMYNCK, R., MEERS, E., JENSEN, L. S. & BRUUN, S. 2023. Constructed wetlands and duckweed ponds as a treatment step in liquid manure handling — A life cycle assessment. *Science of The Total Environment***,** 163956.

BHANTHUMNAVIN, K. & MCGARRY, M. G. 1971. Wolffia arrhiza as a Possible Source of Inexpensive Protein. *Nature,* 232**,** 495-495.

BMJ 2021. The PRISMA 2020 statement: an updated guideline for reporting systematic

reviews. . *In:* PAGE, M., MCKENZIE, J., BOSSUYT, P., BOUTRON, I., HOFFMANN, T. & MULROW, C. (eds.).

CABARET, F., BONNOT, S., FRADETTE, L. & TANGUY, P. A. 2007. Mixing Time Analysis Using Colorimetric Methods and Image Processing. *Industrial & Engineering Chemistry Research,* 46**,** 5032-5042.

CHAKRABARTI, R., CLARK, W. D., SHARMA, J. G., GOSWAMI, R. K., SHRIVASTAV, A. K. & TOCHER, D. R. 2018. Mass Production of Lemna minor and Its Amino Acid and Fatty Acid Profiles. *Frontiers in Chemistry,* 6.

CHEN, G (2018) 'Duckweed systems for eutrophic water purification through converting wastewater nutrients to high-starch biomass: Comparative evaluation of three different genera (*spirodela polyrhiza*, *lemna minor*

and *landoltia punctata*) in monoculture or polyculture', *RSC Advances*, 8(32), pp. 17927–17937. doi:10.1039/c8ra01856a.

CHIN, W. C. 2017. Chapter 16 - Fluid Mechanics of Invasion. *In:* CHIN, W. C. (ed.) *Quantitative Methods in Reservoir Engineering (Second Edition).* Boston: Gulf Professional Publishing.

CONNOLLY, J. & WAYNE, P. 1996. Asymmetric competition between plant species. *Oecologia,* 108**,** 311-320.

COUGHLAN, N., MAGUIRE, D., OOMMEN, A., REDMOND, C., O'MAHONEY, R., WALSH, É., KUEHNHOLD, H., BYRNE, E., KAVOUSI, F., MORRISON, A. & JANSEN, M. 2023. On the rise: Development of a multi-tiered, indoor duckweed cultivation system. *Water Environment Research,* 95. e10964.

COUGHLAN, N., WALSH, É., AHERN, R., BURNELL, G., O'MAHONEY, R., KUEHNHOLD, H. & JANSEN, M. 2022a. Flow Rate and Water Depth Alters Biomass Production and Phytoremediation Capacity of Lemna minor. *Plants,* 11**,** 2170.

COUGHLAN, N. E., WALSH, É., BOLGER, P., BURNELL, G., O'LEARY, N., O'MAHONEY, M., PAOLACCI, S., WALL, D. & JANSEN, M. A. K. 2022b. Duckweed bioreactors: Challenges and opportunities for large-scale indoor cultivation of Lemnaceae. *Journal of Cleaner Production,* 336**,** 130285.

COUNCIL OF EUROPEAN COMMITTEES (2008) *31991L0676 The Nitrates Directive*, *EUR-Lex*. Available at: https://eur-lex.europa.eu/eli/dir/1991/676/oj (Accessed: 01 September 2023).

CRIPPA, M., SOLAZZO, E., GUIZZARDI, D., MONFORTI-FERRARIO, F., N. TUBIELLO & FLEIP, A. 2021. Food systems are responsible for a third of global anthropogenic GHG emissions. *Nature Food,* 2**,** 198-209.

CUI, W. & CHENG, J. J. 2015. Growing duckweed for biofuel production: a review. *Plant Biology,* 17**,** 16-23.

CUI, W., XU, J., CHENG, J. & STOMP, A. 2011. Starch Accumulation in Duckweed for Bioethanol Production. *Biological Engineering,* 3**,** 187-197.

DE BEUKELAAR, M. F. A., ZEINSTRA, G. G., MES, J. J. & FISCHER, A. R. H. 2019. Duckweed as human food. The influence of meal context and information on duckweed acceptability of Dutch consumers. *Food Quality and Preference,* 71**,** 76-86.

DEMANN, J., PETERSEN, F., DUSEL, G., BOG, M., DEVLAMYNCK, R., ULBRICH, A., OLFS, H. W. & WESTENDARP, H. 2022. Nutritional Value of Duckweed as Protein Feed for Broiler Chickens-Digestibility of Crude Protein, Amino Acids and Phosphorus. *Animals (Basel),* 13.

DEPARTMENT OF HOUSING, LOCAL GOVERNMENT, AND HERITAGE (2022) *Fifth Nitrates Action Programme 2022-2025*, *Search for services or information*. Available at: https://www.gov.ie/en/publication/f1d01-fifth-nitrates-action-programme-2022-2025/ (Accessed: 01 September 2023).

DEPARTMENT OF FOOD, AGRICULTURE, AND THE MARINE 2023. Information Note on the 5th Nitrates Action Programme and Changes to the Nitrates Regulation. Kildare Street, Dublin 2. (Accessed: 01 September 2023).

DEPARTMENT OF THE ENVIRONMENT, CLIMATE AND COMMUNICATIONS (2022) The Climate Action Plan 2023. *https://www.gov.ie/en/publication/7bd8c- climate-action-plan-2023/* (Accessed 4 January 2023).

DEVLAMYNCK, R., DE SOUZA, M. F., LEENKNEGT, J., JACXSENS, L., EECKHOUT, M. & MEERS, E. 2021a. Lemna minor cultivation for treating swine manure and providing micronutrients for animal feed. *Plants,* 10.

DEVLAMYNCK, R., DE SOUZA, M. F., MICHELS, E., SIGURNJAK, I., DONOSO, N., COUDRON, C., LEENKNEGT, J., VERMEIR, P., EECKHOUT, M. & MEERS, E. 2021b. Agronomic and Environmental Performance of Lemna minor Cultivated on Agricultural Wastewater Streams-A Practical Approach. *SUSTAINABILITY,* 13.

DORAN, P. M. 2013. Chapter 7 - Fluid Flow. *In:* DORAN, P. M. (ed.) *Bioprocess Engineering Principles (Second Edition).* London: Academic Press.

EDELMAN, M., APPENROTH, K. J., SREE, K. S. & OYAMA, T. 2022. Ethnobotanical History: Duckweeds in Different Civilizations. *Plants (Basel),* 11.

EPA (2022) *Latest Emissions Data*, *Environmental Protection Agency*. Available at: https://www.epa.ie/our-services/monitoring--assessment/climate-change/ghg/latest-emissions-data/ (Accessed: 14 October 2023).

EPA (2018) *CORINE 2018*, *EPA Maps*. Available at: https://gis.epa.ie/EPAMaps/ (Accessed: 14 October 2023).

EUROPEAN PARLIAMENT. (2023) *Circular economy: Definition, importance and benefits: News: European parliament*, *Circular economy: definition, importance and benefits | News | European Parliament*. Available at: https://www.europarl.europa.eu/news/en/headlines/economy/20151201STO05603/circular-economy-definition-importance-and-benefits (Accessed: 10 September 2023).

FAIZAL, A., SEMBADA, A. A. & PRIHARTO, N. 2021. Production of bioethanol from four species of duckweeds (Landoltia punctata, Lemna aequinoctialis, Spirodela polyrrhiza, and Wolffia arrhiza) through optimization of saccharification process and fermentation with Saccharomyces cerevisiae. *Saudi Journal of Biological Sciences,* 28**,** 294-301.

FEMEENA, P. V., COSTELLO, C. & BRENNAN, R. A. 2023a. Spatial optimization of nutrient recovery from dairy farms to support economically viable load reductions in the Chesapeake Bay Watershed. *Agricultural Systems,* 207**,** 103640.

FEMEENA, P. V., ROMAN, B. & BRENNAN, R. A. 2023b. Maximizing duckweed biomass production for food security at low light intensities: Experimental results and an enhanced predictive model. *Environmental Challenges,* 11**,** 100709.

FETTING, C. (2020). "The European Green Deal", ESDN Report, December 2020, ESDN Office, Vienna.

FITSCHEN, J., HOFMANN, S., WUTZ, J., KAMEKE, A. V., HOFFMANN, M., WUCHERPFENNIG, T. & SCHLÜTER, M. 2021. Novel evaluation

method to determine the local mixing time distribution in stirred tank reactors. *Chemical Engineering Science: X,* 10**,** 100098.

FOGLER, H. S. (2006) 'Chapter 13: Distribution of Residence Times for Chemical Reactors', in *Elements of Chemical Reaction Engineering*.

GENERAL HYDROPONICS. 2023a. *FloraGro 3-1-6.* [Hydroponics medium].

GENERAL HYDROPONICS. 2023b. *FloraMicro 5-0-1.* [Hydroponics medium].

GIBLIN, S. M., HOUSER, J. N., SULLIVAN, J. F., LANGREHR, H. A., ROGALA, J. T. & CAMPBELL, B. D. 2014. Thresholds in the response of free-floating plant abundance to variation in hydraulic connectivity, nutrients, and macrophyte abundance in a large floodplain river. *Wetlands,* 34**,** 413-425.

GOOPY, J.P. and MURRAY, P.J. (2003) 'A review on the role of duckweed in nutrient reclamation and as a source of animal feed', *Asian-Australasian Journal of Animal Sciences*, 16(2), pp. 297–305. doi:10.5713/ajas.2003.297.

GUO, L., FANG, Y., JIN, Y., HE, K. & ZHAO, H. 2023. High starch duckweed biomass production and its highly-efficient conversion to bioethanol. *Environmental Technology & Innovation,* 32**,** 103296.

HACH, C. 2017. LCK 138 LATON. *DOC312.53.94004.* 2 ed.: HACH LANGE GMBH.

HACH, C. 2020. LCK348 Phosphorus total. *DOC312.53.94020.* 4 ed.: HACH LANGE GMBH.

HADJIEV, D., SABIRI, N. E. & ZANATI, A. 2006. Mixing time in bioreactors under aerated conditions. *Biochemical Engineering Journal,* 27**,** 323-330.

HASSAN, M. R., & CHAKRABARTI, R. (2009). Use of Algae and Aquatic Macrophytes as Feed in Small-Scale Aquaculture. *A Review. Food and Agricultural Organization Fisheries Technical Paper*, *531*.

HUI, Y., FENG, X., DUAN, X., MAO, Z.-S. & YANG, C. 2023. Experimental and Numerical Study on the Residence Time Distribution in a Stirred Membrane Reactor. *Industrial & Engineering Chemistry Research,* 62**,** 6486-6499.

JANAUER, G. A., SCHMIDT-MUMM, U. & SCHMIDT, B. 2010. Aquatic macrophytes and water current velocity in the Danube River. *ECOLOGICAL ENGINEERING,* 36**,** 1138-1145.

JONES, G., SCULLION, J., DALESMAN, S., ROBSON, P. & GWYNN-JONES, D. 2023. Lowering pH enables duckweed (Lemna minor L.) growth on toxic concentrations of high-nutrient agricultural wastewater. *Journal of Cleaner Production,* 395**,** 136392.

KÖRNER, S., VERMAAT, J. E. & VEENSTRA, S. 2003. The Capacity of Duckweed to Treat Wastewater. *Journal of Environmental Quality,* 32**,** 1583-1590.

LAMBOLL, R. D., NICHOLLS, Z. R. J., SMITH, C. J., KIKSTRA, J. S., BYERS, E. & ROGELJ, J. 2023. Assessing the size and uncertainty of remaining carbon budgets. *Nature Climate Change,* 13**,** 1360-1367.

LANDOLT, E. & KANDELER, R. 1987. Biosystematic investigations in the family of duckweeds (Lemnaceae), Vol. 4: the family of Lemnaceae-a monographic study, Vol. 2 (phytochemistry, physiology, application, bibliography). *Veroeffentlichungen des Geobotanischen Instituts der ETH, Stiftung Ruebel (Switzerland)*.

LEE, K. C. & YIANNESKIS, M. 1997. A Liquid Crystal Thermographic Technique for the Measurement of Mixing Characteristics in Stirred Vessels. *Chemical Engineering Research and Design,* 75**,** 746-754.

LENG, R. A. 1999. Duckweed: A tiny aquatic plant with enormous potential for agriculture and environment. *In:* ANIMAL PRODUCTION AND HEALTH DIV.UNIVERSITY OF TROPICAL AGRICULTURE FOUNDATION, P. P. C. C. A. (ed.). FAO.

LEVENEUR, S., WÄRNÅ, J., ERÄNEN, K. & SALMI, T. 2011. Green process technology for peroxycarboxylic acids: Estimation of kinetic and dispersion parameters aided by RTD measurements: Green synthesis of peroxycarboxylic acids. *Chemical Engineering Science,* 66**,** 1038-1050.

LIU, Y., XU, H., YU, C. & ZHOU, G. 2021. Multifaceted roles of duckweed in aquatic phytoremediation and bioproducts synthesis. *GCB Bioenergy,* 13**,** 70-82.

MA, R. D., DUAN, C. Q., LIU, Y. J., YANG, Y. J., LIN, H., WEI, Y. Y. & ZHAO, Y. G. 2023. Pre-aeration promotes nutrient removal in a pilot-scale duckweed-based pond by influencing the duckweed growth and bacterial community. *JOURNAL OF WATER PROCESS ENGINEERING,* 53.

MAGUIRE, D., COUGHLAN, N., JANSEN, M., BYRNE, E. & KAVOUSI, F. 2023. Where engineering meets biology: The Computational Fluid Dynamic analysis of a stacked duckweed bioreactor. *Aquacultural Engineering,* 104**,** 102375.

MANN, R., WILLIAMS, R. A., DYAKOWSKI, T., DICKIN, F. J. & EDWARDS, R. B. 1997. Development of mixing models using electrical resistance tomography. *Chemical Engineering Science,* 52**,** 2073-2085.

MINOGUE, D., FRENCH, P., BOLGER, T., MURPHY, P.N.C. 2015 'Characterisation of dairy soiled water in a survey of 60 Irish Dairy Farms', *Irish Journal of Agricultural and Food Research*, 54(1), pp. 1–16. doi:10.1515/ijafr-2015-0001.

MOHEDANO, R. A., COSTA, R. H. R., TAVARES, F. A. & BELLI, P. 2012. High nutrient removal rate from swine wastes and protein biomass production by full-scale duckweed ponds. *BIORESOURCE TECHNOLOGY,* 112**,** 98-104.

NADAL-REY, G., MCCLURE, D. D., KAVANAGH, J. M., CASSELLS, B., CORNELISSEN, S., FLETCHER, D. F. & GERNAEY, K. V. 2022. Computational fluid dynamics modelling of hydrodynamics, mixing and oxygen transfer in industrial bioreactors with Newtonian broths. *Biochemical Engineering Journal,* 177**,** 108265.

NERE, N. K., PATWARDHAN, A. W. & JOSHI, J. B. 2003. Liquid-Phase Mixing in Stirred Vessels: Turbulent Flow Regime. *Industrial & Engineering Chemistry Research,* 42**,** 2661-2698.

O'MAHONEY, R., COUGHLAN, N. E., WALSH, E. & JANSEN, M. A. K. 2022. Cultivation of Lemna Minor on Industry-Derived, Anaerobically Digested, Dairy Processing Wastewater. *Plants,* 11.

PAOLACCI, S., HARRISON, S. & JANSEN, M. A. K. 2018. Are alien species necessarily stress sensitive? A case study on Lemna minuta and Lemna minor. *Flora,* 249**,** 31-39.

PAOLACCI, S., STEJSKAL, V., TONER, D. & JANSEN, M. A. K. 2022a. Wastewater valorisation in an integrated multitrophic aquaculture system; assessing nutrient removal and biomass production by duckweed species. *Environmental Pollution,* 302**,** 119059.

PAOLACCI, S., STEJSKAL, V., TONER, D. & JANSEN, M. A. K. 2022b. Wastewater valorisation in an integrated multitrophic aquaculture system; assessing nutrient removal and biomass production by duckweed species. *Environmental Pollution,* 302.

PATEL, B. B., GUNDALIYA, D. P. J., PATEL, D. U. D. & KHARE, D. U. 2021. Hydrodynamics of hybrid upflow anaerobic sludge blanket reactors using tracer studies. *Environmental Challenges,* 5**,** 100358.

PETERSEN, F., DEMANN, J., RESTEMEYER, D., ULBRICH, A., OLFS, H. W., WESTENDARP, H. & APPENROTH, K. J. 2021. Influence of the Nitrate-N to Ammonium-N Ratio on Relative Growth Rate and Crude Protein Content in the Duckweeds Lemna minor and Wolffiella hyalina. *PLANTS-BASEL,* 10.

PETERSEN, F., DEMANN, J., RESTEMEYER, D., OLFS, H. W., WESTENDARP, H., APPENROTH, K. J. & ULBRICH, A. 2022a. Influence of Light Intensity and Spectrum on Duckweed Growth and Proteins in a Small-Scale, Re-Circulating Indoor Vertical Farm. *Plants,* 11.

PETERSEN, F., DEMANN, J., VON SALZEN, J., OLFS, H. W., WESTENDARP, H., WOLF, P., APPENROTH, K. J. & ULBRICH, A. 2022b. Re-circulating indoor vertical farm: Technicalities of an automated duckweed biomass production system and protein feed product quality evaluation. *JOURNAL OF CLEANER PRODUCTION,* 380.

PROSRIDEE, K., OONSIVILAI, R., TIRA-AUMPHON, A., SINGTHONG, J., OONMETTA-AREE, J. & OONSIVILAI, A. 2023. Optimum aquaculture and drying conditions for Wolffia arrhiza (L.) Wimn. *Heliyon,* 9**,** e19730.

REHM, B., CONSULTANT, D., HAGHSHENAS, A., PAKNEJAD, A. S. & SCHUBERT, J. 2008. CHAPTER TWO - Situational Problems in MPD. *In:* REHM, B., SCHUBERT, J., HAGHSHENAS, A., PAKNEJAD, A. S. & HUGHES, J. (eds.) *Managed Pressure Drilling.* Gulf Publishing Company.

ROMAN, B., BRENNAN, R. & LAMBERT, J. 2021. Duckweed protein supports the growth and organ development of mice: A feeding study comparison to conventional casein protein. *Journal of Food Science,* 86.

ROSA-RODRÍGUEZ, R. D. L., LARA-HERRERA, A., TREJO-TÉLLEZ, L. I., PADILLA-BERNAL, L. E., SOLIS-SÁNCHEZ, L. O. & ORTIZ-RODRÍGUEZ, J. M. 2020. Water and fertilizers use efficiency in two hydroponic systems for tomato production. *Horticultura Brasileira,* 38.

RUEKAEWMA, N., PIYATIRATITIVORAKUL, S. & POWTONGSOOK, S. 2015. Culture system for Wolffia globosa L. (Lemnaceae) for hygiene human food. *Songklanakarin Journal of Science and Technology,* 37**,** 575-580.

SADINO-RIQUELME, M. C., RIVAS, J., JEISON, D., DONOSO-BRAVO, A. & HAYES, R. E. 2022. Investigating a Stirred Bioreactor: Impact of Evolving Fermentation Broth Pseudoplastic Rheology on Mixing Mechanisms. *Fermentation* [Online], 8.

SAID, M., CULLEY, D., STANDIFER, L., EPPS, E., MYERS, R. & BONEY, S. 2009. Effect of harvest rate, waste loading, and stocking density on the yield of duckweeds. *Proceedings of the World Mariculture Society,* 10**,** 769-780.

SODA, S., OHCHI, T., PIRADEE, J., TAKAI, Y. & IKE, M. 2015. Duckweed biomass as a renewable biorefinery feedstock: Ethanol and succinate production from Wolffia globosa. *Biomass and Bioenergy,* 81**,** 364-368.

SOŃTA, M., REKIEL, A. & BATORSKA, M. 2018. Use of Duckweed (Lemna L.) in Sustainable Livestock Production and Aquaculture – A Review. *Annals of Animal Science,* 19.

STEJSKAL, V., PAOLACCI, S., TONER, D. & JANSEN, M. A. K. 2022. A novel multitrophic concept for the cultivation of fish and duckweed: A technical note. *Journal of Cleaner Production,* 366**,** 132881.

TEAGASC (2020) *Crops 2030*, *Teagasc*. Available at: https://www.teagasc.ie/publications/2020/crops-2030.php (Accessed: 14 September 2023).

TEAGASC (2021) *Managing farm yards to reduce soiled water losses*, *Teagasc*. Available at: https://www.teagasc.ie/news--events/daily/environment/managing-farm-yards-to-reduce-soiled-water losses.php#:~:text=is%20Soiled%20Water%3F-,Soiled%20water%20is%20defined%20in%20the%20Nitrates%20Directive%20as%20water,chemical%20fertilisers (Accessed: 01 September 2023).

UPENDER, H., KISHORE, K. A., AFZAL, A., ISLAM, M. T. & IBRAHIM, M. 2021. Mean residence time and mass fraction of tracer in a liquid-solid tapered inverse fluidized bed: numerical modelling with experimental validation. *Journal of the Taiwan Institute of Chemical Engineers,* 128**,** 30-40.

VAN HOOFF, T., BLOCKEN, B. & TOMINAGA, Y. 2017. On the accuracy of CFD simulations of cross-ventilation flows for a generic isolated building: Comparison of RANS, LES and experiments. *Building and Environment,* 114**,** 148-165.

VESVIKAR, M. S. & AL-DAHHAN, M. 2005. Flow pattern visualization in a mimic anaerobic digester using CFD. *Biotechnology and Bioengineering,* 89**,** 719-732.

VIITANEN, P. 2005. RADIOCHEMICAL METHODS | Radiotracers. *In:* WORSFOLD, P., TOWNSHEND, A. & POOLE, C. (eds.) *Encyclopedia of Analytical Science (Second Edition).* Oxford: Elsevier.

WALSH, É., CIALIS, E., DILLANE, E. & JANSEN, M. A. K. 2022. Lemnaceae clones collected from a small geographic region display diverse traits relevant for the remediation of wastewater. *Environmental Technology & Innovation,* 28**,** 102599.

XU, J., ZHAO, H., STOMP, A. M. & CHENG, J. J. 2012. The production of duckweed as a source of biofuels. *Biofuels,* 3**,** 589-601.

XU, J., SHEN, Y., ZHENG, Y., SMITH, G., SUN, X. S., WANG, D., ZHAO, Y., ZHANG, W. & LI, Y. 2021. Duckweed (Lemnaceae) for potentially nutritious human food: A review. *Food Reviews International***,** 1-15.

YAHAYA, N., HAMDAN, N. H., ZABIDI, A. R., MOHAMAD, A. M., SUHAIMI, M. L. H., JOHARI, M. A. A. M., YAHYA, H. N. & YAHYA, H. 2022.

Duckweed as a future food: Evidence from metabolite profile, nutritional and microbial analyses. *Future Foods,* 5**,** 100128.

YANG, G.-L. 2022. Duckweed Is a Promising Feedstock of Biofuels: Advantages and Approaches. *International Journal of Molecular Sciences* [Online], 23.

YANG, K., ZHANG, X., LI, M., XIAO, Q. & WANG, H. 2022. Measurement of mixing time in a gas-liquid mixing system stirred by top-blown air using ECT and image analysis. *Flow Measurement and Instrumentation,* 84**,** 102143.

ZAPATA, A., DUCOSTE, J., PEÑA, M. & PORTAPILA, M. 2021. Computational Fluid Dynamics Simulation of Suspended Solids Transport in a Secondary Facultative Lagoon Used for Wastewater Treatment. *Water,* 13.

ZHANG, P., CHEN, G., DUAN, J. & WANG, W. 2018. Mixing characteristics in a vessel equipped with cylindrical stirrer. *Results in Physics,* 10**,** 699-705.

ZHANG, Q., ACHAL, V., XU, Y. & XIANG, W.-N. 2014. Aquaculture wastewater quality improvement by water spinach (Ipomoea aquatica Forsskal) floating bed and ecological benefit assessment in ecological agriculture district. *Aquacultural Engineering,* 60**,** 48-55.

ZHAO, Y., FANG, Y., JIN, Y., HUANG, J., BAO, S., HE, Z., WANG, F. & ZHAO, H. 2014a. Effects of operation parameters on nutrient removal from wastewater and high-protein biomass production in a duckweed-based (Lemma aequinoctialis) pilot-scale system. *Water science and technology : a journal of the International Association on Water Pollution Research,* 70**,** 1195-1204.

ZHAO, Y. G., FANG, Y., JIN, Y. L., HUANG, J., BAO, S., HE, Z. M., WANG, F. & ZHAO, H. 2014b. Effects of operation parameters on nutrient removal from wastewater and high-protein biomass production in a duckweed-based (Lemma aequinoctialis) pilot-scale system. *WATER SCIENCE AND TECHNOLOGY,* 70**,** 1195-1204.

ZHAO, Z., SHI, H., LIU, Y., ZHAO, H., SU, H., WANG, M. & ZHAO, Y. 2014c. The influence of duckweed species diversity on biomass productivity and nutrient removal efficiency in swine wastewater. *Bioresource Technology,* 167**,** 383-389.

ZHOU, Y., STEPANENKO, A., KISHCHENKO, O., XU, J. & BORISJUK, N. 2023. Duckweeds for Phytoremediation of Polluted Water. *Plants* [Online], 12.

ZIEGLER, P., ADELMANN, K., ZIMMER, S., SCHMIDT, C. & APPENROTH, K.-J. 2014. Relative in vitro growth rates of duckweeds (Lemnaceae) − The most rapidly growing higher plants. *Plant Biology,* 17.

Appendices

Appendix 1: Simulation Details

Appendix 1 contains information on the parameter selections for both steady state and transient state simulations that were run as part of this thesis.

Steady State Simulation

Full details on settings used for the steady state CFD model that was solved with ANSYS Fluent can be found in Table 23. For the solution gravity was turned on, and gravitational acceleration of -9.81 (m s^{-2}) in the Y plane selected. Water was selected as the fluid type for the system from the Fluent Database. For pressure-velocity coupling, the coupled scheme was chosen as it has better performance than the solution schemes that are segregated. It is also efficient and robust for steady state simulations (ANSYS, 2009). These settings were used for the model of both system types, system with baffles and system with no baffles.

Table 23: *Steady State Simulation- Selected Parameters*

	Parameter	Selection
Setup		
General	Solver Type	Pressure-Based
	Velocity Formulation	Absolute
	Time	Steady
Models	Viscous	k-epsilon*
	k-epsilon model*	Realizable*
	Near-Wall Treatment	Standard Wall Functions
	Transport Equations	Continuity
		Momentum
		Turbulent Kinetic Energy
		Turbulent Dissipation Rate
Materials	Fluid Density	998.2 (kg m^{-3})
	Fluid Viscosity	0.001 (kg m^{-1} s^{-1})
Solution		
Methods		
Pressure-Velocity Coupling	Scheme	Coupled
Spatial Discretization	Gradient	Least Squares Cell Based
	Pressure	PRESTO!
	Momentum	Second Order Upwind
	Turbulent Kinetic Energy	First Order Upwind
	Turbulent Dissipation Rate	First Order Upwind
	Pseudo Time Method	Global Time Step

*****For the mesh independence studies, as the Re for the inlet of each system was < 2100, the laminar viscous model was selected. Further details can be found in Section *3.1.5.*

Transient Simulation

Table 24 contains details of the parameter selections for the transient models. Any unchanged parameters from steady state to transient were not included and can be found in Table 24. As the transient solution was modelling tracer residence time within each system, the species transport model was turned on. This allows species specific data to be recorded over time, including the molarity of tracer at the outlet. Water was added as a fluid. A second fluid was also added which was named 'tracer' and this was given the same properties as water. The mixture was then called water-tracer-mixture. It was important that water was named first in this sequence as it made up the bulk fluid of the model. PISO was selected for the pressure-velocity coupling as a larger time-step was used for the majority of this solution. PISO increases the stability of the model for these cases (ANSYS, 2009).

Table 24: *Transient State Simulation- Selected Parameters*

	Parameter	**Selection**
Setup		
General	Time	Transient
Models	Energy Equation	On
	Viscous	k-epsilon
	k-epsilon model	Realizable
	Species Model	Species Transport
	Mixture Material	water-tracer-mixture
	Number of Volumetric Species	2
	Transport Equations	Continuity
		Energy
		Momentum
		Species Transport
		Turbulent Kinetic Energy
		Turbulent Dissipation Rate
Materials (water)	Fluid Density	998.2 (kg m^{-3})
	Fluid Viscosity	0.001 (kg m^{-1} s^{-1})
Materials (tracer)	Fluid Density	998.2 (kg m^{-3})
	Fluid Viscosity	0.001 (kg m^{-1} s^{-1})
Methods		
Pressure-Velocity Coupling	Scheme	PISO
Spatial Discretization	Energy	Second Order Upwind
	Tracer	Second Order Upwind

Appendix 2: Further Data from ANSYS Meshing

System with No Baffles

For the mesh independence studies, area-weighted average velocities were recorded at specific locations in the model. They were recorded at increasingly finer mesh sizes. Once the values stopped changing the solution was deemed independent from the mesh. This was discussed in Section *3.1.1.2.* Figure 45 includes the graphs obtained from tracking these parameters for the system with no baffles. These graphs reinforce the selection of Mesh Model number 6 as the mesh independent from the grid.

Graphs of Monitored Parameters from Mesh Independence Study

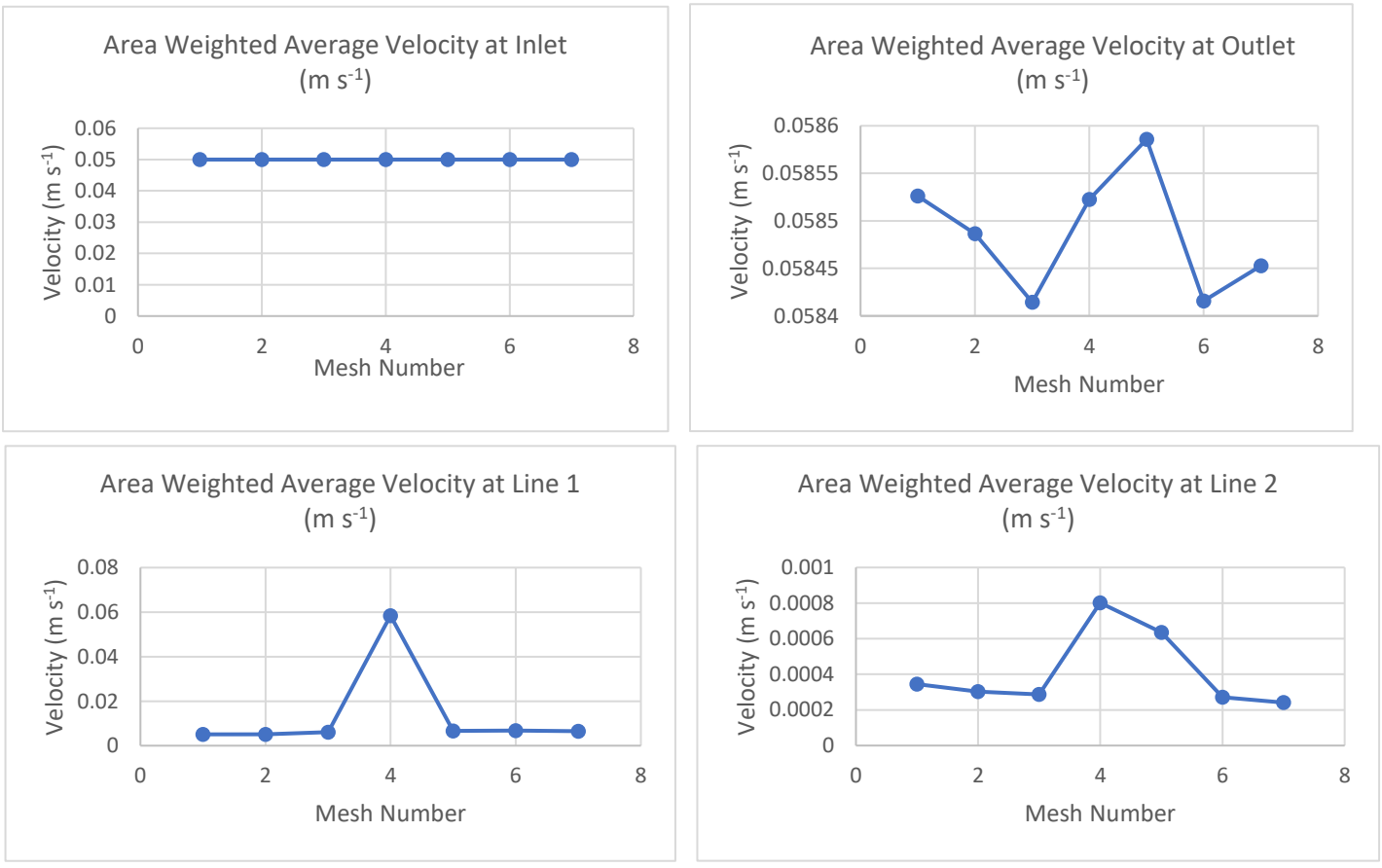

Figure 45: *Monitored Parameters for Mesh Independence Study a) Area-weight average velocity at Inlet, b) Area-weighted average velocity at outlet, c) Area-weighted velocity at line 1, d) Area-weighted average velocity at line 2*

Mesh Analysis

While mesh independence studies focus on achieving a solution independent to the mesh, there are other points of analysis that provide information on mesh quality. Table 25 contains the mesh metric values for Mesh Number 6. The element quality, aspect ratio, skewness, and orthogonal quality all had values in an acceptable range of the desired result. This shows that the mesh is of suitable quality to use for the model.

Table 25: *Mesh Metric Analysis- System with No Baffles*

Mesh Metric	Average Value	Standard Deviation	Desired Result
Element Quality	0.82	0.11	Scale of 0-1, with 1 a perfect 3D shape
Aspect Ratio	1.91	0.49	Closer the ratio is to 1 the better
Skewness	0.26	0.15	Scale of 0-1, below 0.5 is desirable
Orthogonal Quality	0.74	0.15	Scale of 0-1, with value of 1 desired

System with Baffles

Figure 46 includes details of the monitored parameters during the mesh independence study for the system with baffles. Mesh Model 7 was the model chosen, as it the solution is independent from the mesh and requires less computational power than finer meshes.

Graphs of Monitored Parameters from Mesh Independence Study

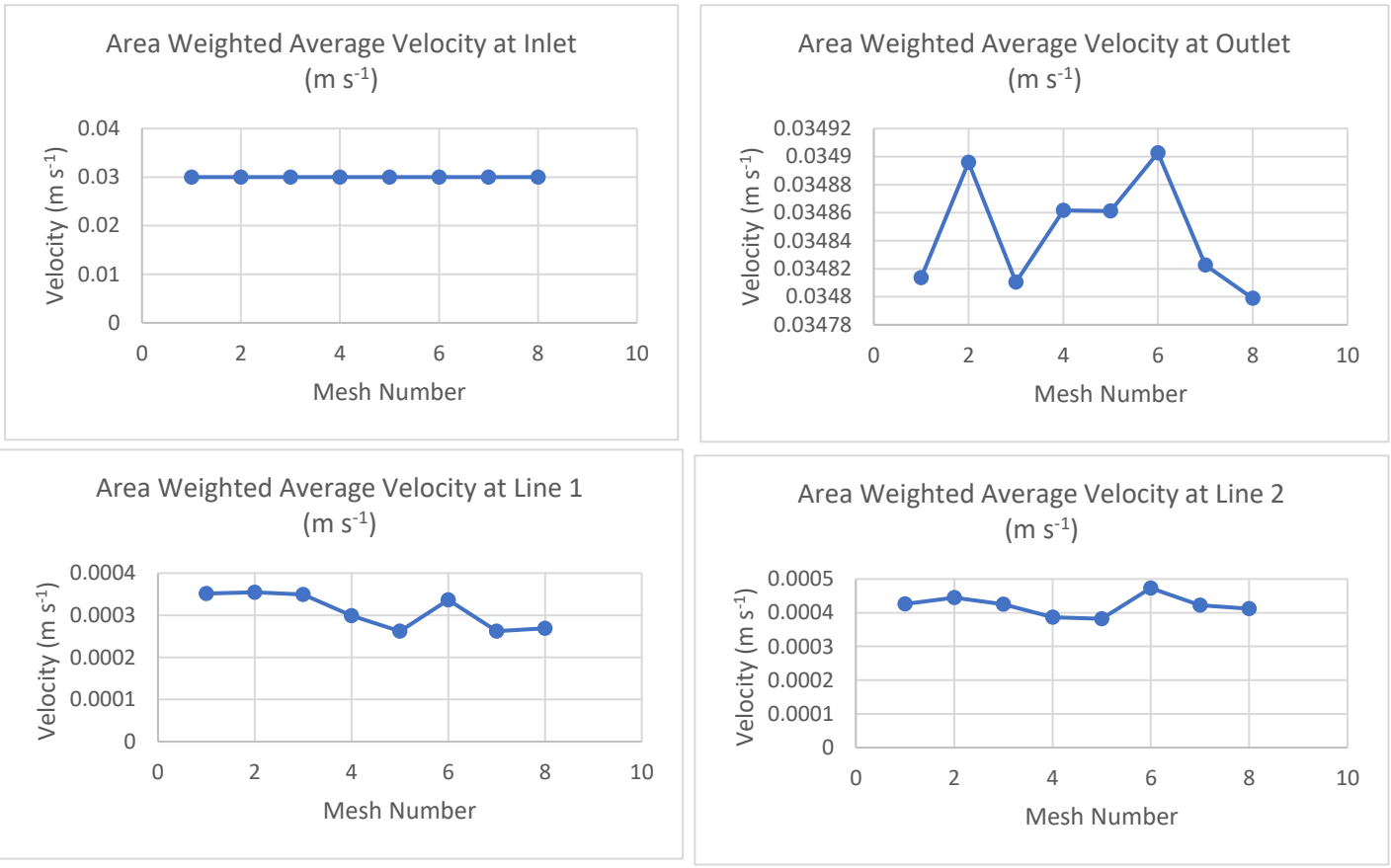

Figure 46: *Monitored Parameters for Mesh Independence Study a) Area-weight average velocity at Inlet, b) Area-weighted average velocity at outlet, c) Area-weighted velocity at line 1, d) Area-weighted average velocity at line 2*

Mesh Metric Analysis

The mesh metric analysis for the system with baffles can be seen in Table 26. The element quality, aspect ratio, skewness, and orthogonal quality are all at appropriate values when compared to the desired result. This analysis shows that the chosen mesh is of good quality, which will ensure a more accurate solution.

Table 26: *Mesh Metric Analysis: System with Baffles*

Mesh Metric	Average Value	Standard Deviation	Desired Result
Element Quality	0.80	0.12	Scale of 0-1, with 1 a perfect 3D shape
Aspect Ratio	2.00	0.74	Closer the ratio is to 1 the better
Skewness	0.29	0.17	Scale of 0-1, below 0.5 is desirable
Orthogonal Quality	0.71	0.17	Scale of 0-1, with value of 1 desired

Appendix 3: Visual Graphics from Mesh Independence Studies

To build on Appendix 2, Appendix 3 contains a visual representation of the mesh independence study. Figure 47 and Figure 49 represent the mesh of each model during the study for the system with no baffles and system with baffles respectively. The velocity contour and velocity vectors of each system are illustrated in Figure 48 and 50.

System with No Baffles

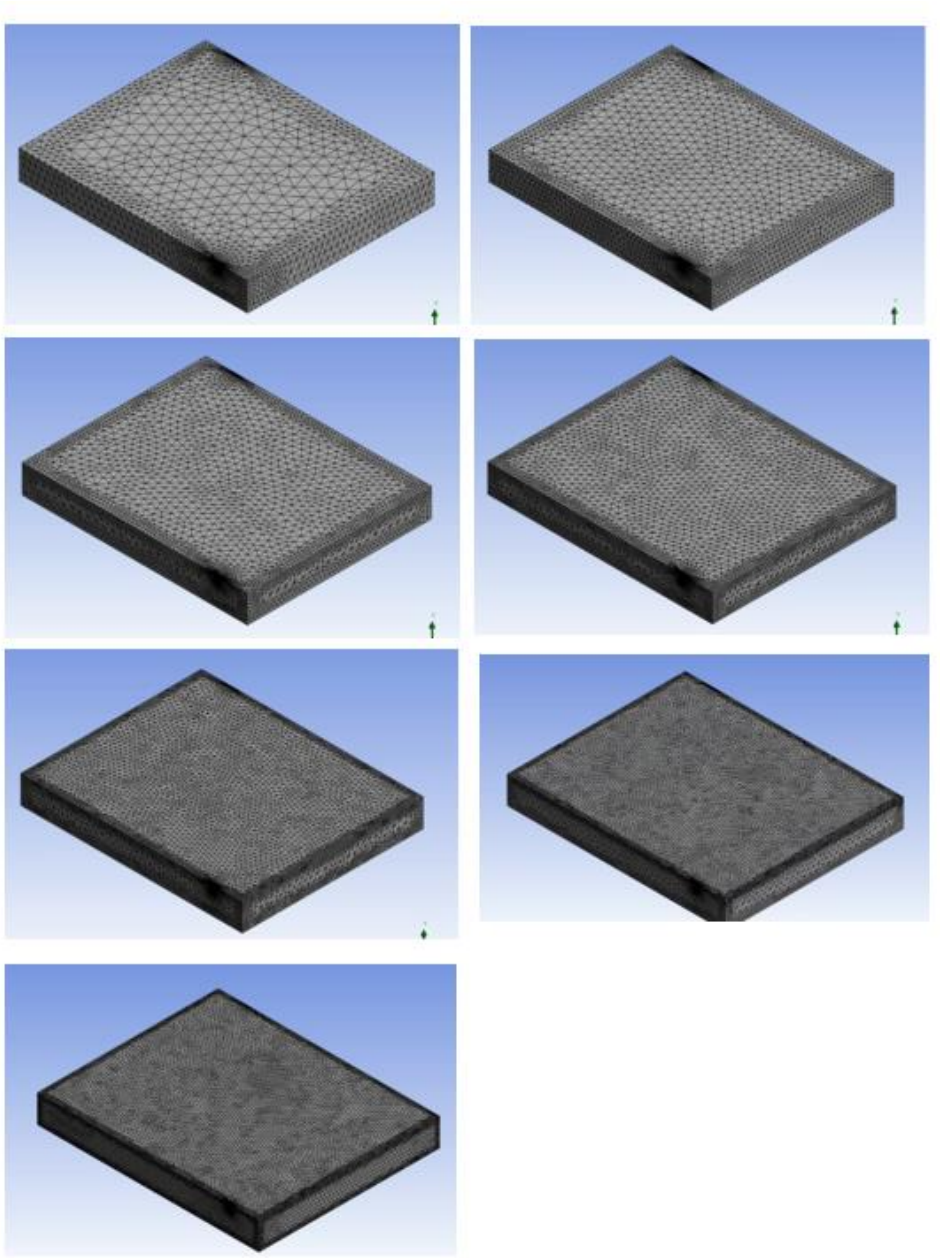

Figure 47: *Mesh for the system with no baffles for each model in the mesh independence study*

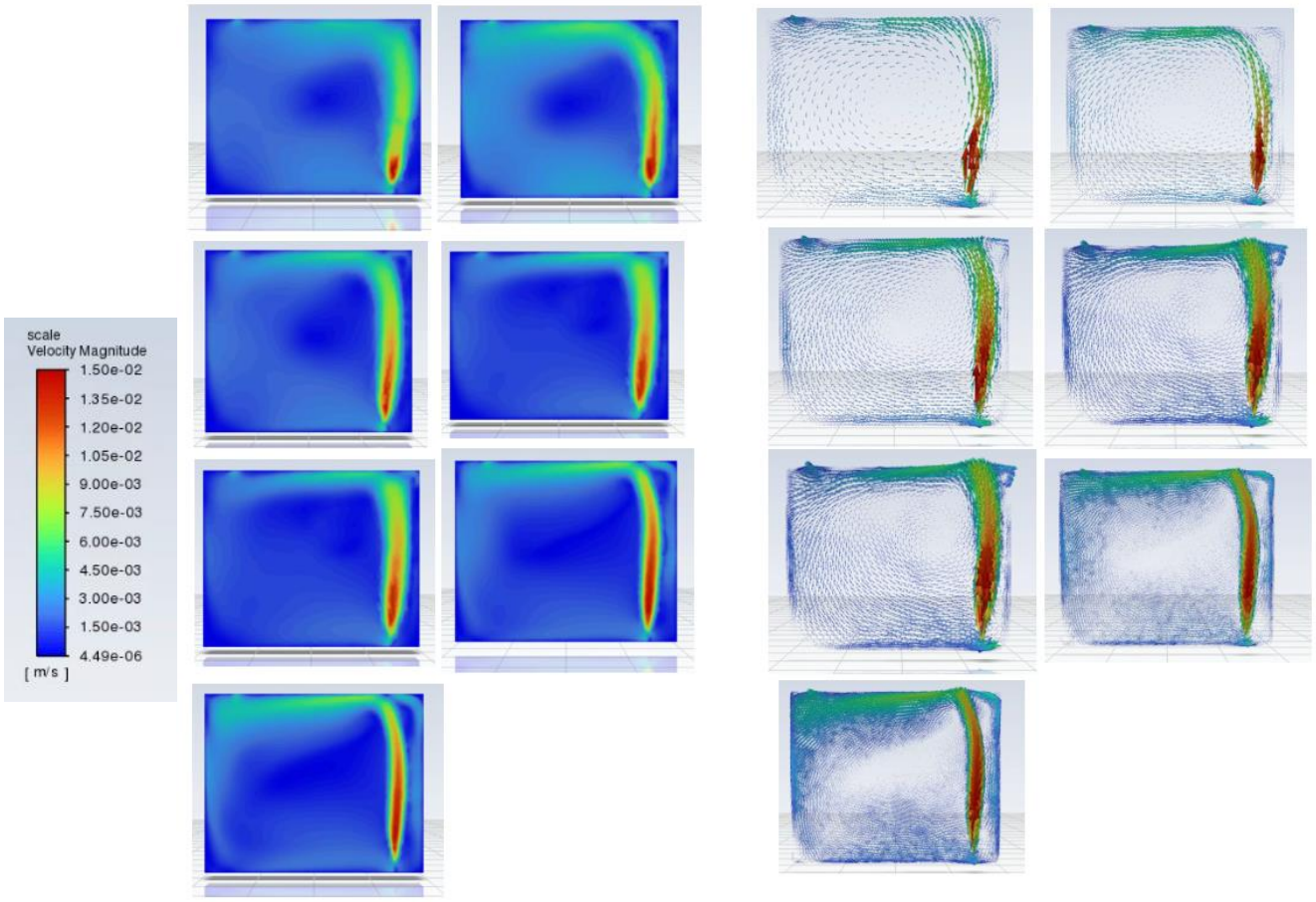

Figure 48: *a) Scale, b) Velocity Contours, c) Velocity Vectors for each model in the mesh independence study for the system with no baffles*

System with Baffles

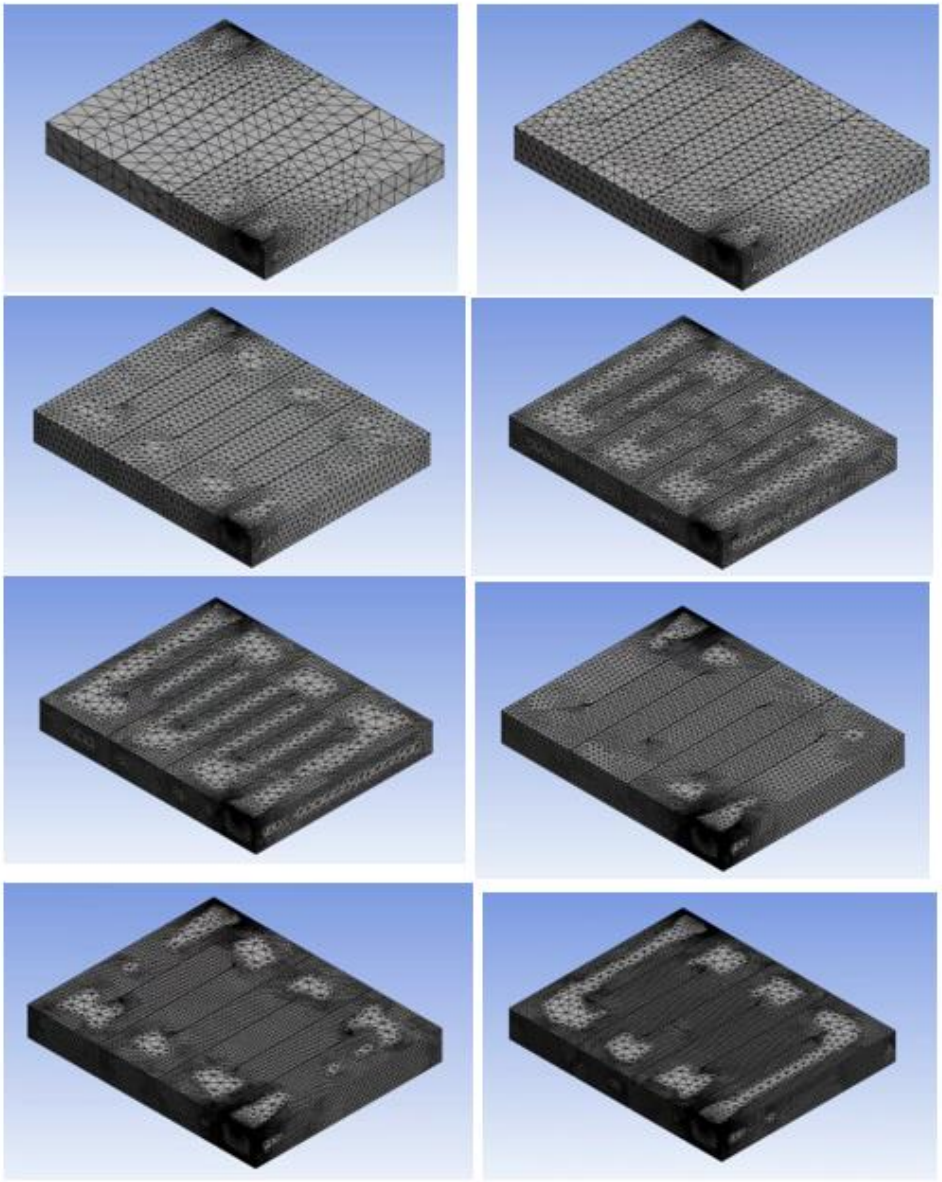

***Figure 49**: Mesh for the system with baffles for each model in the mesh independence study*

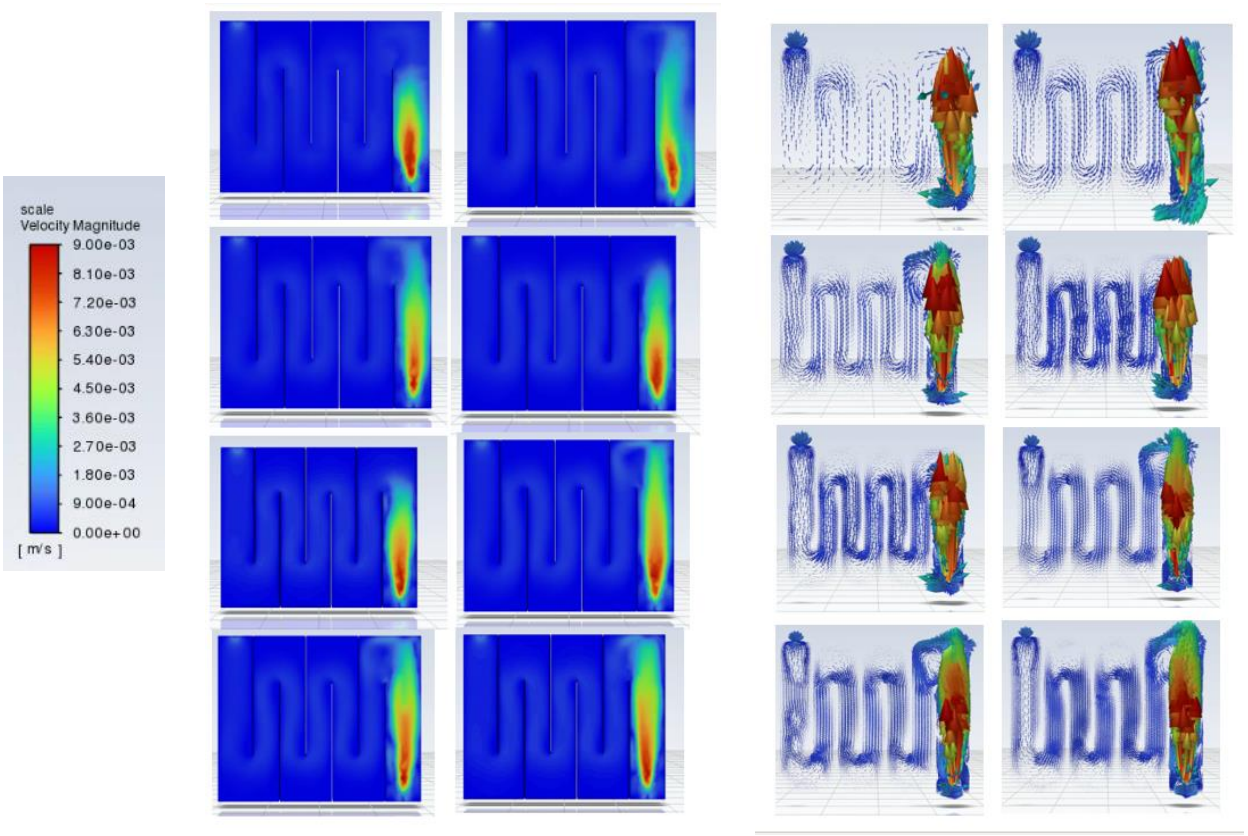

Figure 50: *a) Scale, b) Velocity Contours, c) Velocity Vectors for each model in the mesh independence study for the system with no baffles*

Appendix 4: Hydroponics Media

Appendix 4 contains information on the composition of the hydroponics used in the relative growth rate experiments. Table 27 contains a breakdown of the manufacturer's analysis for TriPart FloraGro 3-1-6. This is a growth fertiliser that contains primary and secondary nutrients needed for perfect growth (General Hydroponics, 2023a). Table 27 contains a breakdown of the manufacturer's analysis for TriPart FloraMicro 5-0-1. This contains micronutrients essential for plant growth as well as pH buffer (General Hydroponics, 2023*b).* For optimal duckweed growth, the concentration of hydroponics recommended is 0.25 mL L^{-1} FloraGro 3-1-6, and 0.25 mL L^{-1} FloraMicro 5-0-1 (Coughlan, 2022a).

Table 27: *(General Hydroponics, 2023a).*

Terra Aquatica TriPart FloraGro, 3-1-6	
Component	**Percentage** %
Total nitrogen	3
(Nitrate nitrogen)	(2)
(Ammoniacal nitrogen)	(1)
Phosphorus pentoxide	1
Potassium oxide	6
Magnesium oxide	0.5

Table 28: *(General Hydroponics, 2023b).*

Terra Aquatica FloraMicro, 5-0-1	
Component	**Percentage** %
Total nitrogen	5
(Nitrate nitrogen)	(4.7)
(Ammoniacal nitrogen)	(0.3)
Potassium oxide	1
Calcium	5
Boron	0.01
Cobalt	0.0005
Copper	0.01
Iron	0.1
Manganese	0.05
Molybdenum	0.0008
Zinc	0.015

Appendix 5: Statistical Analysis of RGR Experiments

(3 System Comparison)

Statistical analysis was used to analyse the significance of the findings for the RGR experiments by multi-linear regression. The RGR achieved for each of the 9 runs was examined in each system. In the IBC with no recirculation, Figure 51, the RGR was tested against light intensity and temperature. The results from the multi-linear regression for the IBC with recirculation, and the IBC with recirculation and baffles are depicted in Figures 52, and 53 respectively.

IBC with No Recirculation

Regression Statistics								
Multiple R	0.138975046							
R Square	0.019314063							
Adjusted R Square	-0.307581249							
Standard Error	0.029952396							
Observations	9							
ANOVA								
	df	*SS*	*MS*	*F*	*Significance F*			
Regression	2	0.000106013	5.3E-05	0.059083	0.943169704			
Residual	6	0.005382876	0.000897					
Total	8	0.005488889						
	Coefficients	*Standard Error*	*t Stat*	*P-value*	*Lower 95%*	*Upper 95%*	*Lower 95.0%*	*Upper 95.0%*
Intercept	0.150527833	0.266107284	0.565666	0.59213	-0.500613233	0.8016689	-0.500613233	0.8016689
Light Intensity	0.000196738	0.000829525	0.237169	0.820416	-0.001833037	0.002226513	-0.001833037	0.002226513
Temperature	-0.001775289	0.015805572	-0.11232	0.914233	-0.040450131	0.036899553	-0.040450131	0.036899553

Figure 51*: Multi-Linear Regression results, RGR in IBC with No Recirculation*

IBC with Recirculation

Regression Statistics								
Multiple R	0.822928271							
R Square	0.677210939							
Adjusted R Square	0.483537502							
Standard Error	0.022567441							
Observations	9							
ANOVA								
	df	*SS*	*MS*	*F*	*Significance F*			
Regression	3	0.005342442	0.001781	3.496664	0.105679668			
Residual	5	0.002546447	0.000509					
Total	8	0.007888889						
	Coefficients	*Standard Error*	*t Stat*	*P-value*	*Lower 95%*	*Upper 95%*	*Lower 95.0%*	*Upper 95.0%*
Intercept	-0.427558134	0.200542086	-2.13201	0.086184	-0.943067978	0.08795171	-0.943067978	0.08795171
Inlet velocity	-0.038366661	0.026527046	-1.44632	0.207725	-0.106556603	0.029823281	-0.106556603	0.029823281
Light Intensity	-0.001234924	0.000626073	-1.97249	0.105587	-0.002844296	0.000374447	-0.002844296	0.000374447
Temperature	0.033056375	0.011966871	2.762324	0.039725	0.002294553	0.063818197	0.002294553	0.063818197

Figure 52: *Multi-Linear Regression results, RGR in IBC with Recirculation*

IBC with Baffles + Recirculation

Regression Statistics								
Multiple R	0.771283341							
R Square	0.594877993							
Adjusted R Square	0.351804788							
Standard Error	0.023124901							
Observations	9							
ANOVA								
	df	*SS*	*MS*	*F*	*Significance F*			
Regression	3	0.003926195	0.001309	2.44732	0.179077614			
Residual	5	0.002673805	0.000535					
Total	8	0.0066						
	Coefficients	*Standard Error*	*t Stat*	*P-value*	*Lower 95%*	*Upper 95%*	*Lower 95.0%*	*Upper 95.0%*
Intercept	-0.314923964	0.205495866	-1.53251	0.18597	-0.843167905	0.213319978	-0.843167905	0.213319978
Inlet velocity	-0.044863842	0.027182315	-1.65048	0.159757	-0.114738208	0.025010525	-0.114738208	0.025010525
Light Intensity	-0.001254324	0.000641538	-1.95518	0.107952	-0.002903449	0.000394802	-0.002903449	0.000394802
Temperature	0.02810102	0.012262476	2.291627	0.070506	-0.003420679	0.059622719	-0.003420679	0.059622719

Figure 53: *Multi-Linear Regression results, RGR in IBC with Recirculation and Baffles*

Appendix 6: Statistical Analysis of Nutrient Remediation Experiments

Statistical analysis was used to analyse the significance of the findings for the TN, and TP experiments by multi-linear regression. The data achieved for each of the 9 runs was examined in each system.

Total Nitrate Results

IBC with No Recirculation

Regression Statistics	
Multiple R	0.191042495
R Square	0.036497235
Adjusted R Square	-0.284670353
Standard Error	1.042434907
Observations	9

ANOVA

	df	*SS*	*MS*	*F*	*Significance F*
Regression	2	0.24697679	0.123488	0.113639	0.894455823
Residual	6	6.52002321	1.086671		
Total	8	6.767			

	Coefficients	*Standard Error*	*t Stat*	*P-value*	*Lower 95%*	*Upper 95%*	*Lower 95.0%*	*Upper 95.0%*
Intercept	10.50089837	9.261346637	1.133841	0.300122	-12.16080047	33.16259722	-12.16080047	33.16259722
Light Intensity	0.011853204	0.028870009	0.410572	0.695646	-0.058789164	0.082495571	-0.058789164	0.082495571
Temperature	-0.150038346	0.55008221	-0.27276	0.794185	-1.496041024	1.195964333	-1.496041024	1.195964333

Figure 54: Multi-Linear Regression results, TN in IBC with No Recirculation

IBC with Recirculation

Regression Statistics	
Multiple R	0.705910358
R Square	0.498309434
Adjusted R Square	0.197295094
Standard Error	0.650758819
Observations	9

ANOVA

	df	*SS*	*MS*	*F*	*Significance F*
Regression	3	2.103165	0.701055	1.655434204	0.28994954
Residual	5	2.117435	0.423487		
Total	8	4.2206			

	Coefficients	*andard Erro*	*t Stat*	*P-value*	*Lower 95%*	*Upper 95%*	*Lower 95.0%*	*Upper 95.0%*
Intercept	15.81769856	5.782868	2.735269	0.041022241	0.952363455	30.68303366	0.952363455	30.68303366
Inlet velocity	1.020747552	0.764939	1.334417	0.239608785	-0.945589943	2.987085048	-0.945589943	2.987085048
Light Intensity	0.032740357	0.018054	1.813514	0.129485491	-0.013667764	0.079148478	-0.013667764	0.079148478
Temperature	-0.530668496	0.345079	-1.53782	0.184704001	-1.417721957	0.356384964	-1.417721957	0.356384964

Figure 55: Multi-Linear Regression results, TN in IBC with Recirculation

IBC with Baffles + Recirculation

Regression Statistics								
Multiple R	0.82942444							
R Square	0.687944901							
Adjusted R Square	0.375889803							
Standard Error	0.570800544							
Observations	9							
ANOVA								
	df	*SS*	*MS*	*F*	*Significance F*			
Regression	4	2.873103	0.718276	2.204562284	0.231360311			
Residual	4	1.303253	0.325813					
Total	8	4.176356						
	Coefficients	*andard Err*	*t Stat*	*P-value*	*Lower 95%*	*Upper 95%*	*Lower 95.0%*	*Upper 95.0%*
Intercept	21.52045338	6.138633	3.50574	0.024767136	4.476876348	38.56403042	4.476876348	38.56403042
Run	-0.032267102	0.199637	-0.16163	0.879433655	-0.586548517	0.522014313	-0.586548517	0.522014313
Inlet velocity	0.910543396	1.193019	0.763226	0.487859358	-2.401809478	4.22289627	-2.401809478	4.22289627
Light Intensity	0.023291934	0.018167	1.282067	0.269081747	-0.027149075	0.073732942	-0.027149075	0.073732942
Temperature	-0.749514876	0.321538	-2.33103	0.080161664	-1.642247953	0.143218201	-1.642247953	0.143218201

Figure 56: Multi-Linear Regression results, TN in IBC with Recirculation and Baffles

Total Phosphate Results

IBC with No Recirculation

Regression Statistics								
Multiple R	0.304635038							
R Square	0.092802506							
Adjusted R Square	-0.209596659							
Standard Error	1.037119583							
Observations	9							
ANOVA								
	df	*SS*	*MS*	*F*	*Significance F*			
Regression	2	0.660186717	0.330093359	0.306887	0.746630154			
Residual	6	6.453702172	1.075617029					
Total	8	7.113888889						
	Coefficients	*Standard Error*	*t Stat*	*P-value*	*Lower 95%*	*Upper 95%*	*Lower 95.0%*	*Upper 95.0%*
Intercept	12.65657294	9.214123487	1.373605743	0.218677	-9.889575016	35.2027209	-9.889575016	35.2027209
Light Intensity	0.020747068	0.028722802	0.722320488	0.497272	-0.049535097	0.091029234	-0.049535097	0.091029234
Temperature	-0.290571577	0.547277368	-0.53094024	0.61453	-1.629711054	1.0485679	-1.629711054	1.0485679

Figure 57: Multi-Linear Regression results, TP in IBC with No Recirculation

IBC with Recirculation

Regression Statistics								
Multiple R	0.425962032							
R Square	0.181443653							
Adjusted R Square	-0.309690155							
Standard Error	0.836579749							
Observations	9							
ANOVA								
	df	*SS*	*MS*	*F*	*Significance F*			
Regression	3	0.775671617	0.258557206	0.369438	0.779012657			
Residual	5	3.499328383	0.699865677					
Total	8	4.275						
	Coefficients	*Standard Error*	*t Stat*	*P-value*	*Lower 95%*	*Upper 95%*	*Lower 95.0%*	*Upper 95.0%*
Intercept	15.27101359	7.4341369	2.054174385	0.095136	-3.839043683	34.38107087	-3.839043683	34.38107087
Inlet Velocity	0.346364784	0.983363108	0.352224708	0.73903	-2.181450561	2.874180128	-2.181450561	2.874180128
Light Intensity	0.0152034	0.023208648	0.655074775	0.541355	-0.044456328	0.074863128	-0.044456328	0.074863128
Temperature	-0.410344623	0.44361441	-0.92500291	0.397413	-1.550691768	0.730002523	-1.550691768	0.730002523

Figure 58: Multi-Linear Regression results, TP in IBC with Recirculation

IBC with Baffles + Recirculation

Regression Statistics								
Multiple R	0.735023558							
R Square	0.540259631							
Adjusted R Square	0.26441541							
Standard Error	0.618528532							
Observations	9							
ANOVA								
	df	*SS*	*MS*	*F*	*Significance F*			
Regression	3	2.247912274	0.749304091	1.958568	0.238649065			
Residual	5	1.912887726	0.382577545					
Total	8	4.1608						
	Coefficients	*Standard Error*	*t Stat*	*P-value*	*Lower 95%*	*Upper 95%*	*Lower 95.0%*	*Upper 95.0%*
Intercept	11.21215768	5.496458395	2.039887665	0.096883	-2.916938427	25.3412538	-2.916938427	25.3412538
Inlet Velocity	1.631144143	0.727053387	2.24349982	0.074885	-0.237806087	3.500094374	-0.237806087	3.500094374
Light Intensity	0.016255011	0.017159405	0.947294576	0.386988	-0.027854644	0.060364666	-0.027854644	0.060364666
Temperature	-0.258592526	0.327988061	-0.78842055	0.466169	-1.101712679	0.584527626	-1.101712679	0.584527626

Figure 59: Multi-Linear Regression results, TP in IBC with Recirculation and Baffles